

STATUS OF THESIS

Title of thesis **DEGRADATION STUDIES ON WASTEWATER CONTAINING METHYL-DIETHANOLAMINE BY USING UV/H₂O₂ ADVANCED OXIDATION PROCESS**

I SABTANTI HARIMURTI

hereby allow my thesis to be placed at the Information Resource Center (IRC) of Universiti Teknologi PETRONAS (UTP) with the following conditions:

1. The thesis becomes the property of UTP
2. The IRC of UTP may make copies of the thesis for academic purposes only.
3. This thesis is classified as

Confidential

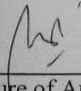
Non-confidential

If this thesis is confidential, please state the reason:

The contents of the thesis will remain confidential for _____ years.

Remarks on disclosure:

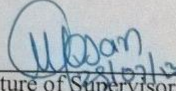
Endorsed by


Signature of Author

Permanent address:

Gendeng GK IV/642
RT 69 RW 17 Baciro,
Yogyakarta, Indonesia

Date: 29/07/2013


Signature of Supervisor

Name of Supervisor

Prof. Dr. T. Murugesan
Chemical Engineering Department
Universiti Teknologi PETRONAS

Prof. Dr. Thanabalan Murugesan

Date: _____

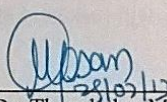
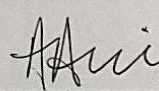
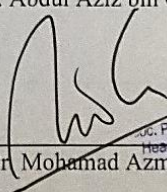
UNIVERSITI TEKNOLOGI PETRONAS

DISSERTATION TITLE:
DEGRADATION STUDIES ON WASTEWATER CONTAINING
METHYL-DIETHANOLAMINE BY USING UV/H₂O₂
ADVANCED OXIDATION PROCESS

By

SABTANTI HARIMURTI

The undersigned certify that they have read, and recommend to the Postgraduate Studies Programme for acceptance this thesis for the fulfilment of the requirements for the degree stated.

Signature Main Supervisor	:	 _____	Prof. Dr. T. Murugesan Chemical Engineering Department Universiti Teknologi PETRONAS
Signature Co Supervisor	:	 _____	Associate Professor Ir. Abdul Aziz Omar Chemical Engineering Department Faculty of Engineering Universiti Teknologi PETRONAS
Signature Head of Department	:	 _____	Assoc. Prof. Dr. Mohamad Azmi Bustam @ Khali Head, Chemical Engineering Department Universiti Teknologi PETRONAS
Date	:	1/8/2013 _____	

DEGRADATION STUDIES ON WASTEWATER CONTAINING
METHYL-DIETHANOLAMINE BY USING UV/H₂O₂
ADVANCED OXIDATION PROCESS

By

SABTANTI HARIMURTI

A Thesis

Submitted to the Postgraduate Studies Programme

As a Requirement for the Degree of

DOCTOR OF PHILOSOPHY
CHEMICAL ENGINEERING DEPARTMENT
UNIVERSITI TEKNOLOGI PETRONAS
BANDAR SERI ISKANDAR,
PERAK

AUGUST 2013

DECLARATION OF THESIS

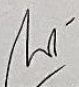
Title of thesis

DEGRADATION STUDIES ON WASTEWATER CONTAINING
METHYL-DIETHANOLAMINE BY USING UV/H₂O₂
ADVANCED OXIDATION PROCESS

I SABTANTI HARIMURTI

here by declare that the thesis is based on my original work except for quotations and citations which have been duly acknowledged. I also declare that it has not been previously or concurrently submitted for any other degree at UTP or other institutions.

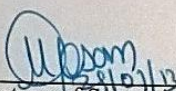
Witnessed by



Signature of Author
Permanent address:

Gendeng GK IV/642
RT 69 RW 17 Baciro,
Yogyakarta, Indonesia

Date: 29/07/2013



Signature of Supervisor
Name of Supervisor
Prof. Dr. T. Murugesan
Chemical Engineering Department
Universiti Teknologi PETRONAS

Prof. Dr. Thanabalan Murugesan

Date: _____

ACKNOWLEDGEMENTS

Alhamdulillah, praise be to Allah, I thank to God the Lord of the worlds, the source of strengths and inspirations for finishing up my PhD program.

I would like to express my deep gratitude to my supervisor Prof. Dr. Thanabalan Murugesan and my co-supervisor Assoc. Prof. Ir. Abdul Aziz Omar for their patient guidance, enthusiastic encouragement, and useful critiques of this research work, as well as providing facilities and chemicals.

I would like to thanks for the assistance given by Mr. M Azhar B A Satar and Mr. Noor Azahari B Arshad for their helpful provides in methyldiethanolamine effluent from Petronas Penapisan Melaka Sdn. Bhd (PPMSB). I would like also to extend my thanks to the technicians of the laboratory Universiti Teknologi PETRONAS for their effort in helping me for setting up of my experiment.

Special thanks to my husband and my sons. Thank you for the love, patience, and faith for all the day during my absence as a wife and mother.

I also would like to thank Universiti Teknologi PETRONAS for the scholarship granted under Graduate Assistantship scheme. Thank you to Chemical Engineering Department and Center for Graduate Studies, Universiti Teknologi PETRONAS for the facilities provided for conducting the research.

Finally, to all that I mention above and to all that I can not list individually including all my friends in Universiti Teknologi PETRONAS, my friends in Yogyakarta Muhammadiyah University, and my friends in Bandar University surely your support cannot be repaid with everything, and may those only be rewarded by Allah.

ABSTRACT

Methyldiethanolamine (MDEA) in aqueous solutions is frequently used for scrubbing carbon dioxide (CO₂) and hydrogen sulfide (H₂S) from natural gas. Large quantity of MDEA disposed into the wastewater during cleaning and maintenance as well as shutdown of the absorption and desorption columns of the gas processing plant. The MDEA is not readily biodegradable and such wastewater cannot be treated using the conventional treatment facility. Advanced Oxidation Processes (AOP's), such as oxidation by Fenton's reagent, UV/H₂O₂ and UV/Ozone have been recommended as a class of techniques used for the total/partial degradation of recalcitrant organics which are not readily amenable to conventional biological oxidation. Based on the advantages of UV/H₂O₂ process such as no formation of sludge during the treatment, applicable for a wide range of pH, and high capability of hydroxyl radical production, the UV/H₂O₂ process was chosen for the treatment of effluents containing MDEA from refinery plant. For this purpose, a synthetic MDEA solution and a real effluent from gas processing unit of a refinery were used for the experiments employing UV/H₂O₂ advanced oxidation process. The degradation of MDEA was found to be highly dependent on the initial concentration of H₂O₂, the initial pH, and the reaction temperature. The important parameters that govern the MDEA degradation by UV/H₂O₂ process were optimized using response surface methodology (RSM). The optimum conditions for degradation process of synthetic MDEA waste were at initial pH = 9.76, ratio between contaminant to oxidant = 1000 ppm of organic carbon to 0.22 M H₂O₂, and temperature = 30°C. Whilst the optimum condition of degradation process of real refinery effluent was at initial pH = 8.13, ratio between contaminant to oxidant = 1000 ppm organic carbon to 0.24 M of H₂O₂, and temperature = 30°C.

At optimum condition of degradation process for 3 hours irradiation using UV intensity at 12.06 mW/cm^2 , the maximum TOC removal achieved for synthetic and real effluent was 85.74% and 92.05%, respectively. Even though the main component of real refinery effluent was MDEA, however the other contaminants such as the presence of organic acids caused a slightly different optimum condition for degradation of refinery effluent from gas plant. During oxidation process, oxalic acid, acetic acid, formic acid, nitrite (NO_2^-), nitrate (NO_3^-), ammonium (NH_4^+), and carbon dioxide (CO_2) were identified as the intermediates formed during degradation. Hydroxyl radical rate constants of MDEA mineralization at different temperatures by using UV/ H_2O_2 in aqueous solution were also estimated. The rate constants of MDEA mineralization were not dependent on temperature when the temperature of reaction was less than 30°C . Based on the estimated hydroxyl radical rate constants of MDEA mineralization at temperature $20 - 50^\circ\text{C}$, the activation energy for mineralization of MDEA by hydroxyl radical was estimated as $10.20 \text{ kJ mol}^{-1}$. The presence of bicarbonate in the solution increased the TOC removal (reached 100 % TOC removal) at an initial $\text{pH} = 7$. This is due to the capability of bicarbonate to act as a good buffer. At $\text{pH} \geq 7$, the active site for hydroxyl radical oxidation was more provided. The biodegradability of partially degraded MDEA after UV/ H_2O_2 was evaluated by estimation of the BOD_5/COD ratio from experimental data collected, and the estimated value (BOD_5/COD), proved that the partially degraded wastewater is readily biodegradable and it can safely be discharged into the environment. The energy efficiency for TOC removal of MDEA using UV/ H_2O_2 is proved as more efficient compared to the other TOC removal technologies.

ABSTRAK

Methyldiethanolamine (MDEA) dalam larutan akuas selalu digunakan untuk menapis karbon dioksida (CO_2) dan hidrogen sulfida (H_2S) daripada gas asli. Kuantiti MDEA yang besar telah dilupuskan ke dalam air kumbahan semasa proses pembersihan dan penyelenggaraan serta penutupan ruangan penyerapan dan nyahpenyerapan loji pemprosesan gas. MDEA tidak boleh terbiodegradasi secara terus dan kemudahan rawatan konvensional tidak boleh digunakan untuk merawat air kumbahan tersebut. Proses Pengoksidaan Lanjutan (AOP), seperti pengoksidaan oleh reagen Fenton $\text{UV}/\text{H}_2\text{O}_2$, dan UV / Ozon telah disyorkan sebagai kelas teknik yang digunakan untuk mendegradasi secara keseluruhan / separa bagi organik degil yang tidak mudah untuk dioksidakan melalui biologi konvensional. Berdasarkan kelebihan $\text{UV}/\text{H}_2\text{O}_2$ proses seperti tiada pembentukan enap cemar semasa rawatan, boleh di aplikasi untuk pelbagai nilai pH, dan keupayaan tinggi untuk menghasilkan radikal hidroksil, proses $\text{UV}/\text{H}_2\text{O}_2$ telah dipilih untuk merawat efluen yang mengandungi MDEA dari loji penapisan. Bagi tujuan ini, penyelesaian MDEA sintetik dan efluen sebenar dari unit pemprosesan gas penapisan telah digunakan untuk eksperimen $\text{UV}/\text{H}_2\text{O}_2$ proses pengoksidaan lanjutan. Degradasi MDEA sangat bergantung kepada kepekatan awal H_2O_2 , nilai awal pH, dan suhu tindak balas. Parameter penting yang mengawal degradasi MDEA oleh proses $\text{UV}/\text{H}_2\text{O}_2$ telah dioptimumkan dengan menggunakan kaedah gerak balas permukaan (RSM). Keadaan optimum proses degradasi sisa sintetik MDEA adalah pada nilai pH awal 9.76, nisbah antara pencemar kepada oksidan adalah 1000 ppm karbon organik kepada 0.22 M H_2O_2 , dan suhu ialah 30 °C. Selain itu keadaan optimum proses degradasi penapisan efluen sebenar adalah pada nilai pH awal 8.13, nisbah antara pencemar kepada oksidan ialah 1000 ppm karbon organik kepada 0.24 M H_2O_2 , dan suhu ialah 30 °C. Pada keadaan optimum proses degradasi selama 3 jam penyinaran menggunakan intensiti UV pada 12.06 mW/cm^2 , penyingkiran TOC maksimum dicapai untuk sintetik adalah 85.74%

manakala 92.05% untuk efluen sebenar. Walaupun komponen utama penapisan efluen sebenar adalah MDEA, namun bahan pencemar lain seperti kehadiran asid organik menyebabkan keadaan optimum untuk degradasi sedikit berbeza. Semasa proses pengoksidaan, asid oksalik, asid asetik, asid formik, nitrit (NO_2^-), nitrat (NO_3^-), ammonium, dan karbon dioksida (CO_2) telah dikenal pasti sebagai perantaraan yang terbentuk semasa degradasi. Hidroksil pemalar kadar radikal mineral MDEA pada suhu yang berbeza dengan menggunakan UV/ H_2O_2 dalam larutan akuas juga dianggarkan. Pemalar kadar MDEA pemineralan tidak bergantung kepada suhu apabila suhu tindak balas adalah kurang daripada 30 °C. Berdasarkan anggaran pemalar kadar radikal hidroksil mineral MDEA pada suhu 20 - 50 °C, tenaga pengaktifan bagi mineral daripada MDEA oleh radikal hidroksil dianggarkan sebagai 10.20 kJ mol⁻¹. Kehadiran bikarbonat dalam larutan meningkatkan penyingkiran TOC (mencapai 100% penyingkiran TOC) pada nilai pH awal 7. Ini adalah disebabkan oleh keupayaan bikarbonat untuk bertindak sebagai penampan yang baik. Pada pH ≥ 7 , tapak aktif untuk pengoksidaan radikal hidroksil adalah lebih banyak. Biodegradasi separa MDEA selepas UV/ H_2O_2 telah ditentukan dengan mengira nisbah BOD₅/COD, dan nilai anggaran (BOD₅/COD), terbukti bahawa biodegradasi separa air sisa telah terbiodegradasi dan ia selamat untuk dilepaskan ke dalam alam sekitar. Kecekapan tenaga untuk penyingkiran TOC MDEA menggunakan UV/ H_2O_2 dibuktikan sebagai lebih cekap berbanding teknologi penyingkiran TOC yang lain.

In compliance with the terms of the Copyright Act 1987 and the IP Policy of the university, the copyright of this thesis has been reassigned by the author to the legal entity of the university,

Institute of Technology PETRONAS Sdn Bhd.

Due acknowledgement shall always be made of the use of any material contained in, or derived from, this thesis.

© Sabtanti Harimurti, 2013

Institute of Technology PETRONAS Sdn Bhd

All rights reserved.

TABLE OF CONTENTS

STATUS OF THESIS.....	i
DECLARATION OF THESIS	Error! Bookmark not defined.
ACKNOWLEDGEMENTS	v
ABSTRAK.....	viii
TABLE OF CONTENTS.....	xi
LIST OF FIGURES	xiv
LIST OF TABLES	xviii
CHAPTER 1	1
INTRODUCTION	1
1.1. Background of Research	1
1.2 Problem Statement	3
1.3 Objectives.....	4
1.4 Scope of the Present Research	4
1.5 Organization of Thesis	5
CHAPTER 2	7
LITERATURE REVIEW	7
2.1 Natural Gas Sweetening Process.....	7
2.1.1 The Removal of Acidic Gas from Natural Gas.....	8
2.1.2 Process Wastewater from Natural Gas Sweetening Operation.....	10
2.2 Wastewater Treatment	11
2.2.1 Wastewater Regulation	12
2.2.2 Wastewater Characteristics	13
2.2.3 Wastewater Treatment Methods	14
2.2.4 The Hybrid Process of Advanced Oxidation followed by Biological Treatment	15
2.3 Advanced Oxidation Processes	16
2.3.1 The Reaction Mechanism of Hydroxyl Radical toward Organic Contaminant in Wastewater.....	18
2.3.2 Fenton’s Process	19
2.3.3 Ozone-based Processes	24

2.3.4	High Voltage Electrical Discharge Processes	26
2.3.5	Others AOP's	29
2.3.6	AOP's based on Ultraviolet Light.....	30
2.4	Response Surface Methodology of Statistical Design of Experiment	47
2.5	Degradation Intermediate	48
2.6	Biodegradability of Pollutants	51
CHAPTER 3	57
EXPERIMENTAL	57
3.1	Materials.....	58
3.1.1	MDEA Contaminated Water/Effluents.....	58
3.1.2	Reagents Used.....	61
3.2	Experimental Set Up	62
3.2.1	UV/H ₂ O ₂ Oxidation Process	62
3.2.2	Biodegradability Test of Partially Degraded MDEA Solution	65
3.3	Analytical Methods	66
3.3.1	Total Organic Carbon (TOC) Determination.....	66
3.3.2	Chemical Oxygen Demand (COD) Determination.....	67
3.3.3	BOD ₅ Determination.....	67
3.3.4	Identification of UV Absorption Spectra of MDEA.....	68
3.3.5	Un-reacted MDEA and Degradation Product Identification using HPLC	68
3.3.6	Nitrate (NO ₃ ⁻) and Nitrite (NO ₂ ⁻) Determination.....	69
3.3.7	Estimation of Ammonium (NH ₄ ⁺)	70
3.3.8	Un-reacted H ₂ O ₂ Determination	70
3.3.9	pH.....	70
3.3.10	Measurement of UV Intensity.....	71
3.4	Statistical Design of Experiments (DOE) for Optimization of Degradation Process by Using UV/H ₂ O ₂	71
CHAPTER 4	73
RESULTS AND DISCUSSION	73
4.1	Preliminary Studies	73
4.1.1	Effect of UV, H ₂ O ₂ , and Combination of UV/H ₂ O ₂ on MDEA Degradation.....	74

4.1.2	Effect of Initial Concentration of MDEA	77
4.1.3	Effect of UV Intensity in Combination with H ₂ O ₂	79
4.1.4	Effect of Initial Concentration of H ₂ O ₂ in Combination with UV.....	81
4.1.5	Effect of pH.....	84
4.1.6	Effect of Temperature	86
4.1.7	Optimization Process of MDEA Degradation by using UV/H ₂ O ₂	88
4.2	Degradation Intermediates Identification and Development of Degradation Mechanism.....	95
4.3	Kinetics of MDEA Mineralization Process.....	102
4.3.1	Determination of Kinetic Constants of MDEA Mineralization	102
4.3.2	Temperature Dependence of MDEA Mineralization.....	113
4.4	Effect of Bicarbonate on MDEA Mineralization by UV/H ₂ O ₂	116
4.5	Degradation of Refinery Effluent (PPMSB Effluent) using UV/H ₂ O ₂	123
4.6	Biodegradability Test on Partially Degraded MDEA Solution.....	129
4.7	Electrical Energy Consumption	130
CHAPTER 5	135
CONCLUSIONS AND RECOMENDATIONS	135
5.1	Conclusions	135
5.2	Recommendations	136
REFERENCES	138
PUBLICATIONS	156
APPENDIX A	157
CALIBRATION CURVE	157
APPENDIX B	164
Rate constant of MDEA mineralization by hydroxyl radical at different temperature based on Figure 4.29		164

LIST OF FIGURES

Figure 2. 1	Chemical Structure of MDEA	9
Figure 2. 2	Flow diagram of a typical amine treating process [13].....	10
Figure 2. 3	Constituent of wastewater.....	14
Figure 2. 4	The concept of coupling AOP-based pre-treatment with biological post-treatment [28].....	15
Figure 2. 5	Generation of hydroxyl radicals using different techniques [30].	16
Figure 2. 6	Range of electromagnetic waves [31].....	31
Figure 2. 7	The general scheme of UV based oxidation reactions in the presence of auxiliary oxidant [32].	33
Figure 3. 1	Scheme of activities in the present research.	57
Figure 3. 2	Correlation of MDEA concentrations with total organic carbon (TOC).	59
Figure 3. 3	Correlation of MDEA concentrations with organic carbon.	59
Figure 3. 4	UV/H ₂ O ₂ oxidation experimental set up.....	63
Figure 3. 5	The schematic diagram of the UV/H ₂ O ₂ photoreactor.	63
Figure 3. 6	Experimental set up for the identification of CO ₂ liberation during UV/H ₂ O ₂ oxidation process.....	64
Figure 3. 7	Experimental set up of biodegradability test.	66
Figure 4. 1	Individual effect of UV, H ₂ O ₂ , and the combination of UV/H ₂ O ₂ on MDEA degradation ([MDEA] ₀ = 1000 ppm TOC; [H ₂ O ₂] ₀ = 0.12 M; pH = 7; Temperature = 30 °C; UV intensity = 12.06 mW/cm ²)	74

Figure 4. 2	Individual effect of UV, H ₂ O ₂ , and the combination of UV/H ₂ O ₂ on the MDEA mineralization ([MDEA] ₀ = 1000 ppm TOC; [H ₂ O ₂] ₀ = 0.12 M; pH = 7; Temperature = 30 °C UV intensity = 12.06 mW/cm ²).	75
Figure 4. 3	UV absorption spectra of MDEA.	76
Figure 4. 4	H ₂ O ₂ profile during the UV/H ₂ O ₂ process.	77
Figure 4. 5	The degradation profile of organic carbon for different initial concentration of MDEA.....	78
Figure 4. 6	Effect of initial concentration of MDEA on TOC removal (after 360 minute reaction time).	79
Figure 4. 7	The degradation profile of organic carbon for different UV intensities.....	80
Figure 4. 8	Effect of different UV intensity on TOC removal.	81
Figure 4. 9	The degradation profile of organic carbon at different.....	82
Figure 4. 10	Effect of initial concentration of H ₂ O ₂ on TOC removal (after 180 min).	83
Figure 4. 11	The degradation profile of organic carbon for different	85
Figure 4. 12	Effect of initial pH condition on TOC removal.	85
Figure 4. 13	The degradation profile of organic carbon at different temperature	87
Figure 4. 14	Effect of temperature on TOC removal.	88
Figure 4. 15	Relation between experimental value and fitted value of TOC removal.	91
Figure 4. 16	Pareto chart of the standardized effect for percentage TOC removal for screening of significant factors for the degradation of MDEA.....	91

Figure 4. 17	3D Contour plots of TOC removal for MDEA.....	93
Figure 4. 18	Comparison of predicted and experimental TOC removal at optimum condition.....	94
Figure 4. 19	Inorganic by-product profile during the UV/H ₂ O ₂ process.	95
Figure 4. 20	Chromatogram of partially degraded MDEA after UV/H ₂ O ₂ process using YMC-PolymerC18 column.....	97
Figure 4. 21	Chromatogram of partially degraded MDEA after UV/H ₂ O ₂ using Transgenomic column.....	98
Figure 4. 22	Organic by-products profile during the UV/H ₂ O ₂ process.	99
Figure 4. 23	The initial stages of MDEA mineralization by hydroxyl radical.....	100
Figure 4. 24	Reaction pathways of intermediate degradation by hydroxyl radical.	101
Figure 4. 25	MDEA mineralization profile at different initial concentration of H ₂ O ₂	102
Figure 4. 26	MDEA mineralization profile at different initial concentration of contaminant.....	103
Figure 4. 27	Plot of $\ln[-d[C]_0/dt]$ vs $\ln[H_2O_2]_0$ at four different temperatures.....	109
Figure 4. 28	Plot of $\ln[-d[C]_0/dt]$ vs $\ln[C]_0$ at four different temperature.....	110
Figure 4. 29	Plot of Equation 4.16 at the initial period of mineralization.....	112
Figure 4. 30	Plot of $\ln k_3$ vs $1/T$	115
Figure 4. 31	The organic carbon profile during the degradation of MDEA using UV/H ₂ O ₂ , in the presence of NaHCO ₃ at initial pH = 7.	117
Figure 4. 32	The pH profile during the degradation of MDEA using UV/H ₂ O ₂ with the presence of NaHCO ₃ at initial pH = 7.	119

Figure 4. 33	The pH profile during the degradation of MDEA using UV/H ₂ O ₂ with the presence of NaHCO ₃ at initial pH = 9.76.	120
Figure 4. 34	The organic carbon profile during the degradation of MDEA using UV/H ₂ O ₂ with the presence of NaHCO ₃ at initial pH = 9.76. .	121
Figure 4. 35	Percentage TOC removal achieved at initial pH = 7, for different concentration of NaHCO ₃	122
Figure 4. 36	Percentage TOC removal achieved at initial pH = 9.76, for different concentration of NaHCO ₃	122
Figure 4. 37	Correlation between the experimental and fitted value (Equation 4.27) of TOC removal for refinery effluent.	125
Figure 4. 38	Pareto chart of the standardized effect for percentage TOC removal for screening of significant factors for degradation of actual effluent.	126
Figure 4. 39	Contour plots of TOC removal for refinery effluent.	127
Figure 4. 40	Comparison of experimental and predicted TOC removal for refinery effluent.	128
Figure 4. 41	The biodegradability evaluation of simulated MDEA solution.	129
Figure 4. 42	The biodegradability evaluation of actual refinery effluent.	130
Figure 4. 43	The TOC for photochemical degradation of MDEA by UV/H ₂ O ₂	131
Figure 4. 44	The TOC for the photocatalytic degradation of MDEA	131
Figure 4. 45	Comparison of energy consumption of MDEA degradation in the present work using UV/H ₂ O ₂ and using ZnO/SnO ₂ coupled photocatalysts.	134

LIST OF TABLES

Table 2. 1	Malaysian effluent standard regulation for sewage and industrial effluents, Environmental Quality Act 1974 [Laws of Malaysia; (act 127) 1999] [24].	12
Table 2. 2	Redox potential standards of some oxidant species [30].	17
Table 2. 3	Sample of chemical species oxidizable by hydroxyl radicals [30].	17
Table 2. 4	Literature review on Fenton processes, Fenton like processes and photo-Fenton processes for various types of pollutants.	21
Table 2. 5	Ozone-based oxidation processes for various contaminants.	27
Table 2. 6	Radiation type and pertaining energy levels [31].	31
Table 2. 7	The review of experimental conditions and results of the UV/H ₂ O ₂ process.	38
Table 2. 8	The photocatalytic degradation on various contaminants with various modifications.	44
Table 2. 9	Application of response surface methodology (RSM) in the advanced oxidation processes (AOP's) area.	49
Table 2. 10	The identified by-products formed during the degradation of organic compounds containing nitrogen using AOP's.	52
Table 2. 11	Condition/concentration of pollutants that requires pre-biological treatment [117].	54
Table 2. 12	Biodegradability enhancement by advanced oxidation processes (AOP).	55
Table 3. 1	Chemicals used in the present work.	58
Table 3. 2	The properties of PPMSB effluent.	60

Table 3. 3	The correlation constants for the calibration curves for MDEA and organic acids.....	69
Table 3. 4	The correlation constants for the calibration curves for nitrate (NO_3^-) and nitrite.....	70
Table 4. 1	The three levels chosen from the preliminary study.....	89
Table 4. 2	Box-Behnken matrix design.	89
Table 4. 3	Box-Behnken matrix design with experimental and fitted value.....	90
Table 4. 4	ANOVA analysis for TOC removal of synthetic MDEA waste.....	92
Table 4. 5	Optimum condition for the degradation of MDEA by using UV/ H_2O_2 at initial TOC = 1000 ppm; UV light intensity = 12.06 mW/cm ²	94
Table 4. 6	Estimated reduction rates at initial 30 minutes.....	104
Table 4. 7	Calculated values for k_{exp} and k_3	111
Table 4. 8	Literature values for hydroxyl radical rate constants for different compounds.	114
Table 4. 9	Activation energies of hydroxyl radical oxidation for different pollutants.....	115
Table 4. 10	Box-Behnken matrix design with observed and fitted value for refinery effluent.	124
Table 4. 11	ANOVA analysis for TOC removal of refinery effluent.	127
Table 4. 12	Optimum condition for the degradation of PPMSB effluent by using UV/ H_2O_2 at initial concentration of contaminant (TOC) = 1000 ppm;	128
Table 4. 13	Comparison of electrical energy efficiency of MDEA mineralization for different process.	133

NOMENCLATUR

Symbol	Description	Unit
ν	frequency	Herzt
h	Planck constant	J.s
c	speed of light	m.s ⁻¹
λ	wavelength	m
t	time	minute/second
TOC	total organic carbon	ppm
COD	chemical oxygen demand	ppm
% TOCremoval _t	percentage of TOC removal at t	ppm
TOC ₀	TOC value at $t = 0$	ppm
TOC _t	TOC value at t	ppm
BOD ₅	biological oxygen demand at 5 days	ppm
DO ₅	dissolved oxygen at 5 days	ppm
y	predicted response	-
β_0	intercept	-
β_i	linear effect	-
β_{ii}	squared effect	-
β_{ij}	interaction effect	-
ε	error term	-
k_{exp}	observed mineralization rate constant	M ⁻¹ s ⁻¹
k_3	rate constant of MDEA mineralization by hydroxyl radical	M ⁻¹ s ⁻¹
C	substrate	M
$\Phi_{H_2O_2}$	quantum yields of the photolysis H ₂ O ₂	mol.E ⁻¹
W_{abs,H_2O_2}	radiation rate absorbed by H ₂ O ₂	E.s ⁻¹
V	volume	L
A ₀	preexponential factor	-
E _a	activation energy	J.mol ⁻¹
R	ideal gas constant	J.K ⁻¹ .mol ⁻¹
T	temperature	°K
ϕ	energy efficiency	g kWh ⁻¹
Δ TOC	total organic carbon removed	ppm
P	electrical power consumed	kWh

CHAPTER 1

INTRODUCTION

1.1. Background of Research

Methyldiethanolamine (MDEA) is one of the common alkanolamines used in the petrochemical industries such as natural gas processing plant, refineries, and ammonia gas plant. MDEA in water solution is used as a solvent for the absorption of acidic gases such as CO₂ and H₂S, which are present in natural gas. Petrochemical industries discharge large amount of alkanolamine in wastewater during the cleaning, maintaining and scheduled inspection of the plant. The presence of this contaminant generates toxic and often non biodegradable substances into the aqueous phase, resulting in severe environmental pollution problem. The toxicity of this wastewater is due to its high content of nitrogen and dissolved organic compounds (i.e. chemical oxygen demand (COD) concentration is approximately 500000 ppm). Toxicity and non biodegradability of alkanolamine have been reported by Sandin *et al.* [1], Duran-Moreno *et al.* [2] and Fürhaker *et al.* [3], respectively.

In the recent two decades, advanced oxidation processes (AOP's) are underlined by significant number of investigations for their application in wastewater treatment, especially for the treatment of recalcitrant organic contaminant which are difficult to degrade using conventional biological oxidation unit. The AOP's can reduce the concentration and toxicity of contaminant to certain limits and could not achieve complete degradation of contaminant present in wastewater even though the modification of the experimental conditions has been reported. In addition, the widely used biological treatment in the removal process of organic and inorganic contaminant in the wastewater could not completely degrade the toxic contaminant

since the toxic contaminant often inhibited or even eliminated the bacteria populations in the conventional wastewater treatment plants. Therefore, a hybrid process i.e. AOP's prior to biological treatment is required to achieve a complete degradation of contaminant. In other words, the toxic wastewater should be pre-treated using AOP's before biological treatment.

In terms of refinery wastewater, the wastewater is commonly generated with high concentration of alkanolamine and often difficult to degrade using the conventional biological degradation. This issue is becoming an interesting research topic for the degradation study of wastewater containing alkanolamine. Therefore, during the recent decade many researchers started to look for developing alternative methods/techniques for refinery wastewater treatment. Ali *et al.* [4] used the ZnO/SnO₂ coupled photocatalysts in the presence of UV light (356 nm) to degrade MDEA in water solution. They successfully reduced the MDEA and total organic carbon (TOC) as much as 39.18% and 23.15% respectively using the photocatalysts for 5 hours of treatment and the initial concentration of MDEA was 1000 ppm. Even though this treatment could partially remove MDEA and TOC, however a better performance method with high efficiency for the complete degradation of refinery wastewater may still be required. One of the considerably demonstrated techniques from AOP's namely, Fenton's treatment has been well studied to degrade the organic contaminant that are commonly present in the refinery wastewater. Fenton's reagent, a mixture of ferrous sulfate and hydrogen peroxide [5] has been used to treat MEA [6], DEA [7], DIPA [8], and real Qilu refinery wastewater in China [9]. The Fenton's process was found to be more effective due to its rapid oxidation process, but the formation of sludge and their applicability at particular pH condition (i.e. acidic) pH, have created a necessity for an alternative technique for the treatment of refinery wastewater. Due to the limitation of photocatalysis (low performance for MDEA degradation) and Fenton's treatment (formation of sludge during the process and applicable only in the low pH), Arrif *et al.* in 2010 [10] used UV/H₂O₂ process to treat monoethanolamine (MEA) in water solution, and a successful degradation was reported. The UV/H₂O₂ has many advantages such as no formation of sludge during the process, high capability of hydroxyl radical production, and applicable for a wide range of pH.

Based on these advantages, in this present research the UV/H₂O₂ technique is proposed to treat MDEA in water solution. MDEA is commonly chosen as the scrubbing agent since this alkanolamine can be used for the absorption and stripping of hydrogen sulfide (H₂S) and carbon dioxide (CO₂) and also can be used to remove carbonyl sulfide (COS) [2]. Even though MDEA is widely used as the scrubbing agent during sweetening process of acidic gas from natural gas, the study pertaining to the degradation of MDEA present in effluents are highly limited.

1.2 Problem Statement

High concentration of alkanolamine in wastewater will be generated during maintaining and cleaning as well as scheduled inspection of absorption and desorption columns of natural gas sweetening plant. The wastewater produced is toxic to the environment and cannot be treated via the conventional wastewater treatment. One of the alternative techniques in advanced oxidation processes (AOP's), Fenton's treatment, has been studied to degrade the alkanolamine wastewater. However, the limitation of Fenton's treatment has inspired to look for an alternative technique which displays better performance and advantages such as no sludge formation during the treatment, applicable for a wide range of pH, and high capability of a hydroxyl radical (HO •) production, which has been identified as an important species in the AOP's. UV/H₂O₂ is one of the methods in the AOP's, which is expected to meet the required criteria, for better performance.

In this context, the present research has been undertaken to experimentally investigate the degradability of MDEA using UV/H₂O₂. Simulated waste and real effluent from Petronas Penapisan Melaka Sdn. Bhd. (PPMSB) were used in this study. Effects of different process parameters such as the initial concentration of the wastewater, the initial H₂O₂ dosage, pH, intensity of UV light, and temperature will be studied, as well as the intermediate products will also be investigated. Mathematical and statistical software will be used for the optimization of the process. In addition, for scale up and commercialization of the method, the kinetic constants of reaction need to be established. Since the UV/H₂O₂ process for degradation of MDEA

is an electric-energy-intensive process and the electric energy can represent major consumption cost, then the evaluation of electrical energy demand is also required.

In order to evaluate the advantage of the hybrid strategy of the combined AOP using UV/H₂O₂ and biological oxidation, a biodegradability test of the partially degraded wastewater as well as untreated wastewater will be investigated following the standard procedure and using locally available activated sludge.

1.3 Objectives

The objectives of the present work are detailed as follows:

1. To study the degradation characteristics of MDEA contaminated wastewater using UV/H₂O₂ advanced oxidation process and to identify the optimum conditions for the process, for both simulated solution and actual effluents from refinery.
2. To identify the formation of intermediate products during the degradation process and to establish the reaction mechanism, the rate equation, kinetic constants for the mineralization process.
3. To study the effect of bicarbonate on the degradation of MDEA using UV/H₂O₂.
4. To study the biodegradability of the partially degraded wastewater and to estimate the electrical energy efficiency of UV/H₂O₂ process for the degradation of MDEA.

1.4 Scope of the Present Research

In order to achieve the objectives of the present research, the simulated MDEA solution and real effluent solution containing MDEA will be used for this research. Simulated wastewater was prepared by dissolving MDEA in distilled water, while real wastewater was collected from Petronas Penapisan Melaka (PPMSB), Malaysia.

Experiments will be conducted to study the individual effect namely intensity of UV radiation, initial concentration of MDEA/H₂O₂, initial pH, and temperature on the UV/H₂O₂ oxidation process and based on these results, the effect of individual parameters and also along with their combination effect will be identified using response surface methodology (RSM) and the optimum conditions will be estimated.

The intermediate products formed, if any, during the mineralization of MDEA, will be identified for proposing the mineralization mechanism. Meanwhile, by using the TOC profile that will be established, the kinetic parameters and the rate constants for MDEA mineralization will be estimated.

Since the presence of bicarbonate in the UV/H₂O₂ oxidation system affects the rate and the efficiency of the process, an attempt will be made to study the effect of bicarbonate (at different concentration levels and different initial pH condition) on the UV/H₂O₂ process.

Biodegradability test will be conducted on the partially degraded MDEA solution, and in order to prove the efficiency of the present process, electrical energy demand of the UV/H₂O₂ process will be estimated.

1.5 Organization of Thesis

This thesis consists of five chapters:

- Chapter 1 provides an overview about the background of the research related to generation of wastewater from sweetening process of natural gas treatment plant, problem statement, objective, and scope of the present research.
- Chapter 2 describes a detailed literature review on various advance oxidation process, with an emphasis on UV/H₂O₂ process. It also presents a detailed merits and demerits of the available process for wastewater treatment.
- Chapter 3 elaborates the materials and the methodologies used for the degradation process, by-product identification, etc, involved in the process.

- Chapter 4 deals with the report on the results obtained in the present research along with a detailed discussion with a view to optimize the parameters involved in the process. The development of kinetic model, the estimating of reaction rate constants, and the by-product identification for the proposal of mechanism etc are discussed in detail.
- Chapter 5 gives a brief summary of the present research outcome along with the conclusion and recommendation for future research.

CHAPTER 2

LITERATURE REVIEW

2.1 Natural Gas Sweetening Process

Natural gas is one of the main energy sources in the world other than petroleum, coal, hydro-electricity, nuclear-electricity, geothermal, wind, solar, and biomass. It is one of the cleanest, safe, and most useful among all energy sources. The global consumption of natural gas grew by 7.4% in 2010, while the production of natural gas increased by 7.3% in 2010 as a cause of the increasing demand of this natural gas as reported in British Petroleum review [11]. Malaysia, one of the important natural gas producers in the world, produced around 2.3 trillion cubic feet of natural gas [12]. Methane (CH_4) is the main hydrocarbon molecule found in the raw natural gas. Acidic gases (i.e. carbon dioxide (CO_2) and hydrogen sulfide (H_2S)), mercaptans (e.g. methanethiol (CH_3SH) and ethanethiol ($\text{C}_2\text{H}_5\text{SH}$)), water vapor, nitrogen (N_2) and helium (He) are present in the raw natural gas as impurities [13 – 15]. High corrosiveness of acidic gas in the presence of water in the raw natural gas is well known for damaging the pipeline and the processing equipments, and also reduces the true heating value which has an effect on the price of natural gas. Hence the removal of acidic gases from raw natural gas is most important to meet the market requirement [13].

2.1.1 The Removal of Acidic Gas from Natural Gas

The common and most widely used gas purification processes can be classified into the following five categories [13, 16]:

1. Absorption using organic solvents.
2. Adsorption onto solid surfaces.
3. Application of membranes.
4. Chemical conversion to convert into another compound.
5. Cryogenic condensation.

Among the five common methods, the most important method for gas purification is the absorption using organic solvent. Alkanolamines such as monoethanolamine (MEA), diethanolamine (DEA), methyldiethanolamine (MDEA), and diisopropanolamine (DIPA) are the most commonly used solvents for the absorption of acidic gases such as CO₂ and H₂S [13]. The capability of alkanolamine to absorb acidic gas depends on the functional groups of alkanolamine (i.e hydroxyl group and amino group). The hydroxyl groups are capable of reducing the vapor pressure and increase the water solubility, whilst the amino group is capable to provide the alkalinity in water solution, that cause the acidic gas absorption.

Methyldiethanolamine (MDEA) is one of the common alkanolamine which is widely used in petrochemical industries. MDEA is used as an intermediate material in the synthesis of pharmaceutical products (e.g. analgesic and antispasmodic agent), personal care products (e.g. fabric softener and foaming agent on the shampoo), and the most importantly in gas processing plants [17]. The structural formula of MDEA is presented in Figure 2.1. MDEA has two ethanol functional groups and one methyl group. Those groups are attached to a nitrogen atom. Due to the existence of nitrogen atom with a pair of free electrons, MDEA forms weak base in aqueous solution, hence MDEA is often used for scrubbing/sweetening of acidic gases (CO₂ and H₂S) from raw natural gas. MDEA chemically binds with the acidic gases and when heated it releases the absorbed gases [13, 18].

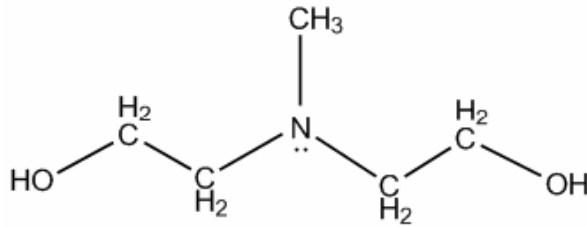


Figure 2. 1 Chemical Structure of MDEA

The acidic gas purification using MDEA solution occurs according to Reactions 2.1 – 2.6 [13, 19 – 20]:

Ionization of water:



Ionization of dissolved H_2S :



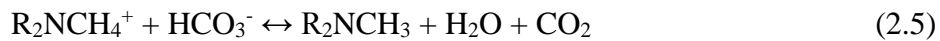
Hydrolysis and ionization of dissolved CO_2 :



Protonation of MDEA:



Acid-basic reaction with the amine:



The basic flow diagram for an acid gas absorption process is shown in Figure 2.2. The gas treating process includes an absorber unit and a regenerator unit. The typical operating range of temperature and pressure are 35 °C to 50 °C and 5 atm to 205 atm respectively in the absorber while in the regenerator at 115 °C to 126 °C and 1.5 atm to 1.7 atm, respectively.

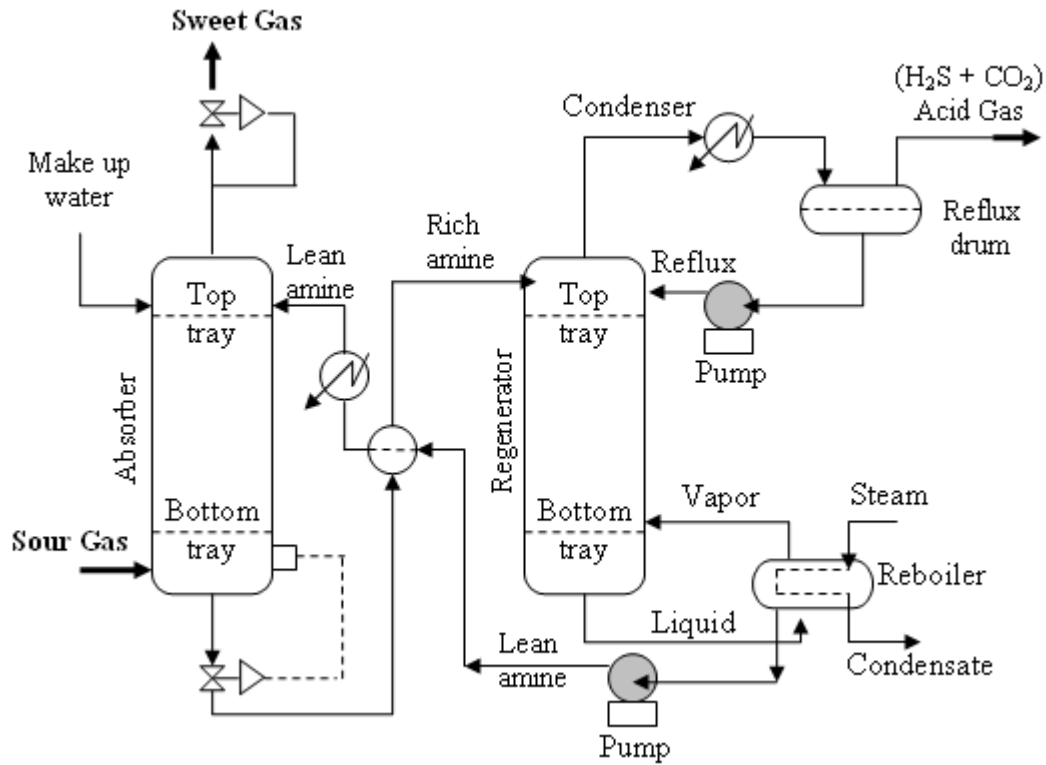


Figure 2. 2 Flow diagram of a typical amine treating process [13].

Acidic gases (such as CO_2 and H_2S) are absorbed in an absorber to produce a purified gas as the product and a rich amine solution (i.e. an amine solution + dissolved CO_2 and H_2S). The rich amine is then routed into the regeneration unit (a stripper with a reboiler) to produce a lean amine that is to be recycled. Further, the H_2S -rich stripped gas stream is then commonly routed into a Claus process to convert it into elemental sulfur, and the CO_2 generated during desorption can be used for enhanced oil recovery (EOR) [13].

2.1.2 Process Wastewater from Natural Gas Sweetening Operation

The turn around process is conducted in order to maintain the satisfactory performance of the process equipments. During the periodical maintenance and also during the regular operations a large amount of wastewater containing alkanolamine is commonly generated as wastewater/effluents.

The general sources of the wastewater containing alkanolamine during the gas operation process come from valve leakage, operational upset and also from the cleaning of reclaimer, absorber, and plant equipments i.e. heat exchanger, pumps, and vessel [21]. A heat-stable salt, degraded alkanolamine, and solid impurities may also be generated as effluents along with alkanolamine. During the gas purification process, those impurities are generated in the reclaimer and absorber of the gas processing unit. These effluents consist of amine as main pollutant and require appropriate treatment before disposal, since this amine solution is not readily biodegradable and toxic to the environment.

The effluent from natural gas processing unit consists of raw alkanolamine solution (MDEA), heat-stable salts, degraded alkanolamine, and insoluble particles, etc. Hence, a preliminary treatment is also required before further treatment, such as treatment using advanced oxidation process (AOP).

2.2 Wastewater Treatment

Wastewater is a combination of all undesired materials either dissolved or in suspended form in water which normally carries the wastes from residence, institution and industry, together with such ground water, surface water, and storm water [22 – 23]. Commonly, the accumulation of untreated wastewater produces unpleasant-smelling gases during the decomposition of organic material present in the wastewater. In addition, wastewater contains numerous pathogenic or disease-causing microorganisms. When the wastewater enters an aqueous ecosystem, it causes oxygen depletion and toxic to the aquatic life. The contaminated drinking water might cause methemoglobinemia. Thus, the immediate removal of wastewater from its generation sources followed by its treatment and disposal are necessary.

2.2.1 Wastewater Regulation

Development and implementation of wastewater treatment is the answer for the concern for public health and unpleasant condition caused by the discharge of wastewater to the environment [22 – 23]. Removal of suspended and floatable material, treatment of biodegradable organics and other contaminants, as well as elimination of pathogenic organism are the basic principle of the water treatment process. USEPA (Water Pollution Control Act of 1972) established the standards for wastewater discharge. Secondary treatment such as removal of suspended solid and biodegradable organics, as well as disinfectant of municipal wastewater must be treated to meet the acceptable levels before releasing into the environment. USEPA and most of other countries' regulation for water pollution insists the industries to use the best available technology to treat their wastewater before its disposal. The admissible maximum values of contaminants in the treated wastewater of different countries are regulated according to their own guidelines. The Malaysian standard for industrial effluents is presented in Table 2.1.

Table 2. 1 Malaysian effluent standard regulation for sewage and industrial effluents, Environmental Quality Act 1974 [Laws of Malaysia; (act 127) 1999] [24].

Parameters	Unit	Standard (A)	Standard (B)
Temperature	°C	40	40
pH value	-	6.0 – 9.0	5.5– 9.0
BOD ₅ at 20°C	mg/L	20	50
COD	mg/L	50	100
Suspended Solids	mg/L	50	100
Phenol	mg/L	0.001	1.0
Free chlorine	mg/L	1.0	2.0
Sulphide	mg/L	0.50	0.50
Ammoniacal Nitrogen	mg/L	10	20
Oil and grease	mg/L	1.0	10

Some more stringent standards have been developed recently to deal with the removal of nutrients and the priority pollutants. When the wastewater is to be reused, standards normally include the requirements for the removal of refractory organic, heavy metals, and in some cases dissolved solids [22]. Hence, in order to achieve the regulation standard, the effluents from the industries have to be treated appropriately before discharging into the environment.

2.2.2 Wastewater Characteristics

Based on the constituents present in wastewater, it can be characterized as physical, chemical and biological. The physical characteristics mainly include the presence of suspended solids in the effluent, degree of turbidity, temperature, color, and odor. Whilst, the chemical characteristics may include the organic compounds (e.g. carbohydrates, phenol, pesticides), dissolved gases (e.g. hydrogen sulfide, methane, oxygen), and inorganics (e.g. alkalinity, heavy metals, nitrogenous substances, pH), etc. [22 – 23]. Organic impurities are the most common and important constituent in domestic and industrial wastewater. Quality of wastewater is determined by the characteristic of wastewater and commonly the organic impurities consist of the mixture of carbonaceous material (not specific). Therefore, the investigation of organic content in the wastewater is not an easy test. The most commonly used tests are the total organic carbon (TOC), chemical oxygen demand (COD), and biochemical oxygen demand (BOD₅) [25]. The biological characteristics include the presence of bacteria, viruses, algae, protozoa, worms, coli forms, etc. Basically, bacteria are used in several wastewater treatment processes particularly for the degradation of biodegradable contaminant. However, the growth of the bacteria especially pathogenic ones (which transmit disease that may cause gastrointestinal symptom) must be controlled. During the aerobic biodegradation of biodegradable contaminant by bacteria, the oxygen is required. Algae are an important supplier for oxygen in the ponds during their photosynthesis. The schematic diagram of wastewater characterization is shown in Figure 2.3.

Natural gas sweetening process will generate high concentration of amine in wastewater and the concentration of amine may reach as high as 15 – 50 % by weight in practice [13]. Hence, the wastewater from the gas processing unit needs to be treated before discharging into the environment [26 – 27].

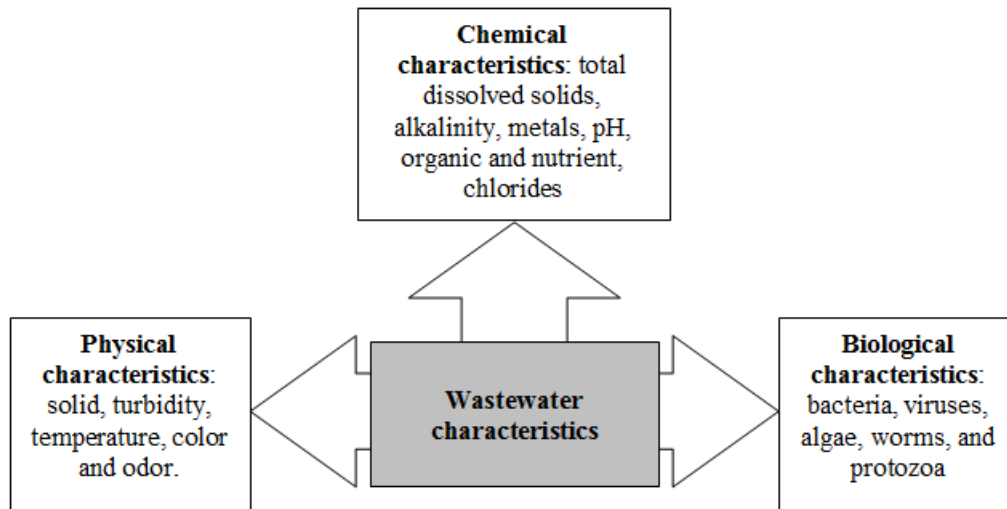


Figure 2. 3 Constituent of wastewater.

2.2.3 Wastewater Treatment Methods

Removal of contaminants in wastewater can be carried out by three methods i.e. physical, chemical, and biological. These methods are typically grouped as physical, chemical, and biological unit operations [22]. However in actual wastewater treatment plants (WWTP), several methods are used individually or in combination with each other. Physical unit operations are commonly used to remove the suspended material in the wastewater and this process is to be used in the preliminary treatment. These processes include: the screening, mixing, flocculation, sedimentation, floatation, filtration, and gas transfer (volatilization and gas stripping) [22]. Chemical unit processes are used for the removal of contaminants inside the wastewater by chemical reaction. In this process, chemicals are added into the wastewater to form more stable components or break down the contaminants into harmless components [22]. Biological unit processes are the removal of biodegradable contaminants present in the wastewater by involving biological activity. In this process, the biodegradable

organic contaminants are changed into gases that can escape into atmosphere or into the biological cell tissue, which can be removed by settling [22].

2.2.4 The Hybrid Process of Advanced Oxidation followed by Biological Treatment

Effluents/wastewater with high concentration of alkanolamine will be generated and leaving the natural gas processing unit and these effluents are often toxic to the bacteria and hence can not be degraded by biological oxidation. Advanced oxidation process is recently chosen by many researchers to treat recalcitrant organic contaminants in the effluent. Fenton's treatment, UV/H₂O₂ treatment, and UV/O₃ treatment are commonly used to degrade the recalcitrant organic contaminant into smaller fragments, which are biodegradable. In order to achieve a complete degradation of recalcitrant organic contaminant, by coupling of chemical oxidation (as pre-treatment) and biological oxidation (as post-treatment) is conceptually beneficial to increase the overall treatment efficiency [28 – 30], as illustrated in Figure 2.4.

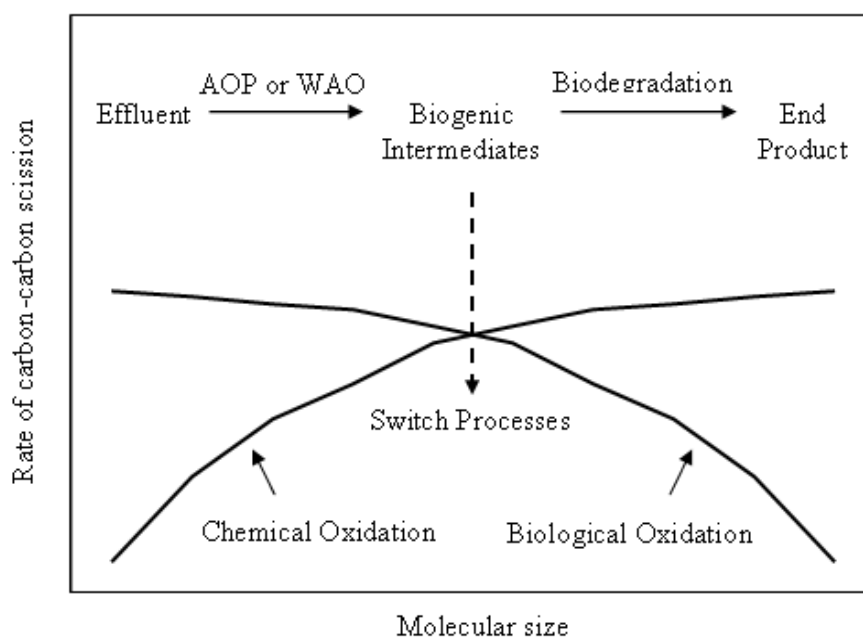


Figure 2. 4 The concept of coupling AOP-based pre-treatment with biological post-treatment [28].

2.3 Advanced Oxidation Processes

In wastewater treatment methods, AOP's are relatively a novel chemical process which involves the generation of hydroxyl radical. The hydroxyl radical is well known as a very reactive oxidant that is capable of degrading a wide range of organic contaminants. Generation of hydroxyl radical in the AOP's including UV irradiation [either direct irradiation of contaminant or photolytic oxidation mediated by hydrogen peroxide (UV/H₂O₂) and/or ozone (UV/O₃)], heterogeneous photo catalysis using semi conductor catalysts (UV/TiO₂), electron beam irradiation, X-ray, γ -ray radiolysis, non-thermal electrical discharge, and ultrasonic irradiation [29]. Generation of hydroxyl radical using different techniques is shown in Figure 2.5.

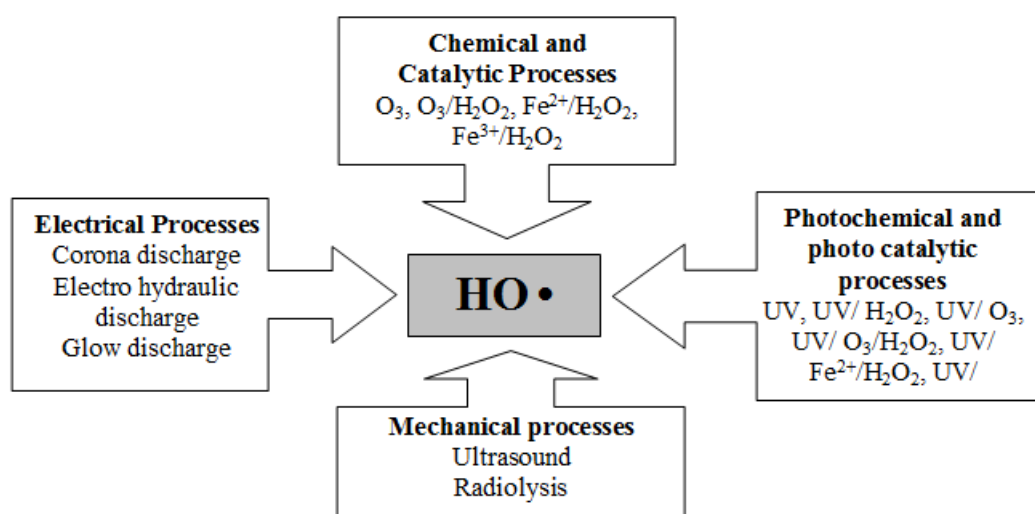


Figure 2. 5 Generation of hydroxyl radicals using different techniques [30].

The AOP's can be a chemical, catalytic, photochemical, photo catalytic, mechanical, and electrical process (Figure 2.5). The chemical and catalytic processes involve the application of ozone/or hydrogen peroxide. Moreover, the catalytic processes (Fenton type processes) involve the usage of some powerful catalyst (iron or copper ion) in combination with hydrogen peroxide to produce hydroxyl radical. UV and solar irradiation are commonly used in the photochemical and photo catalytic processes in combination with some powerful oxidants (ozone and/or hydrogen peroxide) or photo catalyst (e.g. TiO₂, ZnO, etc). Generation of hydroxyl radicals can also be caused by the influence of mechanical (e.g. ultrasound process, radiolysis) or

electrical energy (e.g. electro hydraulic discharge and non thermal plasma processes) [30]. Table 2.2 gives the list of some oxidant species. The redox potential of hydroxyl radical is in the second place after fluorine.

Table 2. 2 Redox potential standards of some oxidant species [30].

Oxidant	Redox Potential, E°, V
Fluorine	3.03
Hydroxyl radical	2.80
Atomic oxygen	2.42
Ozone	2.07
Hydrogen peroxide	1.77
Permanganate ion	1.67
Chlorine	1.36
Chlorine dioxide	1.27

AOP's are the promising chemical processes for the treatment of toxic organic pollutants in aqueous solution. Degradation of the toxic organic pollutants in the AOP's involve a highly reactive species i.e. hydroxyl radical. The hydroxyl radical is a non selective oxidant, hence capable to oxidize any organic contaminant. The reported chemical species that are oxidized by hydroxyl radical are listed in Table 2.3.

Table 2. 3 Sample of chemical species oxidizable by hydroxyl radicals [30].

Group	Details
Acids:	formic, gluconic, lactic, malic, propionic, tartaric.
Alcohols:	benzyl, <i>tert</i> -butyl, ethanol, ethylene glycol, glycerol, isopropanol, methanol, propenediol
Aldehydes:	acetaldehyde, benzaldehyde, formaldehyde, glyoxal, isobutyraldehyde, trichloraldehyde
Aromates:	benzene, chlorobenzene, chlorophenol, PCBs, phenol, catecol, benzoquinone, hydroquinone, <i>p</i> -nitrophenol, toluene, xylene, trinitrotoluene
Amines:	aniline, cyclic amines, diethylamine, dimethylformine, EDTA, propanediamine, <i>n</i> -propylamine
Dyes:	azo, anthraquinone, triphenylmethane
Ethers:	tetrahydrofuran
Ketones:	dihydroxyacetone, methylethylketone

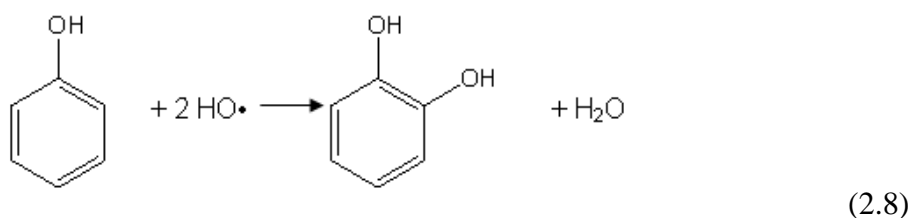
Simple organic acids such as acetic, maleic, and oxalic acid and also acetone, chloroform, and tetrachloroethane can not be readily oxidized by hydroxyl radicals [30].

2.3.1 The Reaction Mechanism of Hydroxyl Radical toward Organic Contaminant in Wastewater

The general reaction mechanism of hydroxyl radical toward organic contaminant in wastewater follows three pathways i.e. hydrogen abstraction, electrophilic addition, and electron transfer reaction [31 – 32]. Most commonly, the hydrogen abstraction is the first dominant step during the hydroxyl radical reactions toward the organic matter (Equation 2.7). The hydroxyl radical will take one hydrogen atom from the active site of organic matter to form one molecule of water (H₂O) [31].



The second pathway of hydroxyl radical reaction toward the organic contaminant is the electrophilic addition. In this step, the hydroxyl radical will attack the organic π -bond system (such as double bond system) to form an intermediate product [33]. Illustration of electrophilic addition by hydroxyl radical is shown below (Equation 2.8):



The third pathway is known as electron transfer reactions. This mechanism generally occurs when the hydroxyl radical react with a halogenated organic contaminant. The hydroxyl radical will be reduced to form OH⁻ [31] as shown below (Equation 2.9):



2.3.2 Fenton's Process

Over a hundred years ago (during 1894), the technology of Fenton's process was first introduced when M.J.H. Fenton reported the application of ferrous ion for the enhanced oxidation of tartaric acid with aqueous hydrogen peroxide. Further, oxidation based on ferrous-catalyzed by H₂O₂ at the acidic pH is known as Fenton's oxidation [29] and the reagent (i.e. combination between Ferrous ion (Fe²⁺) and hydrogen peroxide (H₂O₂)) is known as Fenton's reagent. After 40 years of the Fenton's process was found, hydroxyl radical was proposed by Haber and Weiss as the oxidant species in the Fenton's system. Hydroxyl radical plays an important role in the degradation of pollutants by Fenton oxidation and the capability of the treatment generally depends on the concentration of hydroxyl radical in the system. The generation of hydroxyl radical by Fenton's reagent as reported by Walling [5] is shown in Equation 2.10.



The application of Fenton's oxidation for the wastewater treatment is attractive, since the iron is a highly stable and non-toxic element [34], and hydrogen peroxide can be handled with ease and decompose into environmentally benign products. Also, the Fenton treatment will generate the hydroxyl radical, which can be used to degrade a wide range of pollutants into nontoxic or biodegradable products [30].

Effectiveness of Fenton's treatment to treat many recalcitrant organic pollutants has been reported by many researchers. Degradation of amoxicillin, (which is a common antibiotic that is widely used with high probability of releasing into the environment) was successfully carried out by Homem *et al.* [35]. From the initial amoxicillin concentration of 450 µg/L, after 30 minutes of reaction time, the concentration reduction was reported as 54%. Biodegradability of pharmaceutical wastewater and hospital wastewater were increased by Fenton's treatment as reported by Berto *et al.* [36], Jiang *et al.* [37], and Li *et al.* [38]. Badawy *et al.* [39] reported that even though the biodegradability of the pharmaceutical wastewater did not increase, but the contaminant level was reduced. Lodha and Chaudhari [40] successfully decolorized and reduced the COD levels until approximately 70% from wastewater containing Azo dyes within 30 minutes of reaction time. Boonrattanakij *et al.* [41] and Ramli [42] reported that the continuous addition of Fenton's reagent was more effective to reduce the level of contaminant in the wastewater and also they proposed that the reaction inhibition during the treatment could be reduced because of the controllable hydroxyl radical production. Fenton's treatment was also applied for the degradation of alkanolamines (monoethanolamine [43], diethanolamine [7], and diisopropanolamine [44]) that are commonly present in the refinery wastewater. Zhang and Yang [9] treated the refinery wastewater obtained from Shengli refinery of SINOPEC Qilu Petrochemical Company, China. The effect of inorganic ions on Fenton's catalytic degradation of phenol was studied by Mingyu *et al.* [45]. It was reported that ferric ion (Fe^{3+}) enhanced the Fenton's process but phosphate, chloride, copper ion, and carbonate suppressed the process, whereas sulfate radical, nitrate, and ammonium were found to have no effect on the oxidation process. Fenton process studies used for the degradation of various types of pollutants that were reported by different researchers are summarized in Table 2.4.

Table 2. 4 Literature review on Fenton processes, Fenton like processes and photo-Fenton processes for various types of pollutants.

Contaminant/ References	Experimental						Results
	Fenton's type	Reactor	Feeding reagent	pH	Conc.	Temp. (°C)	
Azo dyes Lodha & Chaudhari, 2007 [40]	Fenton's reagent,	Batch reactor Cap = 1 L	–	2.0 – 7.0	–	Room temp.	The reported optimum pH was 3 and the degradation was increased by increasing H ₂ O ₂ and Fe ²⁺ dose, up to the critical dose. Complete decolorization was achieved and approximately 70% of COD was removed at 30 minutes of reaction time.
Hospital wastewater after biological treatment Berto <i>et al.</i> , 2009 [36]	Fenton's reagent	Batch reactor Cap = 500 ml	–	3.8	–	Room temp.	Using Fenton's treatment, the COD decreased up to 90.6%.
Monoethanolamine (MEA) Harimurti, 2009 [43]	Fenton's reagent	Batch jacketed glass reactor Cap = 1 L	–	2.0 - 5.0	[MEA] = 0.013 - 0.213 M [H ₂ O ₂] = 0.708 - 2.123 M [Fe ²⁺] = 0.014 - 0.058 M	Room temp.	Optimum condition for degradation of [MEA] ₀ = 0.213 M was pH = 3, [H ₂ O ₂] = 2.123 M and [Fe ²⁺] = 0.029 M. The maximum COD reduction was ± 55%. This treatment has also increased the biodegradability.
2,6-dimethyl-aniline Boonrattanakij <i>et al.</i> , 2009 [41]	Fenton's reagent	Batch reactor Cap = 0.5 L	–	3.0±0.05	–	25±0.2	Degradation rate of contaminant was better in the continuous system. Malic, lactic, oxalic and formic acid were identified as degradation products.

Refinery wastewater from Shengli refinery of SINOPEC Qilu Petrochemical Company Zhang and Yang, 2009 [9]	Fenton's reagent	Batch reactor (round-bottom flask) Cap = 500 ml	–	±3.0	$n[\text{Fe}^{2+}] : n[\text{H}_2\text{O}_2] = 1:3 - 1:20$	30-50	The max. COD removal was achieved at $\text{pH} = 2.5 - 3$, $n[\text{Fe}^{2+}] : n[\text{H}_2\text{O}_2] = 1:5$ after 2 hours of reaction time. The treatment was found to be effective as pre-treatment before biological oxidation.
Biologically treated coking plant effluent Jiang <i>et al.</i> , 2009 [37].	Fenton's reagent	Rotated drum bottle as reactor Cap = 40 ml	–	3.0 – 10.0	$[\text{H}_2\text{O}_2] = 5 - 40 \text{ mg/L}$ $[\text{Fe}^{2+}] = 10 - 70 \text{ mg/L}$	–	> 50% COD was removed at optimum condition i.e. $\text{pH} = 6$, $[\text{H}_2\text{O}_2] = 27.2 \text{ mg/L}$, $[\text{Fe}^{2+}] = 56 \text{ mg/L}$. The treated effluents were more biodegradable compared to the un treated effluents.
Pharmaceutical wastewater from El-Nasr Pharmaceutical and Chemical Company, South-East of Cairo Badawy <i>et al.</i> , 2009 [39]	Fenton's process	–	–	3.0±0.2	$[\text{COD}]_0 = 4100 - 13,023 \text{ mg/L}$	Room temp.	The application of Fenton treatment improved the removal efficiency However, it did not improve the biodegradability.
Amoxicillin Homem <i>et al.</i> , 2010 [35]	Fenton's reagent	Batch with thermostatic reactor Cap = 250 ml	–	2.9 - 6.5	$[\text{H}_2\text{O}_2] = 0 - 4.50 \text{ mg/L}$ $[\text{Fe}^{2+}] = 0 - 240 \text{ } \mu\text{g/L}$	22-57	The optimum condition was $\text{pH} = 3.5$, $[\text{H}_2\text{O}_2] = 3.50 \text{ mg/L}$, $[\text{Fe}^{2+}] = 95 \text{ } \mu\text{g/L}$. 54% of amoxicillin was degraded after 30 min of reaction time from the initial concentration of $450 \text{ } \mu\text{g/L}$.
Diethanolamiene (DEA) Dutta <i>et al.</i> , 2010 [7]	Fenton's reagent	Batch jacketed glass reactor Cap = 1 L	–	1.0 – 4.0	$[\text{DEA}] = 800 - 16000 \text{ ppm}$ $[\text{H}_2\text{O}_2 \text{ 30\%}] = 53.33 - 233.33 \text{ ml}$ $[\text{FeSO}_4, 7\text{H}_2\text{O}] = 4 - 16 \text{ gram}$	Room temp.	Optimum condition for the oxidation of $[\text{DEA}]_0 = 16000 \text{ ppm}$ was $[\text{H}_2\text{O}_2 \text{ (30\%)}] = 175 \text{ ml}$, $[\text{FeSO}_4, 7\text{H}_2\text{O}] = 8 \text{ gram}$, $\text{pH} = 2$. Biodegradability of treated DEA was better compared to the un-treated DEA.

Natural gas plant wastewater contains Diisopropanolamine (DIPA) Ramli, 2010 [42]	Fenton's reagent	Jacketed glass reactor Cap = 1 L	Continuous	2.0 – 5.0	[waste] \approx 17000 mg/L COD [H ₂ O ₂]/[Fe ²⁺] = 5 – 30	Room temp.	As much as 73% of COD was removed at the optimum condition, i.e. [H ₂ O ₂]/[Fe ²⁺] = 10, pH = 3 at room temperature.
Phenol Mingyu <i>et al.</i> , 2011 [45]	Fenton's reagent	Cone bottle reactor Cap = 250 ml	–	3.0	[phenol] = 0.61 mmol/L	25	The presence of ferric ion (Fe ³⁺) enhanced the Fenton's oxidation whereas phosphate, chloride, copper ion and carbonate were found to suppress the oxidation process.
Diisopropanolamine (DIPA) Khamaruddin <i>et al.</i> , 2011 [44]	Fenton's Reagent	Jaketed glass reactor Cap = 2 L	–	2.0 – 4.0	[DIPA] ₀ = 3000 ppm n[H ₂ O ₂]/n[Fe ²⁺] = 95	30-60	It was reported that the highest degradation was obtained at 60 °C and at pH = 2.5.
Acrylic fiber manufacturing wastewater Li <i>et al.</i> , 2012 [38]	Fenton's reagent	Batch reactor	–	1.0 – 7.0	[waste] = 4528 mg/L [H ₂ O ₂] = 100 – 800 mg/L [Fe ²⁺] = 100 – 800 mg/L	25	The optimum oxidation condition for degradation of 4528 mg/L COD was [H ₂ O ₂] = 500 mg/L, [Fe ²⁺] = 300 mg/L, pH = 3 with COD removal = 65.5% for 2 hours of reaction time and the biodegradability (BOD ₅ /COD) increased from 0.1 to 0.226.

2.3.3 Ozone-based Processes

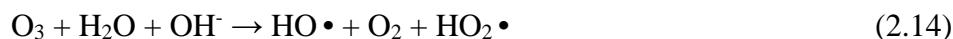
Naturally, ozone (O_3) is present in the atmospheric layer around the earth, and it is formed by the recombination of atomic radical oxygen and diatomic oxygen. The atomic radical oxygen ($O\bullet$) is commonly generated by the photolysis of diatomic oxygen (O_2) and further reacts with the diatomic oxygen (O_2) to form ozone (O_3) [30 – 32]. The reaction of ozone formation can be expressed in Equation 2.11 – 2.12.



Ozone has a redox potential of 2.07 V, therefore ozone is very reactive either in the liquid or in gas. Reaction of ozone with organic contaminant can be considered either on direct or indirect reaction. Equation (2.13) show the direct mechanism which involves organic compound degradation by molecular ozone and occurs in acidic pH range.



Hydroxyl radical is generated from the reaction of ozone and hydroxyl ions present in water (indirect ozone mechanism) at basic pH conditions (Equation 2.14). Further, the hydroxyl radical reacts with an organic compound present in water.



Based on the Equation (2.13) and (2.14), indirect mechanism of ozonization can also be classified as AOP's. Meanwhile, direct mechanism of ozonization can be classified as classical chemical treatment method. Combination of O_3/H_2O_2 has been widely investigated. By this combination, the hydroxyl radical is generated, and this

combination is well known as peroxone or perozonation [30, 46 – 47]. Overall mechanism of reaction can be expressed in Equation 2.15.



The O₃/UV process and O₃/H₂O₂ process have been studied by Andreozzi *et al.* [48] for the degradation of the mineral oil-contaminated wastewater, and they concluded that O₃/UV process was more effective to reduce the COD values compared to the O₃/H₂O₂ process. Within 30 minutes of reaction time, around 80 – 90 % of COD removal was achieved. The UV/O₃ process was also used for acetone removal [49] and improvement of drinking water quality in France [50]. Degradation of acetone using UV/O₃ was the most effective compared to the other processes i.e. H₂O₂/O₃ and UV/H₂O₂. Almost complete degradation was achieved by this process within a short duration (< 30 minutes) of oxidation time. This process was used for disinfection, oxidation of micro-pollutant, and minimization of bromate concentration in the drinking water for the improvement of the quality. Application of UV in drinking water production was also capable of reducing the ozone consumption. Ma and Graham [51] reported an enhancement in the degradation of atrazine by ozone, which was catalyzed by small amount of manganese (Mn²⁺). This enhancement was due to the oxidation of Mn²⁺ to Mn⁴⁺, that enhanced the generation of hydroxyl radical (HO •), which has a very high oxidation potential toward atrazine. Safarzadeh-Amiri [52] used the O₃/H₂O₂ process to degrade methyl-*ter*-butyl ether (MTBE) and proved that the operating cost of O₃/H₂O₂ process was less compared to the UV/H₂O₂ process for reducing the same amount of MTBE and resulted in the same amount of removal efficiency. Biodegradability of carbaryl (a pesticide) was enhanced using photocatalytic ozonization in the presence of TiO₂ as reported by Rajeswari and Kanmani [53]. It was also reported that the ratio of BOD₅/COD increased up to 0.38. Other than the report on the enhancement of biodegradability, they also reported a reduction of COD and TOC up to 92% and 76.5%, respectively, at the experimental concentration of carbaryl, ozon, and TiO₂ are 40 mg/L, 0.28 g/h, and 1 g/L, respectively at pH = 6. In addition, Katsoyiannis *et al.* [54] reported that the energy requirements between O₃/H₂O₂ and UV/H₂O₂ for transformation of micropollutants

(i.e. atrazine (ATR), sulfamethoxazole (SMX), and N-nitrodimethylamine (NDMA)) were quite similar, even though the NDMA transformation was more effective using direct photolysis. Park *et al.* [55] used the combination of microwave/UV and ozone to degrade bromothymol blue in water solution, and reported a complete degradation of bromothymol blue within 10 minutes of reaction time. During ozone based process, phosphate and carbonate were found to be the scavenger of the degradation reaction for sulfamethoxazole using UV/TiO₂/O₃ [56]. The available literature on the ozone based oxidation process for different pollutants are summarized in Table 2.5.

2.3.4 High Voltage Electrical Discharge Processes

High voltage electrical discharge (frequency of 60Hz) process is a process when a strong electrical field induced chemical and physical processes and commonly known as corona discharge. Application of electrical discharge (short high voltage pulse (200 – 100 ns)) in liquid phase and at non-thermal condition results in the formation of various active species such as HO•, H•, •O, HO₂⁻, O₂⁻•, H₂O₂, etc (Equation 2.16 – 2.18).



This process is very effective for treatment of biological microorganism and dissolved chemicals in liquid phase [30, 33]. The radical species present in the system usually react with each other and produce H₂O₂, H₂ or H₂O (Equations 2.19 – 2.21).

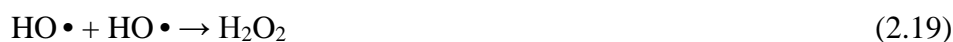


Table 2. 5 Ozone-based oxidation processes for various contaminants.

Contaminat/ References	Experimental					Results
	Reactor	Lamp	Conc.	pH	Temp.	
Mineral oil-contaminated wastewater Andreozzi <i>et al.</i> , 2000 [48]	Semi-connector reactor Cap = 0.2 – 1 L	17 W LP UV $\lambda = 254$ nm	–	4.9 (buffer KH_2PO_4)	25°C	O_3/UV was proved to be more effective to reduce the COD value compared to the $\text{O}_3/\text{H}_2\text{O}_2$. Approximately 80 – 90 % COD was removed within 30 minutes of reaction time.
Atrazine Ma and Graham, 2000 [51]	Reactor & gas bubble-connecting column Cap = 3.651 L	–	Mn^{2+} sol. = 24.8 ml/min	7.0	–	The presence of small amount of Mn^{2+} (0.3 – 1.2 mg/L) greatly enhanced the degradation of atrazine.
Methyl-ter-butyl ether (MTBE) Safarzadeh-Amiri, 2001 [52]	Bubble column as reactor with circulation of mixture 2 L/min Cap = 6 L	–	$[\text{MTBE}]_0 = 80$ mg/L $[\text{O}_3] = 150$ mg/L $[\text{H}_2\text{O}_2] = 50$ mg/L	–	–	The $\text{O}_3/\text{H}_2\text{O}_2$ provides an economical and efficient process for the reduction of MTBE-contaminated water. Nearly complete reduction of MTBE (80 to 0.05 mg/L) was achieved by using 150 mg/L ozone and 50 mg/L H_2O_2 .
Acetone Hernandez <i>et al.</i> , 2002 [49]	Glass borosilicate reactor Cap = 1 L	LPUV & MPUV	Ozone inlet = 35 /weight [acetone] = 5 ppm	7.0 (borate buffer)	20 °C	LPUV/ O_3 was reported as more effective for acetone degradation among UV/ O_3 , $\text{H}_2\text{O}_2/\text{O}_3$, and UV/ H_2O_2 . Acetone removal was > 99% within 30min of reaction time. Increasing O_3 concentration increased the degradation rate.

Pretreated drinking water from Paris area (France) Meunier <i>et al.</i> , 2006 [50]	Brown glass screwed with dispenser fitted for ozone injection Cap = 500 ml	UV at $\lambda = 254$ nm.	–	8.0	$6 \pm 1^\circ\text{C}$ & $25 \pm 1^\circ\text{C}$	Introducing UV in the system reduced the ozone dose and the combination of UV/O ₃ improved the water quality with regard to disinfection, oxidation of micro-pollutant and minimization of bromate concentration.
Carbaryl (Carbamat pesticide) Rajeswari and Kanmani, 2009 [53]	Cylinder photoreactor Cap = 500 ml	125 W MP UV lamp	[carbaryl] ₀ = 40 g/L O ₃ input = 0.28 g/h [TiO ₂] = 5 g	–	$19 \pm 1^\circ\text{C}$	By this process, 92% COD and 76.5% TOC were removed and the ratio of BOD ₅ /COD increased to 0.38.
Sulfamethoxazole (SMT) Beltrán <i>et al.</i> , 2009 [56]	Tubular borosilicate glass Cap = 1 L	HP Hg lamp	[O ₃] = 10-30 mg/L	–	–	The degradation of sulfamethoxazole was caused by direct ozonolysis, direct photolysis, and HO•. Phosphate and carbonate was found to be the scavengers.
Bromothymol Blue (BTB) Park <i>et al.</i> , 2010 [55]	Quartz reactor with Microwave = 2.45 Hz max power 1 kW circulation = 300 cc/min. Cap = 1L	UV-C	O ₃ = 0.75 – 3.26 g/h [BTB] ₀ = 3.0×10^{-5} M	–	–	Decomposition rate of BTB increased significantly with increasing of catalyst dosage, microwave intensity when applied together with ozone. Complete degradation was achieved when 3.26 g/h of O ₃ was injected in the UV/MW/TiO ₂ system.
Micropollutants i.e.: Atrazine,(ATR), sulfamethoxazole (SMX) and N-nitrosodimethylamine (NDMA) Katsoyiannis <i>et al.</i> , 2011 [54]	Batch reactor Cap = 500 ml	15 W LP Hg lamp	[pollutant] ₀ = 0.5 – 1 μM [O ₃] ₀ = 1.5 mM [H ₂ O ₂] ₀ / [O ₃] ₀ = 1:2	8.0	20 °C	Transformation rate of micropollutants increased with the use of O ₃ /H ₂ O ₂ . Energy requirement for O ₃ /H ₂ O ₂ and UV/H ₂ O ₂ is quite similar for the NDMA transformation.

Based on the reactions according to Equations 2.16 – 2.21, the degradation of organic contaminant in the system follow three mechanisms i.e. direct reaction with hydroxyl radical, indirect reaction of radicals formed from stable molecules (H₂O₂), and direct reaction with stable molecule [57].

2.3.5 Others AOP's

There are many other types of promising AOP's are introduced recently. Those are ultrasonic irradiation, radiolysis of water, and electrochemical processes. These processes also involve the radical species to degrade the organic pollutant in the system, which are generated by ultrasonic wave, radio wave, and direct electron transfer, and the details are discussed below:

2.3.5.1 Ultrasonic Irradiation

The frequency of ultrasonic wave that is used in this process ranges from 20 – 40 kHz. Irradiation of ultrasonic wave into the water generate a highly reactive hydroxyl radical (HO•) and H• (Equation 2.22).



During the degradation of organic pollutant, the reactive radicals react with the organic contaminant in the system through oxidation or reduction [33, 57].

2.3.5.2 Water Radiolysis

In water radiolysis process, the high energy ionizing radiation (KeV to MeV) is used. Exposure of this high energy into a dilute aqueous solution results in the excitation

and ionization of water, which further produce reactive radicals, and degrade the organic contaminants present in water [33, 57].

2.3.5.3 Electrochemical Processes

Electrochemical processes are a kind of oxidation-reduction reaction in which one atom or molecule loses an electron to another atom or molecule. During the degradation of organic pollutant, the reaction occurs by the electron transfer reaction of oxidation-reduction or by chemical reaction. General electrolysis of organic matter by electron transfer is shown in Equation 2.23 [33].



2.3.6 AOP's based on Ultraviolet Light

UV light was firstly investigated by Isaac Newton during the early 19th century and he observed the diffraction of white beam when passing through a prism. Infrared and ultraviolet was discovered beyond two ends of spectra of visible light. The light irradiation is later characterized as irradiation with visible (VIS), infrared (IR) or ultraviolet (UV). These three have same characteristics of electromagnetic irradiation, but differed in respect of its frequency. Correlation between electromagnetic energy and frequency (Equation 2.24) is known as Plank relation or Plank-Einstein equation:

$$E = h\nu = \frac{hc}{\lambda} \quad (2.24)$$

where E is the electromagnetic energy, h is the Plank constant (6.6261×10^{-34} J.s), ν is the frequency (s^{-1}), c is the speed of light (3×10^8 m.s⁻¹), and λ is the wavelength (m).

Higher electromagnetic energy will occur at short wavelengths [32]. The radiation type and pertaining energy at specific wavelength are presented in Table 2.6, while the range of electromagnetic wave is presented in Figure 2.6.

Table 2. 6 Radiation type and pertaining energy levels [31].

Radiation	Wavelength (nm)	Energy range (kJ Einstein ⁻¹)
IC	>780	<155
VIS	780 – 400	155 – 300
UV-A	400 – 315	300 – 377
UV-B	315 – 280	377 – 425
UV-C	280 – 100	425 – 1198

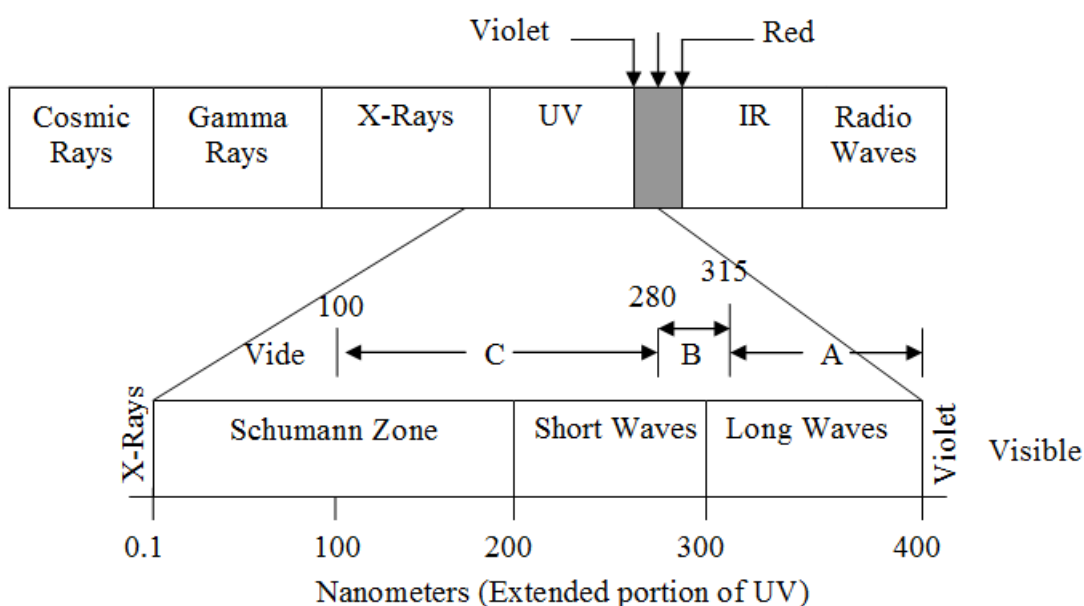


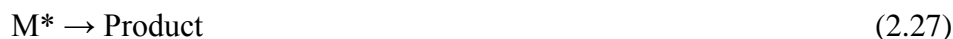
Figure 2. 6 Range of electromagnetic waves [31].

During the earlier days, the UV radiation was used for disinfection. Further, the UV irradiation is used for the enhancement of the rate of reaction and also used for the oxidation process. UV-C (Table 2.4) with wavelength at 254 nm is commonly used in the oxidation process. This UV can be produced by low-pressure mercury vapor lamp which was invented by Hewith in 1901 [31 – 33].

All processes involving UV light for the degradation of organic contaminant or for initiation of oxidation mechanism by irradiation of some powerful oxidant or photocatalyst are considered as UV-based processes. These UV-based processes can be grouped into three categories i.e. UV photolysis, photochemical processes, and photocatalytic processes.

2.3.6.1 UV Photolysis

Most of the molecules have lowest-energy electronic state at room temperature. This condition is called as “ground state”. During the exposure of UV irradiation, the molecules are excited to a higher energy level and called as “excited state”. Lifetime of excited molecules is very short ($10^{-9} - 10^{-8}$ s). Further, the molecule returns to the ground state or decompose to produce different molecules. Direct photolysis of molecules by UV irradiation is expressed in Equation 2.25 – 2.27 [31 – 32, 58].



In order to achieve an efficient process for the degradation of organic contaminant, commonly UV light is combined with some powerful oxidant or photocatalyst. However, the efficiency depends on the following requirements such as [30]:

- a. The solution treated should be clear (the turbidity should be as low as possible) for better UV transmission.
- b. Scavenger reaction of mineralization process of organic pollutant by the presence of excess amount of hydroxyl radical in the system.
- c. Free from heavy metals, oil and grease, etc.

2.3.6.2 Photochemical Processes

Photochemical process normally employ the combination of UV light and some auxiliary/supplementary oxidants such as hydrogen peroxide (H_2O_2), Ozone (O_3), Oxygen (O_2), and water (H_2O). General scheme of UV based oxidation reactions in the presence of auxiliary oxidants in the idealized condition are shown in Figure 2.7.

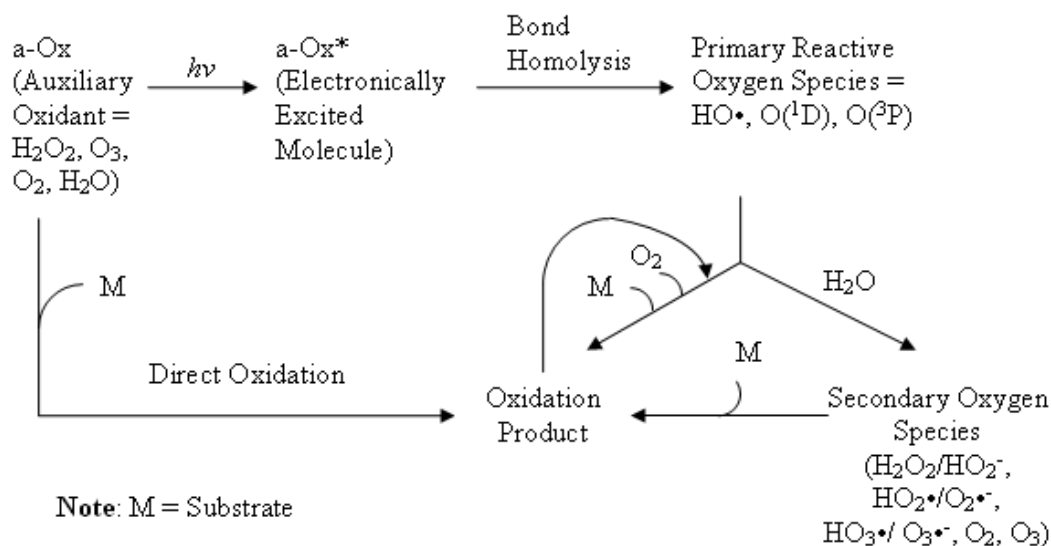


Figure 2. 7 The general scheme of UV based oxidation reactions in the presence of auxiliary oxidant [32].

UV induces the auxiliary oxidant to form electronically excited molecule (a-Ox^*). Subsequently, hemolytic/splitting bond leads the primary reactive oxygen species, which are mostly hydroxyl radical ($\text{HO}\cdot$) or oxygen atoms in the ground state ($\text{O}({}^3\text{P})$) and oxygen atoms in the excited state ($\text{O}({}^1\text{D})$). These primary reactive oxygen species are very reactive and hence immediately react with the substrate M to form the oxidation product. Furthermore, the concentration of primary reactive oxygen species in the medium is very low. In the water or air, the primary reactive oxygen species are possibly transformed by radical to form secondary oxygen species through an electron transfer or an acid/base reaction. These secondary oxygen species are well known to oxidize the substrate M with lower reactivity compared to the primary reactive oxygen species. Carbonate (CO_3^{2-}) and bicarbonate (HCO_3^-) are also able to be transformed by radical to form carbonate radical ($\text{CO}_3^-\cdot$) and bicarbonate radical

(HCO₃ •), respectively, which are able to react with the selective substrate M. These carbonate radical and bicarbonate radical are well known as tertiary selective radical. In the advanced oxidation processes, reactions of secondary oxygen species and tertiary selective radical toward the substrate M are known as scavenger reactions. Other than the primary reactive oxygen species, secondary reactive oxygen species and tertiary selective radical, in fact, the auxiliary oxidant was also found to react with certain substrate M to form oxidation product through direct oxidation, depending on their reduction potential [32].

In UV/H₂O₂ process, high quantity of energy is required to generate the hydroxyl radical from H₂O₂ photolysis. Two hydroxyl radicals are theoretically generated per absorbed energy quantum. In practice, the highest energy quantum required for generation of hydroxyl radical is 0.5 mol of H₂O₂ per Einstein [29, 31 – 33, 57 – 62]. The generation of hydroxyl radical by UV radiation can be expressed as Equation 2.28.



while the scavenger mechanism of H₂O₂ and hydroxyl radical which influences the overall process efficiency can be explained in Equation 2.29 – 2.32 [32, 57 – 58, 60].



UV lamp characteristics, reactor configurations, pH of solution, and initial concentration of H₂O₂ are the important parameters that can affect the performance of the UV/H₂O₂ process, whilst the presence of suspended particle and the presence of iron and potassium salt are the major limitation for the application of UV/H₂O₂ process. Suspended particles must be removed and the iron and potassium salt can be

precipitated by pH adjustment and then filtered before the UV/H₂O₂ process. The UV/H₂O₂ process is commonly used for the following [24]:

- a. Elimination of the micro- and macro- pollutants from drinking water.
- b. Removal of low concentration or organic toxic compounds present in ground water.
- c. Detoxification and faster degradation of smaller volume of recalcitrant organic contaminant, and
- d. Monitoring exhaust gases in the case of volatile organic compound.

During the recent years, several interesting studies related to UV/H₂O₂ process for degrading organic contaminant in water solution have been reported. A detailed review of the literature on UV/H₂O₂ process for the degradation of organic contaminant is listed in Table 2.7. Many kinds of contaminants have been successfully degraded using this process with different types of reactor configurations. UV light at 254 nm is well known to initiate the production of hydroxyl radical through H₂O₂ photolysis, which plays an important role in the degradation process. Low Pressure Mercury lamp (germicidal lamp) is most commonly used as the UV source since this lamp is the most effective technology in generating UV light at a wavelength of 253.7 nm (or commonly known at 254 nm wavelength) [31 – 32].

The degradation of contaminants using UV/H₂O₂ process is mostly done by hydroxyl radical, which is generated through H₂O₂ photolysis. Lopes *et al.* [63] reported that ineffective degradation of 4-chloro-3,5-dinitrobenzoic acid was found in the absence of H₂O₂ and the degradation was improved when H₂O₂ was introduced in the process. This result agreed with many other results reported on UV/H₂O₂ treatment for the contaminants such as herbicide 2,4-D, phenol, carbendazim, azo dyes (Maroon), reactive azo dye (Reactive Orange dye), formaline, amoxicillin, trichloroethene, methyl *ter*-butyl ether (MTBE), and natural organic compounds (NOM) in groundwater. However, opposite trend was observed for the degradation of pharmaceutical compounds using UV/H₂O₂ [64]. At low pH conditions, the degradation was found to be more effective in the absence of H₂O₂.

Other than the decomposition of organic contaminant, the UV/H₂O₂ process can also remove the toxicity of the compounds. As reported by Jung *et al.* [65], antibacterial activity of amoxicillin was completely removed by UV/H₂O₂ process, due to the decomposition of active sites of the parent compound.

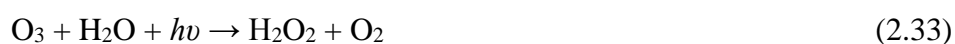
In addition, organic acids are commonly found to be the product of UV/H₂O₂ process. This phenomenon was reported by Li *et al.* [66], who studied the degradation of trichloroethene using UV/H₂O₂. Trichloroethene was converted into formic, oxalic, dichloroacetic, and monochloroacetic acid at the end of UV/H₂O₂ process. Stefan and Bolton [67] also reported a similar result. During the oxidation of 1,4-dioxane, they identified some organic acids such as formic, methoxyacetic, acetic, glycolic, glyoxylic, oxalic, and some aldehydes such as formaldehyde, acetaldehyde, and glyoxal. Further degradation of organic acid lead to the formation of CO₂ as reported by Leitner and Dore in 1996 [68], who studied the decomposition of aliphatic acid by UV/H₂O₂.

The presence of carbonate (CO₃²⁻) during the UV/H₂O₂ process results in the formation of carbonate radical (CO₃^{-•}), which is commonly known as an inhibitor in the advanced oxidation process since this radical has lower reactivity compared to the hydroxyl radical (HO•). Inhibition of carbonate radical in the UV/H₂O₂ process was reported by Mazellier *et al.* [69] and Muruganandhan and Swaminathan [70], who studied the degradation of carbendazim and reactive orange dye, respectively.

Another parameter that affects the UV/H₂O₂ degradation process is the initial pH of the solution, since the mechanism/pathway of degradation reaction by hydroxyl radical is different for individual contaminants. Muruganandhan and Swaminathan (2004) [70] reported that the decolorization of reactive orange dye using UV/H₂O₂ was effective at pH = 3. Opposite result was reported by Riga *et al.* [71] for the decolorization of procion H-exl dye, where decolorization was effective when the pH of the system was greater than 12. In addition, degradation of herbicide (2,4-D) using UV/H₂O₂ was more effective at acidic as well as alkaline conditions compared to that at neutral condition as reported by Chu in 2001 [72]. Ariff [73] reported that UV dose was found to be the most significant parameter that influences the monoethanolamine (MEA) degradation using UV/H₂O₂ process. An increase of UV dose increases the degradation rate of MEA.

Meanwhile other parameters such as initial pH, initial concentration of contaminant, and initial concentration of oxidant (H₂O₂) showed little effect on the degradation. Körbathi and Rauf [74] also reported a degradation of basic red 2 dye (BR2) using UV/H₂O₂ process. The degradation of basic red 2 dye (BR2) was highly dependent on the concentration of dye as well as concentration of H₂O₂. Salari *et al.* [75] studied the degradation of methyl-tert-butyl-ether (MTBE) using combination of UV light and H₂O₂ and reported that the MTBE degradation was dependent of H₂O₂ concentration. Other than for the degradation of recalcitrant organic contaminant, the UV/H₂O₂ was also used for the deactivation of microbe and virus. It was reported by Mamae *et al.* [76] in 2007 that the combination of UV and hydrogen peroxide gave very small effect compared to the degradation with UV alone. The efficiency of UV/H₂O₂ was reportedly depending on the nature of the microorganism.

Another oxidant such as ozone is also commonly used in the photochemical process. Ozone is even better oxidant compared to hydrogen peroxide, since this oxidant has higher molar absorption coefficient at 254 nm (typically the wavelength for UV-C radiation). Photolysis rate of ozone to generate the hydroxyl radical is almost 1000 times higher than hydrogen peroxide [30]. Generation of hydroxyl radical during the UV/O₃ process follows the Equation 2.33. Irradiation of UV light toward ozone in water generates one hydrogen peroxide, which further produce two hydroxyl radicals.



The hydroxyl radical will then react with organic matter present in the water. The degradation mechanism of organic pollutant using UV/O₃ in water follows the order: direct photolysis, hydroxyl radical attack (generated from different sources), and direct ozone attack. Combination of two binary systems i.e. UV/H₂O₂ and UV/O₃ is represented as UV/H₂O₂/O₃. The combination between any two systems is normally conducted to achieve the complete mineralization of organic contaminant that present in water [30 – 32, 57 – 58, 62].

Table 2. 7 The review of experimental conditions and results of the UV/H₂O₂ process.

Contaminant/ References	Experimental					Results
	Reactor	Lamp	Conc.	pH	Temp.	
Aliphatic acid Leitner and Dore, 1996 [68]	Batch reactor Cap = 4 L	LP Hg lamp $\lambda = 253.7$ nm	[TOC] ₀ < 0.1 mg/L	2.9 - 3.5	Room temp.	The O ₂ consumption was accompanied by HO ₂ •/O ₂ • generation followed by recombination into H ₂ O ₂ . CO ₂ was the end product of oxidation.
1,4-Dioxane Stefan and Bolton, 1998 [67]	Semi batch reactor Cap = 6 L	1 kW Hg UV- VIS lamp $\lambda = 200 - 400$ nm.	–	–	–	The reported degradation products are aldehydes (formaldehyde, acetaldehyde and glyoxal) and organic acid (formic, methoxyacetic, acetic, glycolic, glyoxylic and oxalic)
4-chloro-3,5-dinitrobenzoic acid Lopes <i>et al.</i> , 2000 [63]	Annular reactor Cap = 1L & 0.350 L	125 W MP Hg	–	–	25±1°C	Photolysis was ineffective but complete degradation was reported when HO• was introduced.
Isoprene Elkanzi <i>et al.</i> , 2000 [77]	Batch reactor Cap = 250 ml	LP UV $\lambda = 254$ nm	$\frac{[H_2O_2]}{[S]} = 6$ S = isoprene	6.8	24°C	H ₂ O ₂ acted as pseudo catalyst in the process. Complete removal of isoprene was achieved in 120 min of radiation time.
Herbicide 2,4-D Chu, 2001 [72]	Photoreactor Cap = 5 ml	LP Hg $\lambda = 254$ nm	$\frac{[H_2O_2]}{[S]} = 12.5$ S = 2,4-D	Acidic & alkaline	–	Direct photolysis was reported as extremely slow. Acidic condition and alkaline condition gave better removal compared in the neutral pH condition.
Phenol Esplugas <i>et al.</i> , 2002 [78]	Annular reactor Cap = 1.5 L	MP Hg $\lambda = 240$ nm.	–	–	–	Degradation rate of phenol with UV/H ₂ O ₂ process was five times higher compared to UV alone.
Carbendazim Mazellier <i>et al.</i> , 2003 [69]	Batch reactor Cap = 2 L	LP Hg $\lambda = 254$ nm	–	–	–	60% of disappearance caused by HO• and 40% of disappearance caused by CO ₃ • ⁻

Azo dyes (Maroon) Malik and Sanyal, 2004 [79]	Cylindrical reactor Cap = 20 ml	125 W MP Hg	–	–	30°C	The decolorization involved direct photolysis and H ₂ O ₂ catalyzed oxidation. Complete decolorization was end at 12 min of reaction time.
Reactive Azo dye (Reactive Orange dye) Muruganandhan and Swaminathan, 2004 [70]	Multilamp reactor Cap = 50 ml	8 MP Hg (8W) λ = 365 nm	–	3.0	–	The degradation was dependent on pH. The best pH was 3. Na ₂ CO ₃ and NaOH strongly inhibited the photooxidation.
Methyl-ter-butyl ether (MTBE) Salari <i>et al.</i> , 2005 [75]	Batch photoreactor Cap = 500 ml	30 W mercury lamp (UV-C)	–	–	–	HO• has major role in the degradation.
4-nitrophenol (4-NP) Daneshvar <i>et al.</i> , 2006 [80]	Batch reactor Cap = 0.5 L	15 W LP Hg λ = 254 nm	–	–	–	The light intensity, concentration of H ₂ O ₂ , and concentration of 4-NP are the factors affecting the removal efficiency.
Formline Kajitvichyanukul <i>et al.</i> , 2006 [81]	Batch reactor Cap = 1.1 L	10 W germicidal lamp λ = 254 nm	[H ₂ O ₂] = 0.666 M	–	25°C	UV photolysis = 1.5 – 2 % degradation and UV/H ₂ O ₂ = 80% degradation for 80 min of reaction.
E. coli, B. subtilis spores and MS2, T4, and T7 phage Mamane <i>et al.</i> , 2007 [76]	Batch reactor Cap = 100 ml	MP Hp λ = 295 – 400 nm.	–	–	–	The disinfection of the microbe was mostly caused by UV lamp. The presence of HO• gave small effect compared to UV irradiation only.
Procion H-exl dyes Riga <i>et al.</i> , 2007 [71]	Batch reactor Cap = 300 ml	9 W UVC λ = 254 nm	–	> 12.0	20±1°C.	Decolorization was highly dependent on the pH and dye photolysis proceeds was fast when pH >12.
Trichloroethene Li <i>et al.</i> , 2007 [66]	Stainless steel reactor Cap = 28 L	1 kW UV λ = 200 – 300 nm	–	–	–	HO• has major role in the degradation. End products were reported as many kinds of organic acids.

Methyl tert-butyl ether and tertiary butyl alcohol Li <i>et al.</i> , 2008 [82]	Batch reactor	LPUV & MPUV	–	–	–	Energy consumption by using LPUV was lower compared to the MPUV. Pretreatment using NaIX was shown to be the most cost effective.
Natural organic matter (NOM) (Alachlor) Song <i>et al.</i> , 2008 [83]	Batch reactor Cap = 6 L	8 W & 16 W LP Hg $\lambda = 254$ nm	–	–	–	The natural organic matter (NOM) decomposition was due to the direct photolysis and HO• attack.
Basic Red 2 dye (BR2) Körbathi and Rauf, 2008 [74]	Batch reactor Cap = 100 ml,	UVGL-58, J-129 $\lambda = 254$ nm	[BR2]= 20 μ M [H ₂ O ₂]=1.67 mM	7.6	25±2°C	The degradation was highly dependent to the dye concentration and H ₂ O ₂ concentration.
Monoethanolamine Ariff, 2010 [73]	Batch reactor Cap = 0.3 L & 1.1 L	LP Hg $\lambda = 254$ nm	–	–	–	UV dose was reported as the main controlling factor on monoethanolamine degradation.
Pharmaceutical compounds in mix solution Giri <i>et al.</i> , 2011 [64]	Batch reactor Cap = 1.2 L	10 W LP Hg $\lambda = 254$ nm,	–	alkaline	25±2 °C	More than 96% of pharmaceutical compounds were removed by UV photolysis alone and addition of H ₂ O ₂ was not helpful at low pH.
Nitrogenous organic compounds Chen <i>et al.</i> , 2011 [84]	Two reactors Cap = 650 ml & 3 L	14 W LP Hg & 450 W MPUV Hg $\lambda = 254$ nm	–	–	Room temp.	MPUV/H ₂ O ₂ treatment was more effective compared to the LPUV/H ₂ O ₂ . Ammonium was released.
Amoxicillin Jung <i>et al.</i> , 2012 [65]	Batch reactor Cap = 500 ml	LP Hg Arc-UV $\lambda = 254$ nm	–	–	20±2 °C	Degradation of Amoxicillin was caused by direct photolysis and UV/H ₂ O ₂ process. Antibacterial activity was also removed during the process.

2.3.6.3 Photocatalytic Process

Photocatalytic process is another type of oxidation process, which involves UV light as the light source for the irradiation of some powerful photocatalysts such as TiO₂, ZnO, etc. This process also involves a highly reactive species i.e. hydroxyl radical. The generation of the hydroxyl radical in this process follows a mechanism described in Equation 2.34 – 2.36 [32 – 33, 57 – 60, 62, 85].



Irradiation of photon from UV light toward the semiconductor TiO₂ leads to the generation of electron-hole pair since the photons have high transfer energy. The holes in valence band (h_{vb}^+) are very strong oxidants and the electrons in conductance band (e_{cb}^-) are reductants. Reaction between valence band (h_{vb}^+) with water or hydroxyl ion leads to the formation of hydroxyl radical:



While conductance band (e_{cb}^-) reacts with dissolved oxygen to generate hydroperoxyl radical ($\text{HO}_2\cdot$) as shown in Equation 2.37 – 2.38.



Furthermore, the two $\text{HO}_2\cdot$ can recombine to yield hydrogen peroxide (H_2O_2) and oxygen (O_2). Afterwards, the reaction of H_2O_2 with the conductance band will generate the hydroxyl radical (Equation 2.39).



Addition of H_2O_2 at the optimum concentration enhances the efficiency of TiO_2 photocatalysis, whereas the presence of excess H_2O_2 reduces the efficiency. Beside TiO_2 , ZnO , CdS , and SnO_2 are also used on the alternative photocatalysts. These photocatalysts comprised of microcrystalline or microcrystalline particles, which are used in the form of thin layer or as powder dispersion.

Photocatalytic process has been studied by a number of researchers to degrade various contaminants either in the gas phase or in solution. In 2005, Chang *et al.* [86] studied the degradation of gaseous $\text{N,N}'$ -dimethylformamide (DMF) using UV/thin film TiO_2 in a annular pyrex glass reactor at 140°C . Degradation of DMF was reported to be dependent on the initial concentration of DMF, temperature, water vapor, and oxygen content. The reported intermediate products found in this process were NH_4^+ and NO_3^- and these intermediates were also reported to cause deactivation of catalyst. Similar deactivation of catalyst caused by intermediate products NH_4^+ and NO_3^- was also reported by Low *et al.* [87] and Alberici *et al.* [88] when they studied the degradation of organic compounds containing nitrogen atom using TiO_2/UV . The presence of NH_4^+ and NO_3^- were also reported during the degradation of short-chain alkyl- and alkanolamines using TiO_2/UV and $\text{Pt}/\text{TiO}_2/\text{UV}$ by Klare *et al.* [89]. Other than NH_4^+ and NO_3^- , they found NO_2^- as well. It was also reported that the degradation of short-chain alkyl- and alkanolamine was highly dependent on pH. The reported optimum pH for short-chain alkyl- and alkanolamine degradation by hydroxyl radical reported was 10. Higher pH provides more active sites compared to the low pH levels. Hence high pH was more preferable to achieve maximum degradation. TiO_2/UV process has also been reported to enhance the biodegradability of azo dyes and textile plant effluent as reported by Chun and Yizhong [90]. They analyzed the decolorization and biodegradability of yellow KD-3G, reactive red 15, reactive red 24, cationic blue X-GRL), and wastewater from wool processing unit in China. Enhancement of TiO_2/UV performance by the addition of H_2O_2 has also been reported for the degradation of phenolic compounds by Barakat *et al.* [91] and Dixit *et al.* [92].

The efficiency of phenolic degradation was accelerated/enhanced by using the combination of $\text{TiO}_2/\text{H}_2\text{O}_2/\text{UV}$. Nitrification of phenol was identified when nitrate ion was present in the treatment of phenol photocatalysis [93]. Other than the addition of H_2O_2 , for the enhancement of TiO_2/UV performance, experiments were conducted by the addition of O_3 or air in the system, which was later used to degrade the oxalate ions present in aqueous solutions [94]. Maximum degradation of oxalate ion was achieved at $\text{pH} = 10$ and no intermediate product was observed. Behnajady *et al.* [95] used UV/TiO_2 along with oxygenation (bubbling O_2) to study the rate of degradation of four dyes with different structures ((C.I. Acid Red 27 (AR27), Methyl Orange (MO), Malachite Green (MG)) and 4-Nitrophenol (4-NP)), and reported that the photocatalysis rate constants followed the order: $\text{MG} > \text{AR27} > \text{MO} > 4\text{-NP}$. Méndes-Arriaga *et al.* [96] studied the degradation of ibuprofen (IBP) using the combination of solar/ $\text{H}_2\text{O}_2/\text{TiO}_2$. The solar energy was used as light source and as a result, the process was found to be cheaper since the solar light is abundant in nature. Ali *et al.* [4], for his experiments replaced TiO_2 with ZnO/SnO to degrade MDEA, which results in the MDEA removal of 30.18% and 23.38% for synthetic MDEA solution and refinery plant wastewater respectively. Anipsitakis and Dionysious [97] also made attempts to modify the photocatalysis process by using iron, cobalt, and silver instead of TiO_2 to degrade 2,4-dichlorophenol (2,4-DCP) in the presence of three different oxidants i.e. H_2O_2 , KHSO_5 , and $\text{K}_2\text{S}_2\text{O}_8$. The order of efficiency for $\text{UV}/\text{Metal}/\text{Oxidant}$ processes tested was: $\text{UV}/\text{Fe}^{3+}/\text{H}_2\text{O}_2 > \text{UV}/\text{Fe}^{2+}/\text{H}_2\text{O}_2 > \text{UV}/\text{Co}^{2+}/\text{KHSO}_5 > \text{UV}/\text{Ag}^+/\text{K}_2\text{S}_2\text{O}_8$. This was due to the higher photosensitivity of Fe^{3+} in water compared to the other metals (Co^{2+} and Ag^+). A detailed review and comparison of the available literatures on the photocatalytic degradation for various contaminants are compiled in Table 2.8.

Table 2. 8 The photocatalytic degradation on various contaminants with various modifications.

Contaminant/ References	Experimental						Results
	Catalyst	Lamp	Reactor	Conc.	pH	Temp	
Organic compounds containing nitrogen atoms Low <i>et al.</i> , 1991 [87]	TiO ₂	20 W lacklight blue fluorescent tube	Borosilicate glass spiral wound Cap = 40 ml	–	–	–	Using TiO ₂ /UV process, the organic compounds containing nitrogen atoms were degraded to form NH ₄ ⁺ and NO ₃ ⁻ .
Azo dyes and wool textile effluents. Chun and Yizhong, 1999 [90]	TiO ₂	500 W MP Hg	Cylindrical glass body Cap = 500 ml	[dye] _o = 100 ppm, [catalyst] = 1 g/L for dye and 5 g/L for effluent [Air] = 240 ml/min	–	–	> 90% decolorization was achieved within 20 – 30 min, the (BOD ₅ /COD) of pollutants was enhanced from 0 to 0.75.
Nitrogen-containing organic compounds Alberici <i>et al.</i> , 2000 [88]	TiO ₂	30 W UV lamp λ = 365 nm	Glass cylinder Cap = 850 ml	–	–	Room temp.	Intermediate products such as NH ₄ ⁺ and NO ₃ ⁻ were found and trapped at the TiO ₂ surface and they were considered as responsible for the deactivation of TiO ₂ .
Short-chain alkyl- and alakanolamines Klare <i>et al.</i> , 2000 [89]	TiO ₂ & Pt doped in TiO ₂	1100 W Xenonlamp	Round bottom three-neck vessel. Cap = 50 ml	–	–	–	The optimum pH was achieved at pH = 10. As much as 80% nitrogen was converted to form NH ₃ /NH ₄ ⁺ , NO ₃ ⁻ and NO ₂ ⁻ .
Mixture of phenol and nitrate Vione <i>et al.</i> , 2001 [93]	TiO ₂	40 W UV lamp λ = 360 nm	Cylindrical pyrex glass cell Cap = 5 ml	–	–	–	Phenol nitration was found, and the nitration rate was slow in the presence of TiO ₂ .

(2,4-DCP) Anipsitakis and Dionysious, 2004 [97]	Fe ²⁺ or Fe ³⁺ or Co ²⁺ or Ag ⁺	15 W germicidal lamp $\lambda = 253.7$ nm	Stirred rectangular batch reactor Cap = 2 L	[2,4-DCP] ₀ = 20 ppm, [catalyst] = 1-50 ppm.	3.0	Room temp	The order of efficiency was: UV/Fe ³⁺ /H ₂ O ₂ > UV/Fe ²⁺ /H ₂ O ₂ > UV/Co ²⁺ /KHSO ₅ > UV/Ag ⁺ /K ₂ S ₂ O ₈ .
Phenolic compounds Barakat <i>et al.</i> , 2005 [91]	TiO ₂	1600 W MP Hg lamp $\lambda = 365$ nm	Pyrex glass tube Cap = 5 ml	[cont.] ₀ = 10 ⁻³ M [TiO ₂] = 0.15 g/L	–	25°C.	The degradation efficiency increased by 40% after applying the UV and H ₂ O ₂ .
Gaseous N,N'- dimethylformamide (DMF) Chang <i>et al.</i> , 2005 [86]	TiO ₂	10 W black light lamp $\lambda = 365$ nm	Pyrex annular Cap = 110 cm ³	–	–	140°C	The degradation rate was reported to be dependent on DMF concentration, temperature, water vapor, and oxygen content. Inorganic ion such as NH ₄ ⁺ and NO ₃ ⁻ were reported to be the cause for the deactivation of catalyst.
Oxalate ion Addamo <i>et al.</i> , 2005 [94]	TiO ₂	700 W MP Hg $\lambda = 365$ nm	Batch reactor Cap = 2.5 L	[Oxalate] ₀ = 0.22 - 2mM, [TiO ₂] = 0.24 g/L, [air] = 1.3 x 10 ⁻³ M, [O ₃] = 1 – 20 mmol/h,	10.0	–	Mineralization was found at pH = 10 and no intermediate product was reported. Combination of photocatalyst and O ₃ greatly enhanced the degradation.
Ibuprofen (IBP) Méndes- Arriaga <i>et al.</i> , 2009 [96]	TiO ₂	solar irradiation	PC-1.5, CPC-6 & CPC-35.	–	–	–	Solar/H ₂ O ₂ /TiO ₂ was found to be useful for the degradation. The biodegradability was enhanced after treatment
N-methyl-diethanolamine (MDEA) Ali <i>et al.</i> , 2010 [4]	ZnO/ SnO ₂	100 V 12 W UV lamp $\lambda = 365$ nm	Beaker Cap = 250 ml	[MDEA] ₀ = 1000 ppm, [catalyst] = 1.5 g/L	–	–	MDEA degradation by ZnO/SnO ₂ (2:1) photodegradation gave a degradation of 30.18% and 23.38% for synthetic and petroleum wastewater, respectively.

Phenol and Chlorophenol Dixit <i>et al.</i> , 2010 [92]	TiO ₂	MP UV lamp 125 W	250 ml	[cont.] ₀ = 2 – 5 mg/L	4.0	–	Optimum condition for degradation were pH = 4, [H ₂ O ₂] = 200 – 550 ml/L, [TiO ₂] = 1 – 2 g/L in UV/H ₂ O ₂ /TiO ₂ system.
Dyes (C.I. Acid Red 27 (AR27), Methyl Orange (MO), Malachite Green (MG)) and 4-Nitrophenol (4-NP) Behnajady <i>et al.</i> , 2011 [95]	TiO ₂ ,	15 W Hg lamp λ = 254 nm	Batch quartz Cap = 100 ml	O ₂ = 0.5 ml/min, [TiO ₂] = 4g/L, [MG] ₀ = 5 mg/L, [AR27] ₀ = 20 mg/L, [MO] ₀ = 10 mg/L, [4-NP] ₀ = 20 mg/L	–	Room temp.	The photocatalysis rate constants followed this order: MG > AR27 > MO > 4-NP.

2.4 Response Surface Methodology of Statistical Design of Experiment

Design of experiment (DOE) is a systematic approach for the investigation of a system or process. The aim of DOE is to enable the collection of maximum information from a series of structured experiments using the minimum amount of time and data. In the experimental research using conventional approach method, the investigation of the effect of each factor is conducted by varying the factor while maintaining all other factors as constant. The disadvantage of experimental research by applying the conventional method is the total number of experiments to complete the test factor-level combinations will be very large. For example, if there are 4 factors and each factor containing 5 levels, the total experiments will be 5^4 that equals to 625 experiments. By applying DOE, the disadvantage of conventional method will be solved.

There are four engineering problems that may be solved by DOE i.e. comparative, screening characterization, modeling, and optimizing. In terms of comparative, DOE is able to assess the change in a single factor that in fact results in a change to the process as a whole. As a tool for screening characterization, DOE is applicable for the determination of the important and unimportant factors that affect the system or process. Meanwhile in terms of modeling, using DOE a good-fitting mathematical function and estimation of coefficients can be derived. In terms of optimizing, DOE enables to determine the optimum value of each factor that gives maximum or minimum response towards the objective of the research [98].

Later, Frank Yates and Oscar Kempthorne extended the fractional factorial design to reduce the number of experiments [99]. In 1951, Box and Wilson introduced the response surface methodology (RSM) [100]. The motivation of conducting this method was to run experiments efficiently, to select a proper design of experiments, and to determine the optimum operating conditions using a set of controllable variables that give rise to an optimal response. RSM was developed using linear polynomial models, mainly first-order and second-order models [100].

Using RSM, the dependency of effect on treatment can be directly represented as a response curve or as response surface, and this curve or surface can be used to make decision not only about treatment structure but also about the relationship between treatment and response. Knowledge of this relationship is important to find the treatment combination which gives the optimal (highest or lowest) response. The exact relationship is never known but the approximation can be determined [101].

RSM has been widely used for the optimization of AOP's for the degradation of various contaminants. The reported literature on the application of RSM for the optimization of AOP experiments for the treatment of several pollutants are summarized in Table 2.9.

2.5 Degradation Intermediate

Advanced oxidation process for the degradation of organic contaminants is ideally designed to completely mineralize the organic contaminant of concern to inorganic products such as carbon dioxide (CO_2) and water (H_2O), involving a highly reactive species i.e. hydroxyl radical. Since the reactivity of hydroxyl radical is very high, the reaction between hydroxyl radical toward an organic contaminant occurs rapidly. Nevertheless, this reaction by itself does not directly results in mineralization but produces organic oxidation by-products, which can further reacts with hydroxyl radical. Accumulation of by-product during advanced oxidation process might occur when the reaction rate of hydroxyl radical toward the by-product is slow. Thus, this step can limit the rate of the complete mineralization of organic contaminant. Some simple organic compounds such as acetic, maleic, and oxalic acid, as well as acetone, chloroform, and tetrachloroethane can not be readily oxidized using hydroxyl radical [30]. However, they degrade slowly. The process may be enhanced considerably by selecting conducive process conditions.

Table 2. 9 Application of response surface methodology (RSM) in the advanced oxidation processes (AOP's) area.

Contaminant/ References	AOP type	Experimental			
		Factors	Response	Experimental design	Tool
Olive oil processing wastewater (OMW) Ahmadi <i>et al.</i> , 2005 [102]	Fenton peroxidation	H ₂ O ₂ and Fe ²⁺ ratio, pH and OMW concentration	Total phenolics, color removal and aromatic removal	Central Composite design 2 ³ full factorial	Design Expert version 5
Chemical laboratory wastewater Benatti <i>et al.</i> , 2006 [103]	Fenton oxidation	[COD] and [H ₂ O ₂] ratio, [H ₂ O ₂] and [Fe ²⁺] ratio and pH	COD removal	2 ³ factorial with 6 center runs	Werkema and Aguiar (1996) online
Basic Red 2 (BR2) dye Körbahti and Rauf, 2008 [74]	UV/H ₂ O ₂	BR2 concentration, H ₂ O ₂ concentration and pH	% BR2 degradation and % decolorization	D-optimal design, with 3 replicates	Design Expert 6.0
Terasil Red R dye Lim <i>et al.</i> , 2009 [108]	Fenton-like (H ₂ O ₂ /pyridine/Cu(II) system)	Screening process: pH, H ₂ O ₂ concentration, Pyridine concentration and Cu (II) concentration	COD reduction	2 ⁴ full factorial in triplicate, 3 blocks and 2 center point each	Minitab 14 (PA, USA)
		Optimization process: concentration of H ₂ O ₂ , pyridine and Cu(II)	COD reduction	2 ³ full factorial plus 4 center points, 3 replicates	Minitab 14 (PA, USA)
Azo dye (C.I. Basic Red 46 (BR46)) Khataee <i>et al.</i> , 2010 [109]	Oxalate photoelectron-Fenton process using carbon nanotube-PTFE cathode	initial concentration of dye, Fe ³⁺ , oxalate and electrolysis time	Decolorization efficiency (%)	Central Composite Design (CCD) with total 31 experiments and 7 replication at the center point	Minitab 15 software

Leachate Li <i>et al.</i> , 2010 [105]	Fenton treatment	HRT (hydraulic retention time), Nitrogen concentration, C/N ratio	COD and total nitrogen (TN) reduction	(i) 8 runs of 3 level factorial design, (ii) 6 runs at the so called star points and (iii) 1 center point with 5 replicate each	Design Expert version 7.1.3, Stat-Ease
Amoxicillin Homem <i>et al.</i> , 2010 [35]	Fenton oxidation	Concentration of H ₂ O ₂ , concentration of Fe ²⁺ and temperature	C/Co ratio (C= concentration of amoxicillin at t and Co= concentration of amoxicillin at t=0)	Central Composite Design (CCD) with total 16 experiments: 8 factorial design, 6 expansions and 2 center points	JMP 5.01 software
Acid Red 27 (AR 27) dye mix with Methyl Red (MR) dye Naseri and Ayadi-Anzabi, 2011 [106]	Fenton treatment	Concentration of MT, AR 27, H ₂ O ₂ and Fe ²⁺	Decolorization efficiency (%)	24 factorial points, 8 axial points (star points) and 5 replications at center point	MINITAB® (Minitab Inc.) Realease 14.0
Phenol Hasan <i>et al.</i> , 2011 [104]	Fenton's peroxidation	Phenol concentration, H ₂ O ₂ and Phenol ratio, H ₂ O ₂ and Fe ²⁺ ratio, reaction time	% TOC Removal	Central Composite Design (CCD) with 2 level factorial plus additional experimental star point at 3 repetitions	OVAT
Oxitetraacycline-HCl (OTC) Rahmah <i>et al.</i> , 2012 [107]	UV/H ₂ O ₂	Ratio [OTC] to [H ₂ O ₂], pH, and Temperature	%TOC removal	Box-Behnken	Statgraphics Centurion 15.2.11.0.

Oxidation of an organic compound containing nitrogen by hydroxyl radical may proceed through the abstraction of hydrogen atoms and electrophilic addition leading to the formation of carboxylic acids which is further degraded to smaller fragments and eventually to CO_2 , NH_4^+ , NO_2^- , NO_3^- , N_2 , and H_2O when enough hydroxyl radicals are generated in the reaction medium [89]. Organic acid and inorganic compound containing nitrogen such as nitrite (NO_2^-), nitrate (NO_3^-) and ammonia (NH_3)/ammonium (NH_4^+) were found during the degradation of organic contaminant containing nitrogen using advanced oxidation processes [43, 63, 73, 80, 87 – 88, 110 – 112]. Glycine and ammonium was identified during the degradation of monoethanolamine and diethanolamine by using Fenton's reagent [43]. Alberici *et al.* reported that ethylacetamide, acetaldehyde, pyrazine, acetic acid, carbon dioxide, ammonium (NH_4^+) and nitrate (NO_3^-) were found as the by-products during the degradation of diethylamine using $\text{TiO}_2/\text{UV-VIS}$ [88]. Identified by-products obtained from the mineralization process for different organic compounds containing nitrogen using AOP's are listed in Table 2.10.

2.6 Biodegradability of Pollutants

The term biodegradable means that the compound can be broken down and absorbed in a natural environment or susceptible to being broken down by microorganisms into simple compounds such as water and carbon dioxide [113]. Therefore, 'biodegradable' substances or products mean that the compounds are capable of being degraded by microorganism. In the wastewater treatment area, biological treatment is one of the common methods used for the removal of substances in the wastewater, involving the bacterial activity. Only wastewaters containing biodegradable substances can be treated in this method.

Table 2. 10 The identified by-products formed during the degradation of organic compounds containing nitrogen using AOP's.

Contaminant	AOP type	Identified by-product	References
Organic compound containing nitrogen atoms	UV/TiO ₂	NH ₄ ⁺ and NO ₃ ⁻	Low et al., 1991 [87]
Nitrogen containing organic compounds	Photo-Fenton	Ammonia	Maletzky and Bauer, 1998 [110]
Nitrogen containing organic compounds (alkylamines, alkanolamine, heterocyclic and aromatic N-compounds)	UV/TiO ₂ /O ₃	NO ₂ ⁻ , NO ₃ ⁻ and NH ₄ ⁺	Mare <i>et al.</i> , 1999 [111]
4-chloro-3,5-dinitrobenzoic acid	UV/H ₂ O ₂	Cl ⁻ , NO ₃ ⁻ and NO ₂ ⁻	Lopez <i>et al.</i> , 2000 [63]
Alkyl- and alkanolamines	TiO ₂ - and Pt/TiO ₂ -assisted photocatalysis	NH ₃ /NH ₄ ⁺ , NO ₃ ⁻ and NO ₂ ⁻	Klare <i>et al.</i> , 2000 [89]
Diethylamine	TiO ₂ /UV-VIS	Ethylacetamide, acetaldehyde, pyrazine, acetic acid, carbon dioxide, ammonium (NH ₄ ⁺) and nitrate (NO ₃ ⁻)	Alberici <i>et al.</i> , 2000 [88]
4-nitrophenol (4-NP)	UV/H ₂ O ₂	4-nitrocatecol, 1,2,4-benzonitrol, hydroquinone, and nitrite (NO ₂ ⁻)	Daneshvar <i>et al.</i> , 2007 [80]
Monoethanolamine (MEA) and Diethanolamine (DEA)	Fenton treatment	Glycine and NH ₄ ⁺	Harimurti, 2009 [43]
Monoethanolamine	UV/H ₂ O ₂	Formate and nitrate (NO ₃ ⁻)	Ariff, 2010 [73]
Organic compound containing nitrogen atom (nitrobenzene, aniline, piperidine, pyridine, pyrrole, imidazole, pyridazine, pyrimidine, pyrazine)	UV/TiO ₂	Carboxylic acid, N ₂ , CO ₂ , NH ₄ ⁺ and NO ₃ ⁻	Jing <i>et al.</i> , 2011 [112]

In 1995, Eckenfelder and Musterman [25] proposed the following guidelines on relationship between biodegradability and molecular structures:

- a. Aliphatic compound containing carboxyl ($R-COOH$), ester ($R-COO-R$), or hydroxyl ($R-OH$) groups are nontoxic and readily biodegradable. A compound with higher number of carboxyl group substituted in the compound (such as dicarboxylic ($HOOC-R-COOH$)) needs longer acclimatization compared to the less one (such as a single carboxyl groups).
- b. Slow acclimatization and moderate degradation is found for compounds with carbonyl groups ($R-C=O$) or double bonds ($R=R$).
- c. Decrease in the biodegradability of compounds with amino ($R-NH_2$) or hydroxyl groups ($R-OH$) follows the degree of saturation (primary > secondary > tertiary carbon atom attachment).
- d. An increase in halogen substitution of halogenated compounds ($R-X$) decreases the biodegradability.

Hazardous compounds are generated into the environment through many routes i.e.: during the manufacturing process, industrial use of the compounds, atmospheric discharge from industrial facilities, wastewater discharges, disposal of products and used products containing hazardous compounds [114]. Sheha and Someda [115] expressed the definition of hazardous waste according to USEPA [116] i.e. “hazardous waste means waste requires special precaution in its storage, collection, transportation, treatment or disposal to prevent damage to person or property and includes explosive, flammable, volatile, radioactive, toxic, and pathological waste.”

The presence of hazardous material in biological treatment commonly inhibits the growth of microorganism or often toxic to the microorganism. Therefore, pretreatment may be required for contaminants, which are toxic to the microorganism. Eckenfelder *et al.* [117] listed the limiting condition of different pollutants that make pre-biological treatment desirable (Table 2.11).

Table 2. 11 Condition/concentration of pollutants that requires pre-biological treatment [117].

Pollutant or System Condition	Limiting Condition/Concentration	Kind of Pretreatment
Suspended solids	> 125 mg/L	Sedimentation, flotation, lagooning
Oil and grease	>35 mg/L	Skimming tank or separator
Toxic ion		Precipitation or ion exchange
Pb	≤0.1 mg/L	
Cu + Ni + CN	≤1 mg/L	
Cr ^{+b} + Zn	≤3 mg/L	
Cr ³⁺	≤10 mg/L	
pH	6 to 9	Neutralization
Alkalinity	0.5 lb alkalinity as CaCO ₃ /lb BOD removed	Neutralization for excessive alkalinity
Acidity	Free mineral acidity	Neutralization
Organic load variation	>2:1	Equalization
Sulfides	>100 mg/L	Precipitation or stripping
Phenols	>100 mg/L	Extraction, adsorption, internal dilution
Ammonia	>500 mg/L (as N)	Dilution, ion exchange, pH adjustment and stripping
Temperature	> 38 °C in reactor	Cooling, steam addition

Especially for organic contaminants, the common pre-biological treatments used are equalization, absorption, extraction, and dilution. Nevertheless, in the recent years, there is an effective method i.e. advanced oxidation process (AOP) that is frequently used to treat the recalcitrant organic contaminants before biological treatment. Basically, the pre-biological treatment is proposed to make the contaminant becoming readily biodegradable. A material is described or classified as ‘readily biodegradable’ if it fulfill the standard tests that it will be broken down by living organisms and thus removed from the environment. Organization of economic cooperation and development (OECD) in Europe has defined standards of a material to be called as readily biodegradable. Among them, there are two standards that are commonly used for this determination; i) at least 60 – 70% of the material must be broken down within 30 days by microorganism in the bioreactor; ii) the ratio of BOD₅/COD value

is more than 0.5 [118 – 119]. BOD₅ is a measure for the dissolved oxygen consumption during biological oxidation of organic contaminant and COD is a measure for the oxygen required to oxidize the chemical present in a sample. The second standard is frequently used by a number of researchers since it is simple. Numerous kinds of wastewater from different sources have been reported as readily biodegradable after advanced oxidation process (AOP) (Table 2.12).

Table 2. 12 Biodegradability enhancement by advanced oxidation processes (AOP).

Contaminant	Type of AOP	Results	References
Azo dyes (reactive yellowKD-3G, reactive red 15, reactive red 24, cationic Blue X-GRL) and wool textile wastewater	Photocatalytic (UV/TiO ₂)	All dyes are readily biodegradable (BOD ₅ /COD ratio increased from 0 to 0.75) after UV/TiO ₂ process for time >60 minutes of reaction time.	Chun and Yizhong, 1999 [90]
Hospital wastewater	Photo-Fenton (UV-Fenton)	The BOD ₅ /COD ratio increased from 0.30 to 0.52	Kajitvichyanukul and Suntronvipart, 2006 [120]
Textile wastewater	Electron beam irradiation	The BOD ₅ /COD ratio increased from 0.68 to 0.79	Kim <i>et al.</i> , 2007 [122]
Pharmaceutical wastewater	Mw/Fenton-like process	The BOD ₅ /COD ratio changed from 0.165 to 0.470	Yang <i>et al.</i> , 2009 [123]
Hospital wastewater	Septic tank/Fenton reaction	The BOD ₅ /COD ratio changed from 0.46 to 0.48	Berto <i>et al.</i> , 2009 [36]
Carbaryl (a carbamate pesticide)	UV/TiO ₂ /O ₃	The BOD ₅ /COD ratio increased up to 0.38	Rajeswari and Kanmani, 2009 [52]
Pharmaceuticals wastewater from El-Nasr Pharmaceutical and Chemical company, South-East of Cairo	Fenton process	The BOD ₅ /COD ratio increased from 0.25 to 0.39	Badawy <i>et al.</i> , 2009 [39]
Landfill leachate (from Changshengqiao landfill (Chongqing, China)	Fenton process	The BOD ₅ /COD ratio increased from 0.18 to 0.38	Guo <i>et al.</i> , 2010 [121]
Acrylic fiber manufacturing wastewater	Fenton process	The BOD ₅ /COD ratio increased from 0.100 to 0.529 after 2 hours of reaction time.	Li <i>et al.</i> , 2012 [38]

Kajitvichyanukul and Suntronvipart [120] in 2006 followed by Berto *et al.* [36] in 2009 reported the enhancement of biodegradability of hospital wastewater after treating with Photo-Fenton process and Fenton process. Using the photo-Fenton and Fenton process, hospital wastewater was partially degraded to becoming more biodegradable component. Kajitvichyanukul and Suntronvipart reported that BOD₅/COD ratio for hospital wastewater increased from 0.30 to 0.52 after photo-Fenton process, while Berto *et al.* reported that the BOD₅/COD ratio for hospital wastewater increased from 0.46 to 0.48 after Fenton process. Pharmaceutical wastewater [39], acrylic fiber manufacturing wastewater [38], and landfill leachate from Changshengqiao landfill (Chongqing, China) [121] were also successfully partially degraded using Fenton process and the biodegradability of all these three wastewaters increased after treatment, i.e. from 0.25 to 0.39 for pharmaceutical wastewater, from 0.100 to 0.529 for acrylic fiber manufacturing wastewater, and from 0.18 to 0.38 for landfill leachate. Similar reports on the increase in biodegradability of wastewater after AOP are listed in Table 2.12.

CHAPTER 3

EXPERIMENTAL

This chapter deals with the description on the material, equipment set-up and the procedures, and also the details of analytical techniques, involved in the present research. The details of each experiment are also elaborated in this chapter. The details of the present study include three main activities:

- i) Experiments involving UV/H₂O₂ treatment of wastewater containing MDEA (both simulated and actual effluents).
- ii) Optimization of the process using response surface methodology (RSM).
- iii) Analysis and identification of the intermediate products formed during mineralization process and also the biodegradability test.

The scheme of the activities involved in the present research is shown in Figure 3.1.

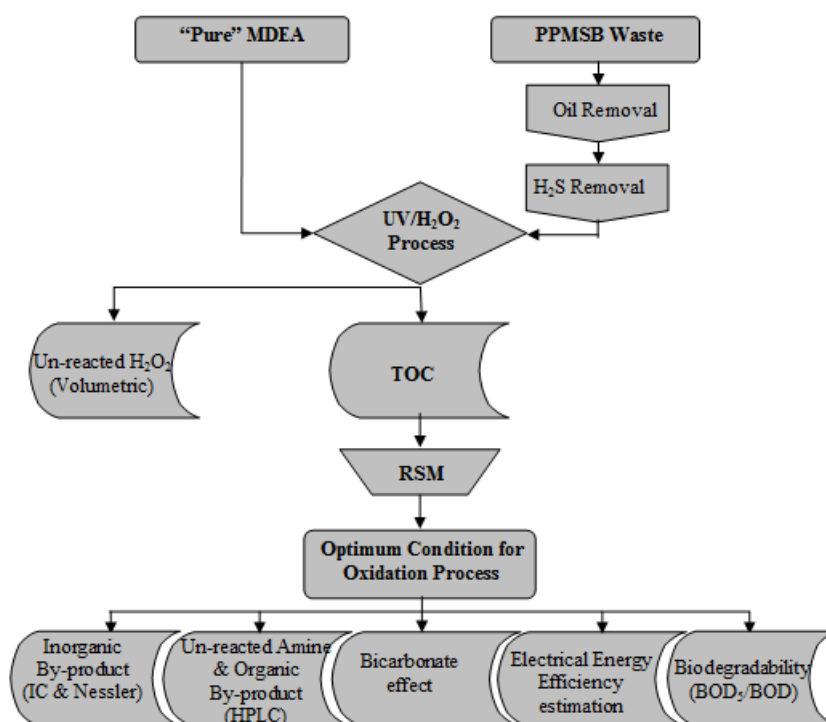
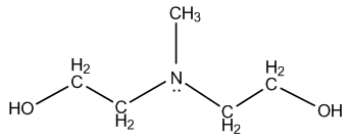


Figure 3.1 Scheme of activities in the present research.

3.1 Materials

The details of the chemicals used in the present research are presented in Table 3.1. All the purchased chemicals were used without further purification.

Table 3. 1 Chemicals used in the present work.

Chemicals	Supplier	MW g·mol ⁻¹	T _m °C	T _b °C	ρ(T = 25 °C) g·cm ⁻³
Methyldiethanolamine (MDEA)	Merck	119.16	-55	247.30	1.04
					
Hydrogen Peroxide (H ₂ O ₂) 30%	Merck	34.01	-0.43	150.20	1.11
Potassium Permanganate (KMnO ₄)	Merck	158.03	240	-	2.70
Disodium Hydrogen Phosphate (Na ₂ HPO ₄)	Merck	141.96	250	-	1.7
Calcium Hydroxide (Ca(OH) ₂)	Merck	74.09	580	-	2.21
Sulfuric Acid (H ₂ SO ₄)	Merck	98.08	10	337	1.84
Sodium Hydroxide (NaOH)	R & M Chemical	39.99	318	1338	2.13

3.1.1 MDEA Contaminated Water/Effluents

For the present experiments, two kinds of MDEA contaminated wastewater were used i.e. simulated wastewater and actual wastewater from gas processing unit. Synthetic wastewater was prepared by dissolving a required quantity of MDEA into distilled water. For example, for the preparation of a 2000 ppm of MDEA solution, 1.92 ml of MDEA was dissolved into 1 liter of distilled water. This concentration is approximately equals to 1020 ppm of total organic carbon (TOC) or approximately equals to 0.085 M organic carbon (C). Figure 3.2 and Figure 3.3 show the correlation between the MDEA concentration with the total organic carbon (TOC) value and the MDEA concentration with the organic carbon (C) concentration, respectively.

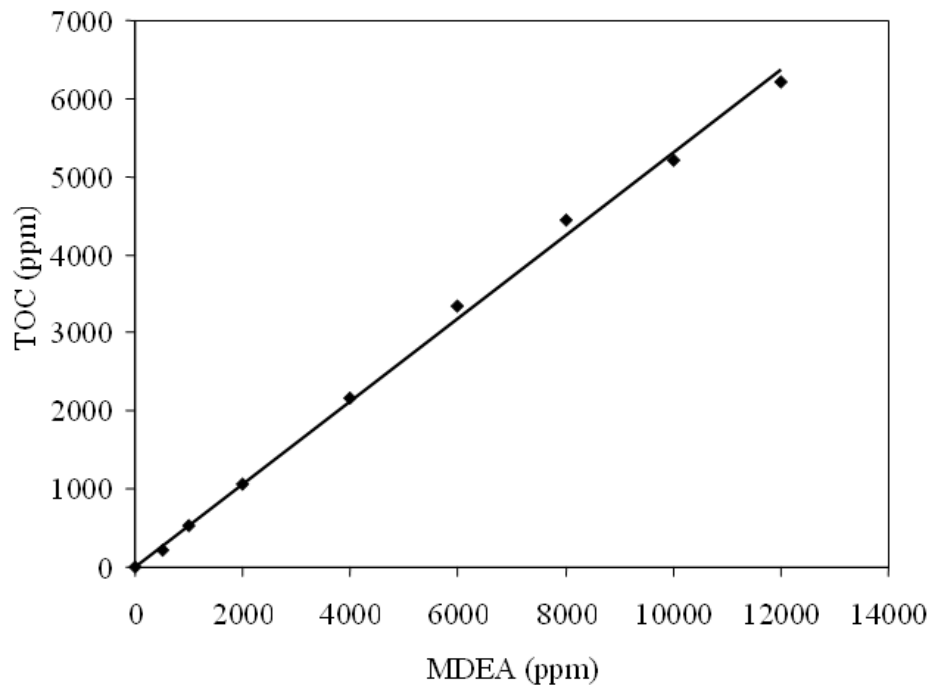


Figure 3.2 Correlation of MDEA concentrations with total organic carbon (TOC).
 $Y = 0.5302X$; $R^2 = 0.9977$

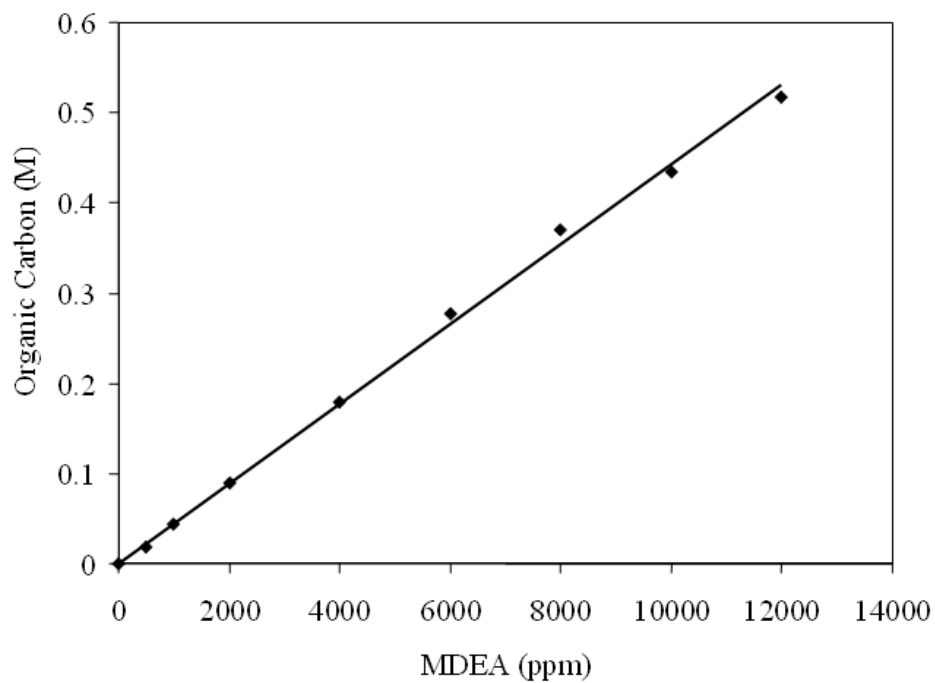


Figure 3.3 Correlation of MDEA concentrations with organic carbon.
 $Y = 5 \times 10^{-4} X$; $R^2 = 0.9977$

Actual wastewater was obtained from Petronas Penapisan Melaka Sendirian Berhad (PPMSB), Malaysia. The concentrations of various compounds present in the obtained effluent solution are shown in Table 3.2. Based on the preliminary studies, conducting the experiment at high concentration of contaminat was a time consuming, therefore the PPMSB effluent which has a very high MDEA concentration was further diluted before subjecting to the degradation process using UV/H₂O₂ oxidation process.

Table 3. 2 The properties of PPMSB effluent.

Measures	Remarks
MDEA	340000 ppm
TOC	175000 ppm
COD	500000 ppm
S ²⁻	500 ppm
NH ₄ ⁺	4156 ppm
Acetic acid	1566 ppm
Oxalic acid	13847 ppm
Oil and grease	250 ppm
pH	10

The real wastewater (obtained from gas processing unit) contain H₂S (toxic gas) apart from oil and grease, which will certainly affect the demineralization of MDEA, and hence these contaminants have to be removed before further treatment.

Initially, the oil and grease were separated by allowing the effluent to settle in separating funnel for overnight. The oil and grease free solution which settled at the upper layer were separated. The removal of H₂S was conducted using the following oxidation process (Equation 3.1):



For the oxidation purpose 2 ml of 30% H₂O₂ was added to every 100 ml of effluents, and the obtained yellow precipitate (sulphur) was then removed by filtration.

3.1.2 Reagents Used

3.1.2.1 Potassium Permanganate (KMnO₄) Solution

KMnO₄ solution was used for the determination of un-reacted H₂O₂ during UV/H₂O₂ oxidation process. The standard KMnO₄ solution was prepared by dissolving 4 gram of KMnO₄ into 1 liter of distilled water, which was standardized using 0.1 N sodium oxalate solution [124].

3.1.2.2 HPLC Mobile Phase

Two mobile phases were used in the HPLC analysis i.e. mobile phase for YMC-Pack PolymerC18 column and mobile phase for Transgenomic column. The HPLC mobile phase for YMC-Pack PolymerC18 column was a mixture of 0.1 M Na₂HPO₄ and 0.1 M NaOH solutions in water. Na₂HPO₄ solution (0.1 M) was prepared by dissolving 14.19 grams of Na₂HPO₄ into 1 liter of distilled water, while 0.1 M NaOH was prepared by dissolving 4 grams of NaOH into 1 liter of distilled water. The ratio of the mixture used was 60% of Na₂HPO₄ and 40% of NaOH at pH of 12. The mobile phase for Transgenomic column used was 0.01 N H₂SO₄, which was prepared by dissolving 0.275 ml of 98% H₂SO₄ in 1 liter of distilled water. Before use, the stock solutions were filtered using paper filter of 0.45 μm pore diameter. This filtration was conducted to eliminate the presence of solid particles in the stock solution, which will create disturbances/uncertainties during HPLC analysis.

3.1.2.3 Calcium Hydroxide (Ca(OH)₂) Solution

Generally, water (H₂O) and carbon dioxide gas (CO₂) are produced during/end of the oxidation of organic compound. Identification of CO₂ liberated during UV/H₂O₂ oxidation process of MDEA was conducted using Ca(OH)₂. The Ca(OH)₂ solution

was prepared by dissolving 1.5 grams of $\text{Ca}(\text{OH})_2$ into 1 liter of distilled water and kept overnight for allowing the solid particle to settle down and the resulted clear solution from the mixture was used to absorb the liberated CO_2 into the solution.

3.1.2.4 Sodium Hydroxide (NaOH) Solution

Sodium hydroxide (1 M NaOH) solution was prepared by dissolving 40 gram of NaOH into 1 liter of distilled water. Since the sample was a strong solution, a concentrated NaOH solution was used for initial pH adjustment.

3.1.2.5 Sulphuric Acid (H_2SO_4) Solution

Two different concentrations of H_2SO_4 solutions were used for the present experiments. A concentrated H_2SO_4 solution i.e. 98% H_2SO_4 was used during the UV/ H_2O_2 process for the adjustment of the pH. In the mean time, determination of unreacted H_2O_2 was conducted using 2 N H_2SO_4 solutions. The 2 N H_2SO_4 solutions were prepared by dissolving 50 ml of 98% of H_2SO_4 into 1 liter of distilled water.

3.2 Experimental Set Up

3.2.1 UV/ H_2O_2 Oxidation Process

The experiments on UV/ H_2O_2 oxidation process was conducted in 700 ml jacketed glass reactor. The reaction zone is a cylindrical borosilicate glass tube, 14 inch long with 2 inch internal diameter. The photo reactor equipped with 8 Watt low pressure Hg vapor lamp (GPH295T5L, S. No. EC90277, USA) which produces UV light at 254 nm was used along with a current-voltage control unit, and a small opening (at the top) for collecting the samples.

The experimental set up is shown in Figure 3.4 and the schematic diagram of the reactor is shown in Figure 3.5.



Figure 3. 4 UV/H₂O₂ oxidation experimental set up.

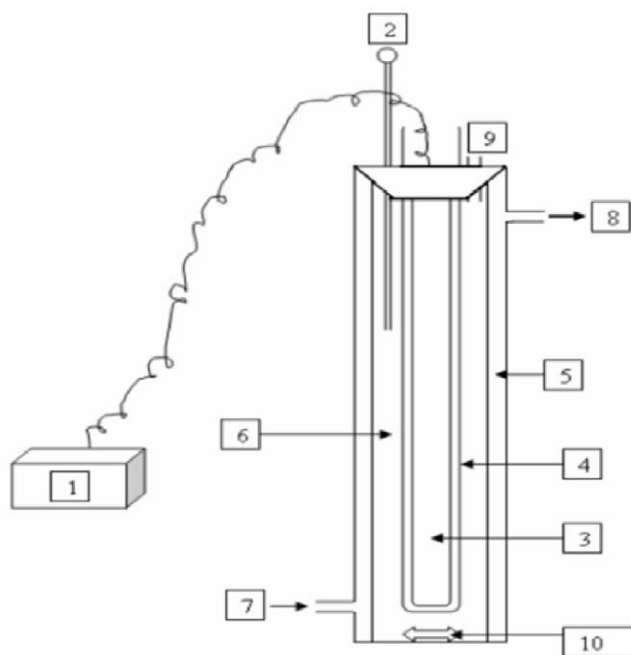


Figure 3. 5 The schematic diagram of the UV/H₂O₂ photoreactor. 1). Current-voltage control unit; 2). Thermometer; 3). UV lamp; 4). Quartz tube; 5). Jacket; 6). Reaction zone; 7). Water inlet; 8). Water outlet; 9). Sample port; and 10). Stirrer bar.

MDEA solution with a desired concentration was taken in the glass reactor. A required amount of H_2O_2 was then added into the solution. The total operating volume of the reactor was maintained at 400 ml. The pH adjustment was made using 1 M NaOH or 98% H_2SO_4 . The temperature was maintained by circulating cooling water through the jacket at a required temperature. During the process, 3 ml of liquid sample was withdrawn from time to time and then diluted for the determination of total organic carbon (TOC) and also for the estimation of un-reacted H_2O_2 . The H_2O_2 concentration was estimated by titration method using KMnO_4 solution [124]. For other analysis, such as, by-product identification and biodegradability test, new samples were prepared before conducting the analysis.

The CO_2 liberation during UV/ H_2O_2 oxidation process of MDEA was identified by conducting the UV/ H_2O_2 oxidation process using sealed reactor. The seal was made using parafilm paper. Sampling port was connected to a vial filled with $\text{Ca}(\text{OH})_2$ solution (lime water). The experimental set up is shown in Figure 3.6.

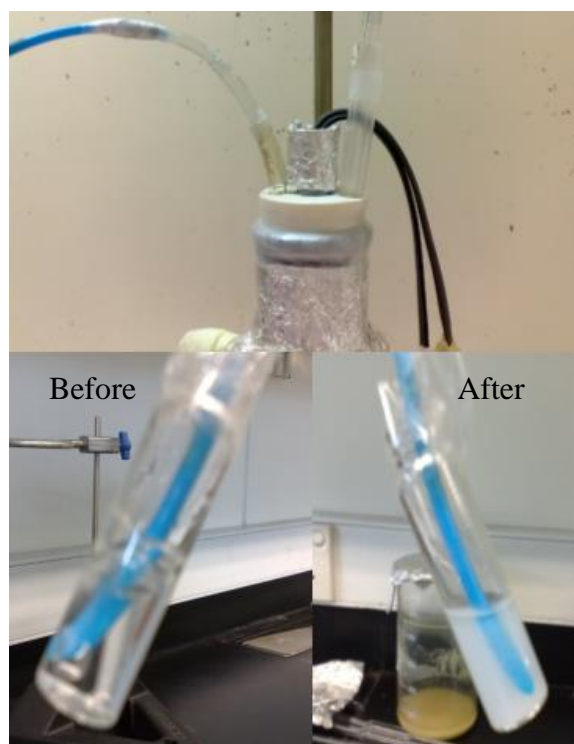
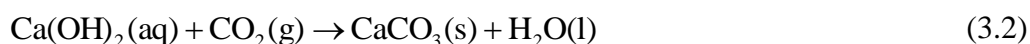


Figure 3. 6 Experimental set up for the identification of CO_2 liberation during UV/ H_2O_2 oxidation process.

Before running the oxidation experiments, the reactor was flushed by nitrogen gas for about 30 minutes. This step was conducted to eliminate any possible presence of CO₂. The CO₂ gas that was liberated from the oxidation process reacted with lime water and then converted into CaCO₃ (a white solid), according to the following reaction (Equation 3.2):



The excess of CO₂ during the test would result in colorless solution of Ca(HCO₃)₂, as shown in Equation 3.3.



3.2.2 Biodegradability Test of Partially Degraded MDEA Solution

During the mineralization of effluents containing MDEA using UV/H₂O₂ process, approximately 85% of total organic carbon (TOC) was removed from the initial TOC concentration of 1000 ppm. A biodegradability test for the partially degraded MDEA after UV/H₂O₂ was also conducted. This test was carried out in order to make sure that the treated effluents must be readily biodegradable when disposed into the environment. The test of partially degraded MDEA after UV/H₂O₂ process was conducted by calculating the ratio of BOD₅ value to COD value [118 – 119]. The BOD₅ was measured using the HACH method for BOD₅ determination (HACH-BODTrak™). Experimental set up for the BOD₅ determination is shown in Figure 3.7. Activated sludge was used as the seed for bacteria for BOD₅ determination which was collected from wastewater treatment plant (WWTP) at Universiti Teknologi Petronas Malaysia. This seed was selected because it is a very common bacterium available in the wastewater treatment plant.



Figure 3. 7 Experimental set up of biodegradability test.

Therefore, no special or adapted bacteria are needed to reproduce the results. The chemical oxygen demand (COD) was measured by using COD TestNTube (HACH) and the value of COD was measured using spectrophotometer (DR 5000). Furthermore, the biodegradability of partially degraded MDEA was determined from the ratio of BOD_5/COD . The compound is considered readily biodegradable when the ratio of BOD_5/COD is greater than 0.5 [118 – 119].

3.3 Analytical Methods

3.3.1 Total Organic Carbon (TOC) Determination

The determination of total organic carbon (TOC) was conducted using TOC analyzer (Shimadzu – Model TOC-V_{CSH}, S. No. H 51104600672, Japan). The collected sample (1 ml) was diluted to obtain 20 ml of sample as required for TOC measurement.

The actual reading of TOC value was calculated from the TOC reading from the analyzer multiplied by dilution factor. This measurement was used to monitor the degradation of organic compound during UV/H₂O₂ process. The percentage of TOC removal at time “*t*” was calculated as follows (Equation 3.4):

$$\% \text{TOC removal}_t = \frac{\text{TOC}_0 - \text{TOC}_t}{\text{TOC}_0} \times 100\% \quad (3.4)$$

where: %TOC removal_{*t*} = percentage of TOC removal at *t*,
TOC₀ = TOC value at 0 minute, and
TOC_{*t*} = TOC value at *t*.

3.3.2 Chemical Oxygen Demand (COD) Determination

Chemical oxygen demand (COD) is a measure of oxygen required for oxidizing oxidizable organic content in the water sample. COD is defined as mg of O₂ consumed per liter of sample. The measurement of COD value was performed using COD analytical equipment (HACH) according to Method 8000. Method 8000 was USEPA approved (5220 D) for wastewater analysis [125 – 126]. Two ml of sample was oxidized using the standard chemicals supplied by HACH and digested at 150 °C for two hours on the DRB HACH digester. The COD reading was obtained by using HACH DR 5000 spectrophotometer.

3.3.3 BOD₅ Determination

The measurement of BOD₅ was performed by using HACH method for BOD₅ determination (HACH-BODTrak™), (Figure 3.7). A total sample of 95 ml was used for the BOD₅ test.

Activated sludge was used as seed and was collected from WWTP Universiti Teknologi PETRONAS Malaysia. Incubation was conducted for 5 days in the incubator at a temperature of 20 ± 1 °C. The BOD₅ value was estimated as follows (Equation 3.5):

$$\text{BOD}_5 = \frac{\text{DO}_{5\text{sample}} - \left[\frac{\text{v.s}}{\text{v.t}} \times \text{DO}_{5\text{control}} \right]}{\frac{\text{v.tc}}{\text{v.t}}} \quad (3.5)$$

where: BOD₅ = BOD₅ of test compound,
 DO_{5sample} = DO₅ of test compound + DO₅ of seed,
 DO_{5control} = DO₅ of seed
 v.s = volume of seed = 30 ml,
 v.tc = volume of test compound = 65 ml, and
 v.t = total volume = 95 ml.

3.3.4 Identification of UV Absorption Spectra of MDEA

Direct photolysis of an organic compound by UV light usually occurs when the organic compound absorb UV light. Identification of the UV spectrum region absorbed by MDEA was conducted using UV-VIS-NIR spectrophotometer (SHIMADZU UV-3150, Japan). MDEA solution was prepared and tested at $\lambda = 200$ to 600 nm regions.

3.3.5 Un-reacted MDEA and Degradation Product Identification using HPLC

An Agilent series 1100 brand of HPLC was used to monitor the degradation products and un-reacted MDEA after UV/H₂O₂ treatment. YMC-Pack PolymerC18 reverse phase column was utilized. A solution consisting of 60% Na₂HPO₄ (100mM) and 40% NaOH (100mM) at pH = 12 was used for elution.

UV light at 215 nm was used as detector. Transgenomic (Model ORH801) column was used for organic acid determination with 0.01 N H₂SO₄ as mobile phase. Refractive index was used as detector. Degradation product determination was performed by the comparison of sample with the standard compound. Qualitative analysis was based on the retention time of each compound in the chromatogram, while quantitative analysis was based on the calibration curve prepared using standard compound. The details of the calibration curves for different compounds tested are presented in Table 3.3 and the plots of concentration vs. area are presented in Figure 1, 2, 3, and 4 of Appendix.

Table 3. 3 The correlation constants for the calibration curves for MDEA and organic acids.

Compound	Column name	Calibration curve	R ²	Remark
MDEA	YMC-Pack PolymerC18	[MDEA] = 0.5354(Area)	0.9998	Figure A1 of Appendix A
Oxalic Acid	YMC-Pack PolymerC18	[Oxalic Acid] = 0.8558(Area)	0.9994	Figure A2 of Appendix A
Formic Acid	Transgenomic-ORH801	[Formic Acid] = 0.0236(Area)	0.9999	Figure A3 of Appendix A
Acetic Acid	Transgenomic-ORH801	[Acetic Acid] = 0.0177(Area)	0.9999	Figure A4 of Appendix A

3.3.6 Nitrate (NO₃⁻) and Nitrite (NO₂⁻) Determination

The profiles of the nitrate (NO₃⁻) and nitrite (NO₂⁻) were evaluated by using ion chromatography (Metrohm-761 Compact IC), which was equipped with Metrosep A Supp 5-150 column. Mixture of 1.0 mM of NaHCO₃ and 3.2 mM of Na₂CO₃ in one liter deionized water was used as mobile phase. Meanwhile, a conductivity meter was used as detector. The concentrations of both nitrate (NO₃⁻) and nitrite (NO₂⁻) were determined based on the calibration curves listed in Table 3.4, and the plots of concentration vs. area are shown in Figure 5 and 6 of Appendix 1, respectively.

Table 3. 4 The correlation constants for the calibration curves for nitrate (NO_3^-) and nitrite.

Compound	Column name	Calibration curve	R ²	Remark
Nitrate (NO_3^-)	Metrosep A Supp 5-150	$[\text{NO}_3^-] = 0.1347$ (Area)	0.9998	Figure A5 of Appendix A
Nitrite (NO_2^-)	Metrosep A Supp 5-150	$[\text{NO}_2^-] = 0.1356$ (Area)	0.9949	Figure A6 of Appendix A

3.3.7 Estimation of Ammonium (NH_4^+)

The estimation of NH_4^+ was made using Nessler's reagent [127 – 128] according to Method 8038 Nitrogen (HACH) [125]. A sample of 25 ml was required for this measurement. The (NH_4^+) concentration was measured using spectrophotometer DR 2000 (HACH) based on the intensity of color formed.

3.3.8 Un-reacted H_2O_2 Determination

The determination of un-reacted H_2O_2 during the UV/ H_2O_2 process was performed by titration method using 0.062 N KMnO_4 solution. Titration of acidified sample from UV/ H_2O_2 process was conducted. The end point was the change in color of the solution from colorless to light pink. Sodium oxalate was used to standardize the KMnO_4 solution [124].

3.3.9 pH

The pH measurements were made using pH meter (HACH sension 1). The pH meter was calibrated and standardized regularly. Measurement of pH during oxidation process was conducted to monitor the change in pH condition during the oxidation process in the reactor.

3.3.10 Measurement of UV Intensity

During the study of effect of UV intensity in the mineralization process of MDEA using combination of UV and H₂O₂, the UV intensity used was varied. Variation of UV intensity was made by connecting the UV lamp to adjustable dimmer. The different UV intensities produced were measured using UV radiometer (Cole-Parmer model: 97651-10 with sensor UV at 254 nm model: 97651-20).

The factors affecting the optimization process of the degradation of wastewater containing MDEA using UV/H₂O₂ process are the intensity of UV, initial concentration of waste (organic contaminant), initial concentration of H₂O₂, initial pH and temperature. Based on the preliminary study, the factor of UV intensity and initial concentration of waste were found to have no optimum value. Hence for the optimization of UV/H₂O₂ process, these two factors were always kept constant at 12.06 mW/cm² and 1000 ppm of total organic carbon. The UV intensity was chosen at this value due to the limitation of UV lamp available in the laboratory. This UV intensity of 12.06 mW/cm² was the highest intensity that could be provided by the available facilities in the laboratory. Increasing UV intensity would increase the degradation rate, thus the highest UV intensity can be used for better efficiency. Similar trend without optimum value was found for the initial concentration of waste. In this case, increasing initial concentration of waste would decrease the degradation rate. Hence, 1000 ppm of total organic carbon was chosen as the initial concentration of waste since the degradation process was easier to monitor.

3.4 Statistical Design of Experiments (DOE) for Optimization of Degradation Process by Using UV/H₂O₂

Optimization process was carried out using response surface methodology (RSM). Portable Statgraphics Centurion 15.2.11.0 was used for RSM analysis. RSM is a method used in modeling and analysis of problem in which a response of importance get influenced by several factors. The objective of this method is to optimize this

response. Response surface is normally represented graphically where the contour plot are often drawn to visualize the shape of the response surface [80].

Determination of the optimum conditions for the degradation process was carried out according to the Box-Behnken design. This design was chosen since for three factors evaluated, the Box-Behnken design offers some advantage in requiring a fewer number of runs compared to other design such as central composite circumscribed (CCC) design and central composite inscribed (CCI). Three level factorial designs which consist of a 2^2 full factorial with 3 center points were created. The three level factors chosen based on the preliminary experiment and coded as low (-1), middle (0), and high (+1). The factors included initial concentration of H_2O_2 (range 0.12 M to 0.24 M), pH (range 7 to 11), and temperature (range $30^\circ C$ to $50^\circ C$). Percentage of TOC removal was measured as influence response. The levels indicated the presence of a curvature which wished-for that the experimental ranges were relatively close to the optimum. When the process is close to optimum, the second order model that incorporates curvature is represented in Equation 3.6.

$$y = \beta_0 + \sum_{i=1}^k \beta_i x_i + \sum_{i=1}^k \beta_{ii} x_i^2 + \sum_{i < j} \beta_{ij} x_i x_j + \varepsilon \quad (3.6)$$

where y is the predicted response, β_0 is the intercept, β_i is the linear effect, β_{ii} is the squared effect, β_{ij} represents the interaction effect, and ε is the error term. After conducting the screening of factors by the factorial design, a response surface analysis was employed to optimize the highest TOC removal of the waste. The results of experimental design was analyzed using Portable Statgraphics Centurion 15.2.11.0 statistical software to estimate the dependent response variable and to find the effects, coefficients, standard deviation of coefficients as well as other parameters of the model. Optimized condition was obtained from contour plot graphically and also by solving the polynomial regression equation. Quality of fit was expressed by the coefficient of determination R^2 . Statistical significance was analyzed using the analysis of variance (ANOVA), with 5% probability level [108].

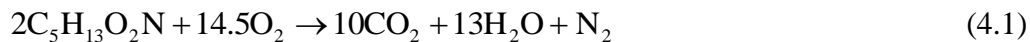
CHAPTER 4

RESULTS AND DISCUSSION

The present chapter deals with the details of the results obtained in the present research and the interpretation of the same. Accordingly the discussion includes the details of the preliminary studies conducted, proposal of degradation mechanism of MDEA, kinetic study, UV/H₂O₂ treatment of a real effluent obtained from a refinery plant (PPMSB), biodegradability test of partially degraded simulated wastewater and real effluent and then the estimation of electrical energy efficiency of the UV/H₂O₂ process. The detailed discussion follows:

4.1 Preliminary Studies

Initial step before conducting the experiments was the estimation of theoretical oxidizing agent (H₂O₂) required for the complete mineralization of MDEA. The estimation was based on the general oxidation reaction of MDEA to form inorganic products as expressed below (Equation 4.1):



Based on the above reaction, for the complete mineralization of 2 moles of MDEA requires 14.5 moles of O₂ (29 atoms of oxygen). In the UV/H₂O₂ process, H₂O₂ is considered as the main source of oxygen atom in the system. One mole of H₂O₂ provides 2 atoms of oxygen, thus 14.5 moles of H₂O₂ are capable to provide 29 atoms of oxygen for complete oxidation of MDEA.

In others words, for complete oxidation of 2 moles of MDEA require 14.5 moles of H_2O_2 . Further, (for example) when we want to conduct the experiment at 2000 ppm of initial concentration of MDEA, the estimation of theoretical amount of H_2O_2 required for complete oxidation of MDEA is as much as 0.12 M.

4.1.1 Effect of UV, H_2O_2 , and Combination of UV/ H_2O_2 on MDEA Degradation

The objective of the study is to visualize the individual effect of UV and H_2O_2 , and the combination of UV/ H_2O_2 , on the degradation of MDEA.

The capability of UV light to degrade the organic compound follows photolysis mechanism. The organic compound absorbs UV spectrum and then results in an excited (organic) compound, which later decomposed to form a product [31 – 32, 129 – 130]. The results of the present experiments showed no degradation was found when the UV alone was applied (Figure 4.1).

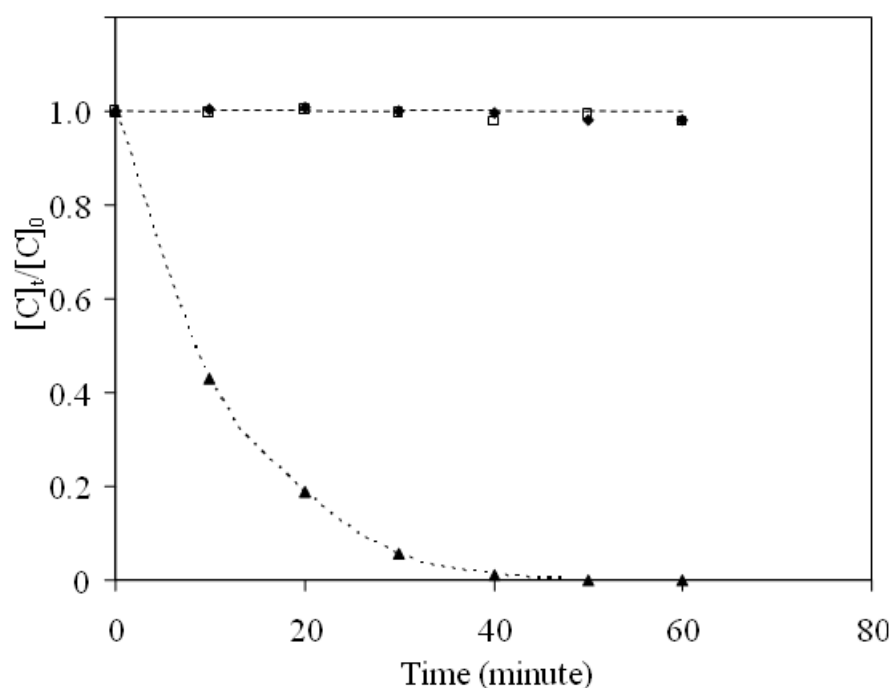


Figure 4. 1 Individual effect of UV, H_2O_2 , and the combination of UV/ H_2O_2 on MDEA degradation ($[MDEA]_0 = 1000$ ppm TOC; $[H_2O_2]_0 = 0.12$ M; pH = 7; Temperature = 30 °C; UV intensity = 12.06 mW/cm²)

◆ UV alone; □ H_2O_2 alone; ▲ UV/ H_2O_2

UV spectrum at 254 nm that was used in this experiment was not capable to degrade the MDEA and to remove the total organic carbon from the system (Figure 4.2), and the reason could be attributed to the fact that MDEA did not absorb the UV light at 254 nm. Based on the screening of UV spectrum (Figure 4.3), the region of the spectrum absorbed by MDEA was at spectrum below than 254 nm region, and therefore the direct photolysis did not occur.

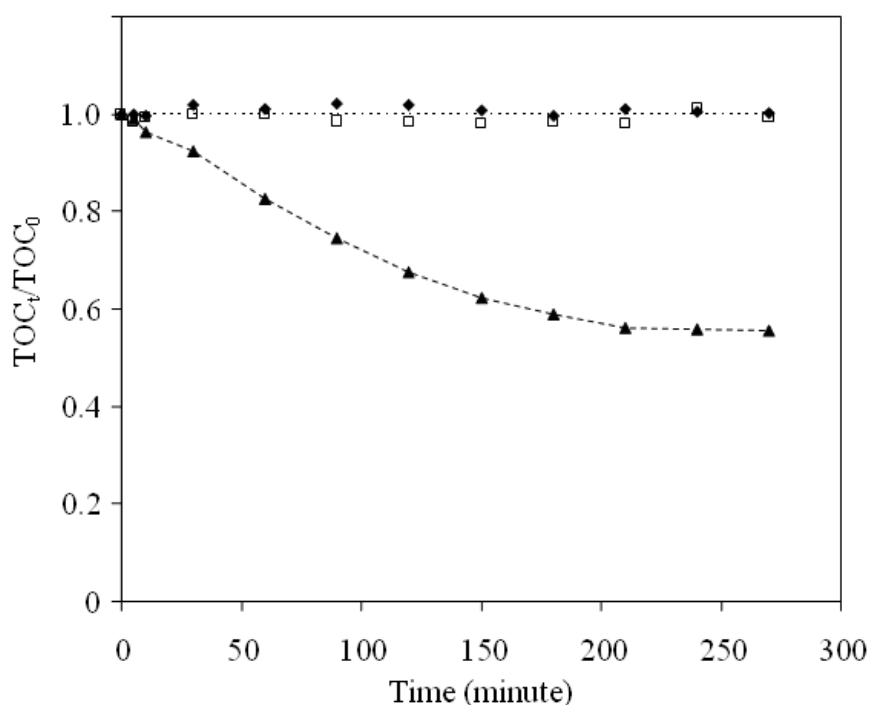


Figure 4. 2 Individual effect of UV, H₂O₂, and the combination of UV/H₂O₂ on the MDEA mineralization ([MDEA]₀ = 1000 ppm TOC; [H₂O₂]₀ = 0.12 M; pH = 7; Temperature = 30 °C; UV intensity = 12.06 mW/cm²).
 ◆ UV alone; □ H₂O₂ alone; ▲ UV/H₂O₂

Meanwhile, the capability of H₂O₂ to degrade organic compound is mainly due to the high redox potential of H₂O₂ i.e. + 1.8 V. This reduction potential indicates the high tendency of H₂O₂ to act as an oxidant, which refers to direct electron-transfer reaction between organic compound and H₂O₂ [131]. The results of the present experiments showed no degradation when the H₂O₂ alone was used. H₂O₂ alone was not capable to degrade the MDEA (Figure 4.1) and to remove the total organic carbon in the system (Figure 4.2).

This might be due to the redox potential of H_2O_2 that is not sufficient for the oxidation process. The photolysis resistance of MDEA toward UV light and H_2O_2 was in agreement with the observation of Xua *et al.* [132], based on their studies on the photolysis resistance of dimethyl phthalate against UV photolysis and H_2O_2 .

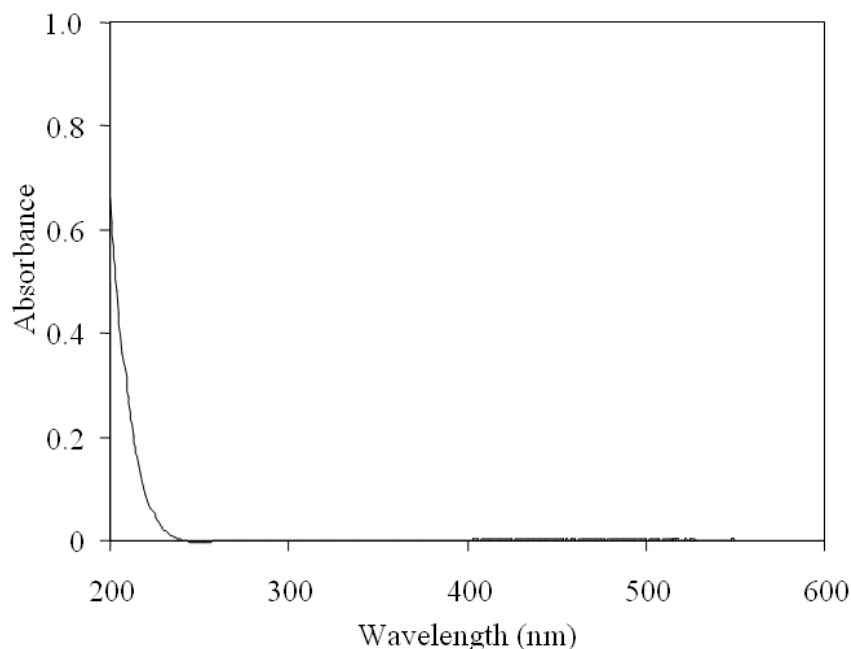


Figure 4. 3 UV absorption spectra of MDEA.

However, the reduction of MDEA and total organic carbon was found when the UV and H_2O_2 were applied in combination. Complete (100%) degradation of MDEA was achieved at 40 minutes of reaction time (Figure 4.1) and the total organic carbon was reduced to a certain level i.e. 41.23% TOC removed (Figure 4.2), which was due to hydroxyl radical generated from H_2O_2 photolysis. It is well known that H_2O_2 strongly absorbs UV spectrum at 254 nm [31]. Therefore the probability of H_2O_2 photolysis to generate hydroxyl radicals is very high. Due to the photolysis of H_2O_2 the concentration of H_2O_2 in the system gets reduced during the UV/ H_2O_2 process, and the profile of H_2O_2 is shown in Figure 4.4. Hence, it can be concluded that the combination of UV and H_2O_2 will generate hydroxyl radical, which plays an important role in the degradation of many recalcitrant organic contaminant [80, 129, 133 – 134].

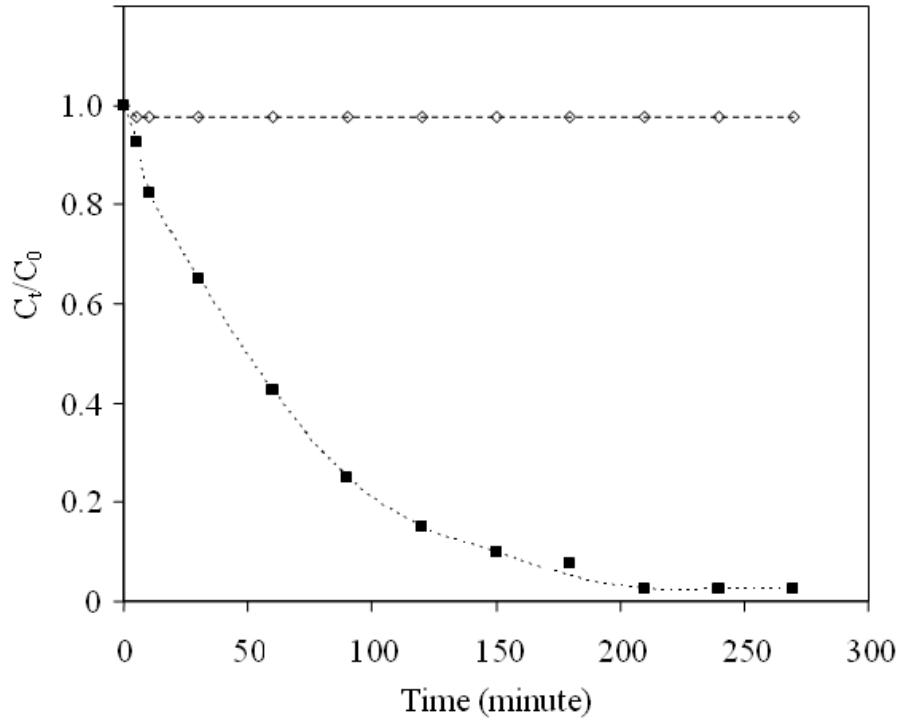


Figure 4. 4 H₂O₂ profile during the UV/H₂O₂ process.

◇ H₂O₂ alone; ■ UV/H₂O₂

4.1.2 Effect of Initial Concentration of MDEA

The effect of initial MDEA concentration on the UV/H₂O₂ oxidation process was studied using eight different initial concentrations (Figure 4.5). The concentrations were varied from 500 ppm to 12000 ppm of MDEA. The other variables namely volume (400 ml), UV intensity (12.06 mW/cm²), temperature (30°C), pH (7), and ratio between concentrations of MDEA to oxidant H₂O₂ (2 moles of MDEA to 14.5 moles of H₂O₂) were retained at constant values.

In order to show a better clarity of the data on TOC removal, a plot of $(TOC)_t/(TOC)_0$ with time was made. Figure 4.5 shows the dependency of TOC removal on the initial concentration of MDEA present in the solution. Based on the trends and the profiles seen in Figure 4.5, the degradation efficiency decreases with an increase in the initial concentration of contaminant. This result is in good agreement with the reported literatures [133, 135 – 136].

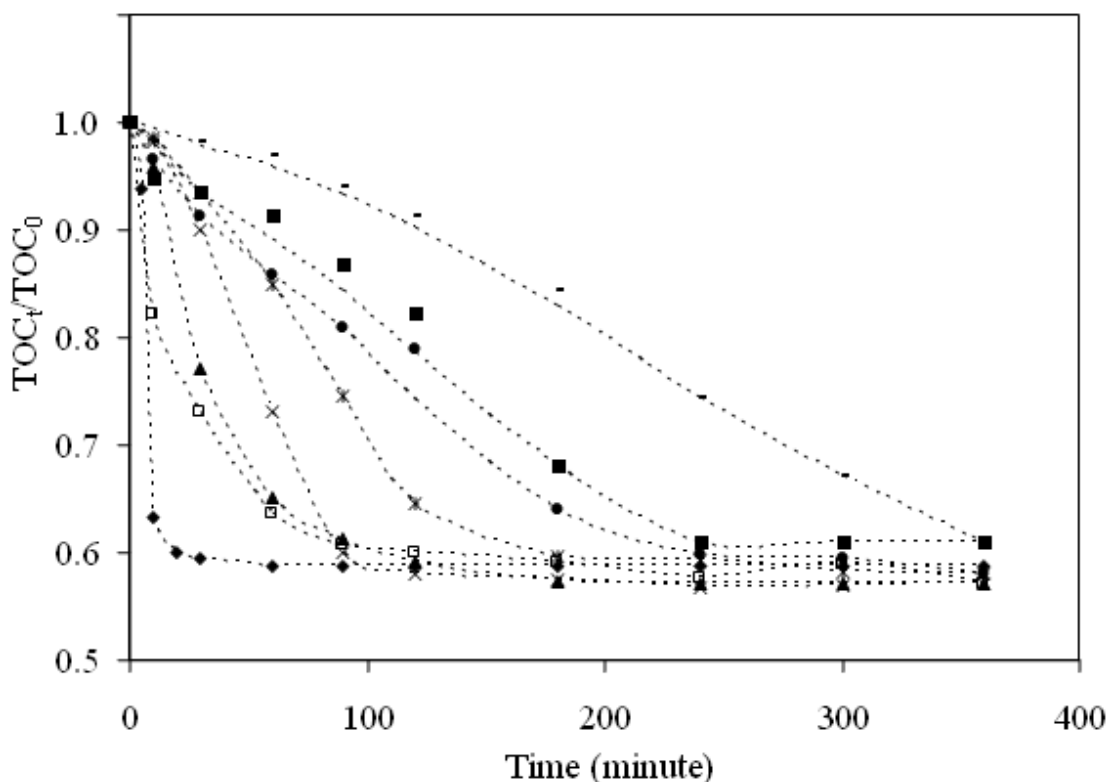


Figure 4. 5 The degradation profile of organic carbon for different initial concentration of MDEA

- ◆--- 500 ppm MDEA; 0.03 M H₂O₂
- ▲--- 2000 ppm MDEA; 0.12 M H₂O₂
- *--- 6000 ppm MDEA; 0.36 M H₂O₂
- 10000 ppm MDEA; 0.60 M H₂O₂
- 1000 ppm MDEA; 0.06 M H₂O₂
- ×--- 4000 ppm MDEA; 0.24 M H₂O₂
- 8000 ppm MDEA; 0.48 M H₂O₂
- 12000 ppm MDEA; 0.72 M H₂O₂

Haji *et al.* [135] reported that higher initial concentration of dye with excess H₂O₂ took longer time to achieve a specific degradation, whilst, Behnajady *et al.* [133] reported that decolorization decrease with an increase in the initial concentration of Malachite Green for a constant initial concentration of H₂O₂. Ochuma *et al.* [136] also reported a similar behavior for the degradation rate of 2,4,6-trichlorophenol (TCP), and concluded that at constant UV lamp intensity, the higher concentration of TCP required longer radiation time for complete degradation.

The percentage of TOC removal (Figure 4.6) for all the different initial concentrations of MDEA was found to be approximately 40% at the end of reaction. At the end of the reaction all H₂O₂ has been consumed and hence no further organic carbon was removed.

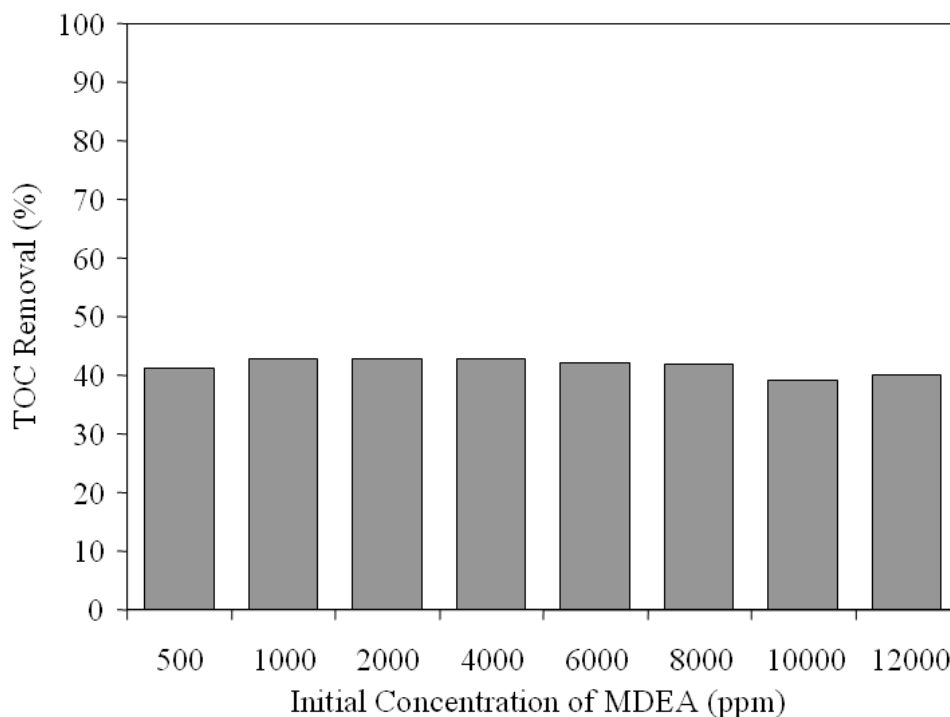


Figure 4. 6 Effect of initial concentration of MDEA on TOC removal (after 360 minute reaction time).

In this preliminary study on effect of initial concentration of MDEA, there was found no optimum concentration for degradation. However, based on the observed results, the suitable initial concentration for this experiment was found to be 2000 ppm of MDEA (=1000 ppm TOC). The maximum degradation occurs at 3 hours, and for this concentration it was found to be accurate and easy to follow the TOC profile with time. Hence all the further experiments were conducted using 2000 ppm of MDEA.

4.1.3 Effect of UV Intensity in Combination with H₂O₂

Experiments were conducted to study the effect of the UV intensity on the organic carbon degradation at three intensity level (3.67 – 12.06 mW/cm²). For an initial concentration of MDEA = 2000 ppm, initial concentration of H₂O₂ = 0.12 M, initial pH = 7.0, temperature = 30 °C, the percentage of TOC removal was found to be

19.37%, 42.42%, and 58.95%, for the UV intensity of 3.67 mW/cm², 7.35 mW/cm², and 12.06 mW/cm² respectively with 180 minutes of reaction time (Figure 4.7).

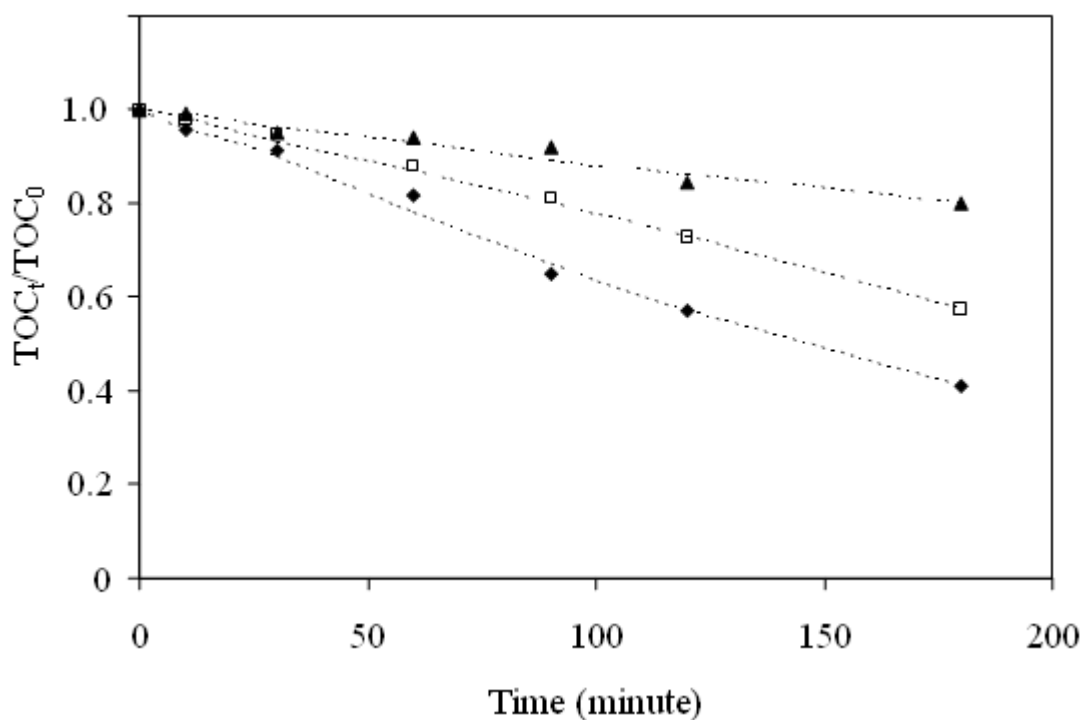


Figure 4. 7 The degradation profile of organic carbon for different UV intensities.

◆ 12.06 mW/cm²; □ 7.35 mW/cm²; ▲ 3.67 mW/cm²

The results showed that degradation rate increased with an increase in UV intensity, which might be attributed to the reason that the effective role of light power towards the formation of high amount of hydroxyl radical in the solution, which are in concurrence with the reported literature [137 – 140]. Qiao *et al.* [135] reported that by increasing UV intensity from 0 to 7.35 mW/cm², the degradation of microcystin-RR was complete within 60 minutes of reaction time Asilian *et al.* [138] reported the same trend for the degradation of polychlorinated biphenyl (PCB) in the water solution by using photochemical process. The degradation efficiency of this compound significantly increased with an increase in UV intensity. Increasing UV intensity will increase the driving force for photolysis reaction, which involves UV energy to excite PCB molecule followed by the cleavage of C-Cl bond. Xu *et al.* [129] reported that increasing UV intensity enhances the degradation of diethyl phthalate in the UV/H₂O₂ process. In addition, oxidative degradation of microcystin-

LR by using UV/H₂O₂ also enhanced by increasing the UV intensity as reported by Ren *et al.* [140].

Based on the results of these experiments and also based on our laboratory limitation, the UV intensity at 12.06 mW/cm² was the highest intensity that gave the highest degradation efficiency i.e. 58.95% TOC removal (Figure 4.8), and hence an intensity of 12.06 mW/cm² was used for further degradation experiments.

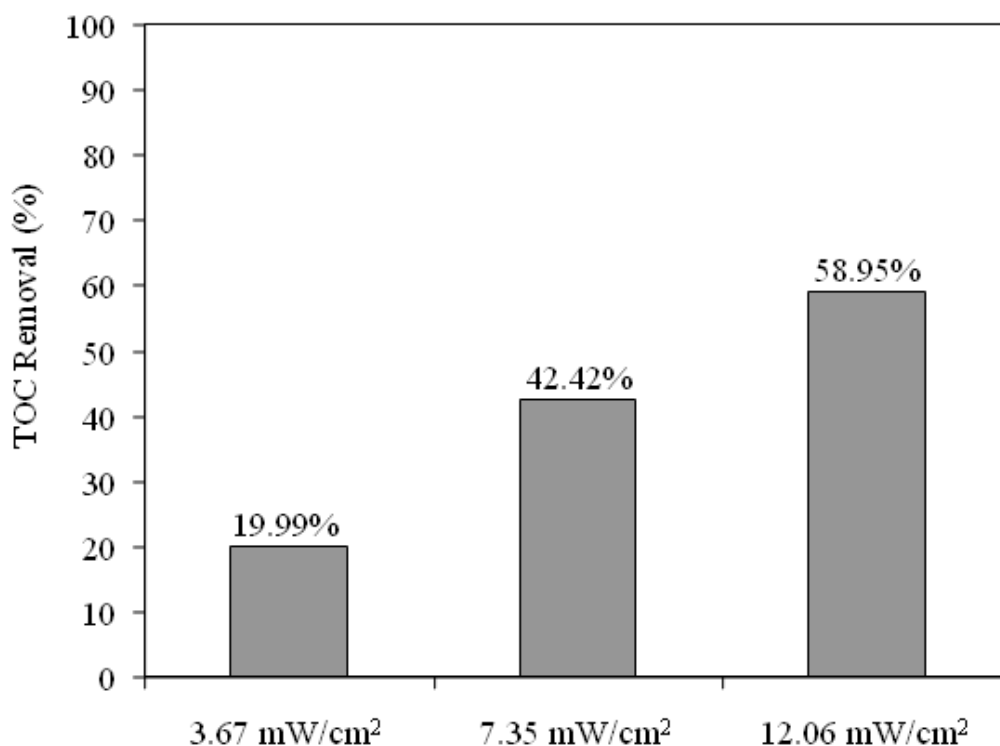


Figure 4. 8 Effect of different UV intensity on TOC removal.

4.1.4 Effect of Initial Concentration of H₂O₂ in Combination with UV

In order to investigate the effect of initial concentration of H₂O₂, six different H₂O₂ concentrations (0.06 M, 0.09 M, 0.12 M, 0.18 M, and 0.24M) were used. The volume of liquid (400 ml), UV intensity (12.06 mW/cm²), MDEA concentration (2000 ppm), pH (7), and temperature (30 °C) were maintained at constant values, while the H₂O₂ concentration was varied from 0 – 0.24 M. Degradation profile of organic carbon at

various initial concentration of H₂O₂ is shown in Figure 4.9 and the TOC removal profile is presented in Figure 4.10.

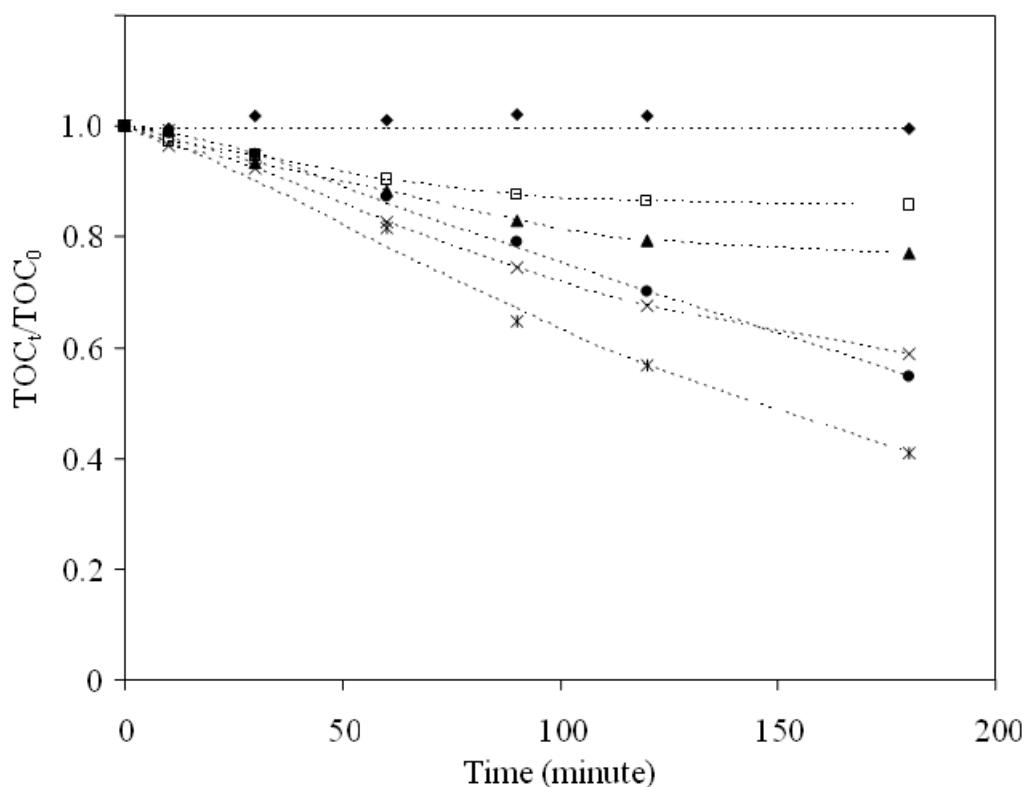


Figure 4. 9 The degradation profile of organic carbon at different initial concentration of H₂O₂.

◆ 0 M; □ 0.06 M; ▲ 0.09 M; × 0.12 M; ✱ 0.18 M; ● 0.24 M

Based on the initial experiments (section 4.1.1), it was found that the hydroxyl radical is the main species to cause the degradation of organic matter. Organic matter was degraded into simpler compounds by oxidation reaction. The hydroxyl radicals were generated from UV photolysis of H₂O₂.



A higher concentration of H₂O₂ is expected to generate more hydroxyl radicals, which enhanced the TOC removal. Based on our preliminary study, the maximum TOC removal i.e. 59.02% was achieved at 0.18 M of H₂O₂, and further increase in

hydrogen peroxide concentration decreased the TOC removal, which might be due to the scavenging effect of H₂O₂ to the hydroxyl radical.

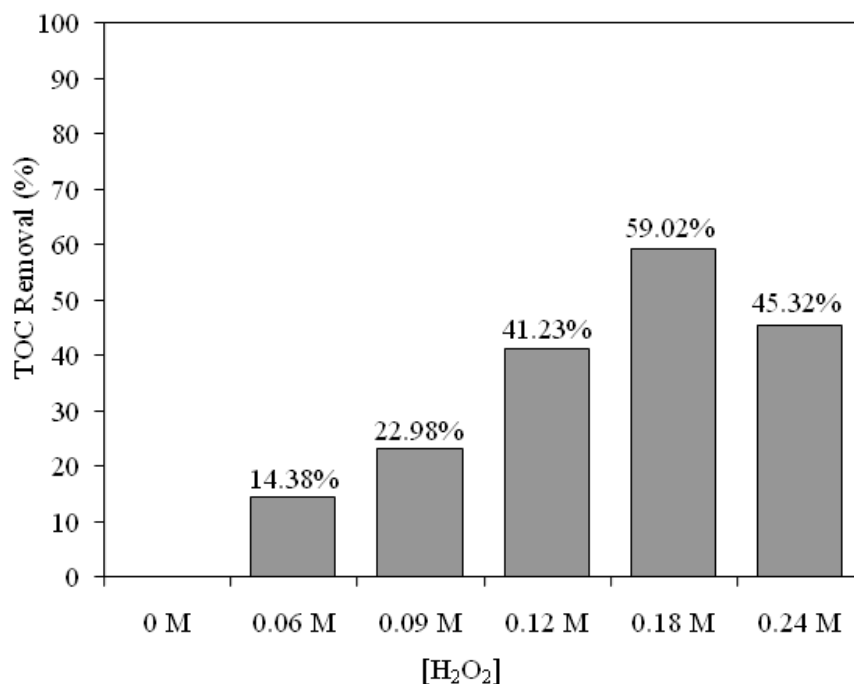
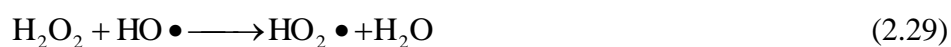


Figure 4. 10 Effect of initial concentration of H₂O₂ on TOC removal (after 180 min).

The reactions of scavenging mechanism of H₂O₂ toward the hydroxyl radical are expressed in Equation 4.29 – 4.30.



Hydroperoxyl radicals (HO₂•) are generated from reaction between hydrogen peroxide (H₂O₂) and hydroxyl radical (HO•) (Equation 2.29). Even though the hydroperoxyl radical is also well known to oxidize the organic matter, but the reactivity of hydroperoxyl is less compared to the hydroxyl radical. In addition, the reaction between hydroperoxyl radical (HO₂•) and hydroxyl radical (HO•) (Equation 2.30) also probably reduce the concentration of hydroxyl radical in the system, which plays as an important species in the degradation process. Hence, the TOC removal was less at higher H₂O₂ concentrations. Similar reports on the optimum

concentration of hydrogen peroxide for UV/H₂O₂ process have also been made by many researchers. Muruganandhan and Swaminathan [70] reported that the optimum hydrogen peroxide concentration was at 20 mmol for the decolorization of azo dye (Reactive Orange 4), and further increase in the initial concentration of H₂O₂ decreased the percentage decolorization. Similarly Malik and Sanyal [79], concluded that the decolorization of azo dye was optimum at 5.88 x 10⁻³ M, and further increase in the H₂O₂ concentration reduced the percentage of decolorization. An optimum concentration of H₂O₂ was also reported for the decolorization of azo dye by UV/H₂O₂ process by Chang *et al.* in 2010 [141]. Increasing H₂O₂ concentration in the system lead to the decomposition rate of azo dye to certain level and further increase in H₂O₂ concentration decreased the decomposition rate.

4.1.5 Effect of pH

The effect of initial pH of the system was studied at five different pH values (pH = 3 to 11) while maintaining the volume of liquid (400 ml); UV intensity (12.06 mW/cm²), concentration of MDEA (2000 ppm); concentration of H₂O₂ (0.18 M); and same temperature (30 °C) as constant. The influence of the initial pH on MDEA degradation using UV/H₂O₂ process is shown in Figure 4.11. The degradation rate of organic carbon increased with an increase in pH up to 9, and further increase in pH reduced the degradation rate of organic carbon. At this optimum pH (pH = 9), the removal of TOC was found to be 79.28%. Figure 4.12 presents the percentage of TOC removal at different initial pH conditions. Further increase in pH beyond 9, resulted in approximately a constant TOC reduction, which might be due to the decomposition of hydrogen peroxide itself at higher pH levels.

At high pH conditions, H₂O₂ tend to ionize to form hydroperoxide anion (HO₂⁻) with pK_a equal to 11.6 (Equation 2.31) [132, 140]. Hydroperoxide anion is well known to be a strong scavenger to hydroxyl radical:



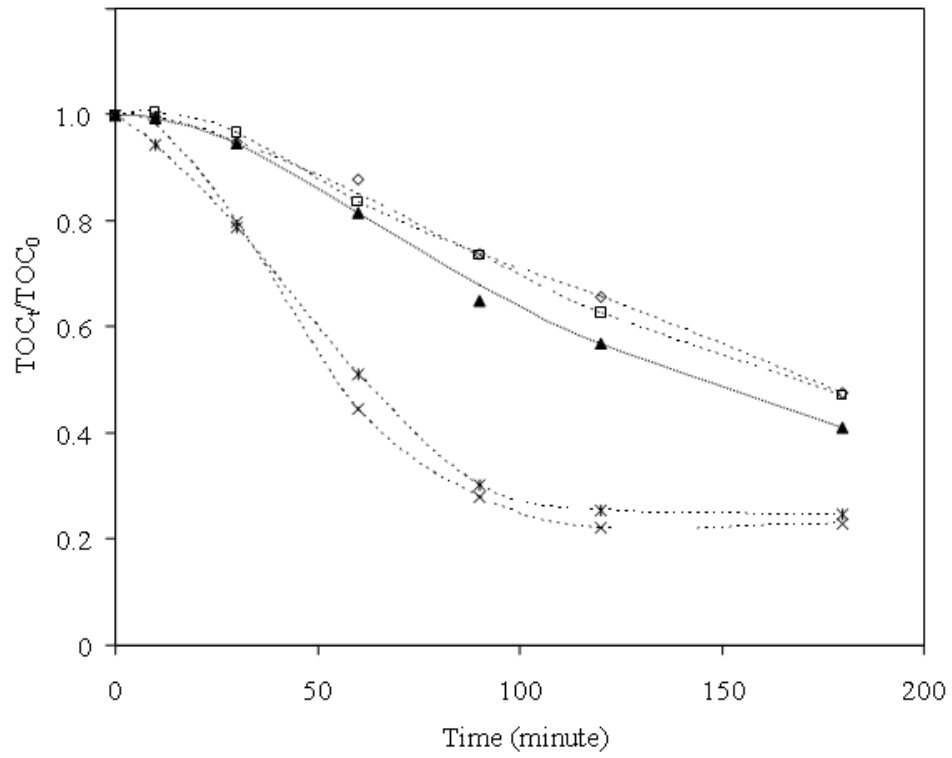


Figure 4. 11 The degradation profile of organic carbon for different initial pH conditions

◇ pH 3; □ pH 5; ▲ pH 7; × pH 9; ✱ pH 11

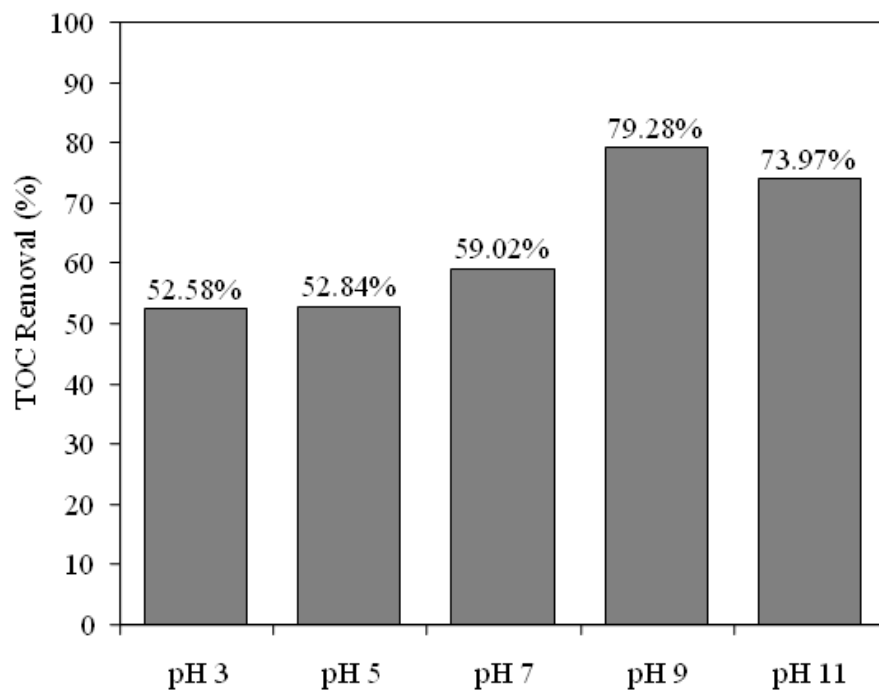


Figure 4. 12 Effect of initial pH condition on TOC removal.

Reaction between hydroperoxide anion (HO_2^-) and hydroxyl radical ($\text{HO}\bullet$) generates a less reactive radical i.e. hydroperoxyl radical ($\text{HO}_2\bullet$) (Equation 2.32) and hence decrease in degradation rate. Similar trend was also reported for the degradation of dimethyl phthalate (DMP) and microcystin-LR (MCLR) using UV H_2O_2 by Xu *et al.* and Ren *et al.*, respectively [132, 140]. They concluded that, the optimum pH for MCLR was at 7.2 and that for DMP was 4.0, for the degradation of the respective compounds using UV/ H_2O_2 process. The optimum pH condition for the degradation of different compounds using UV/ H_2O_2 process depends mainly on the characteristic of the individual compounds.

4.1.6 Effect of Temperature

The effect of reaction temperature on the removal of organic carbon during the MDEA degradation using UV/ H_2O_2 is shown in Figure 4.13. The experiments were carried out at four different temperatures while maintaining the volume of liquid (400 ml), UV intensity (12.06 mW/cm^2), concentration of MDEA (2000 ppm), concentration of H_2O_2 (0.18 M), and pH (7) as constant. Range of temperature studied was $20^\circ\text{C} - 50^\circ\text{C}$.

The effect of temperature was reported by Xu *et al.* [139] for the degradation of diethyl phthalate (DEP) using UV/ H_2O_2 . They concluded that, by varying reaction temperature from 15°C to 31°C did not show any significant change in DEP removal (76.2% to 80.5%, respectively). However it can be seen from Figure 4.13 that by an increase in the temperature up to 40°C , reduction of organic carbon increases very little and beyond which the degradation rate of organic carbon started decreasing.

An increase in the degradation rate of organic carbon with an increase in temperature (20 to 40°C) may be due to the increasing collision frequency between MDEA and hydroxyl radical in the system [142]. Masschelein [31] also stated that the highest effectiveness of LP Hg UV lamp (the UV lamp that was used) to emit the photon was at 40°C . Therefore more photons were provided for photolysis of H_2O_2 .

Hence, more hydroxyl radicals were generated and hence increased the removal of organic carbon up to 67.94 % during the MDEA degradation using UV/H₂O₂ process (Figure 4.14). This result is in agreement with those reported by Li *et al.* [142]. They reported that the degradation rate of clofibric acid in the effluent using UV/H₂O₂ increased by increasing the reaction temperature.

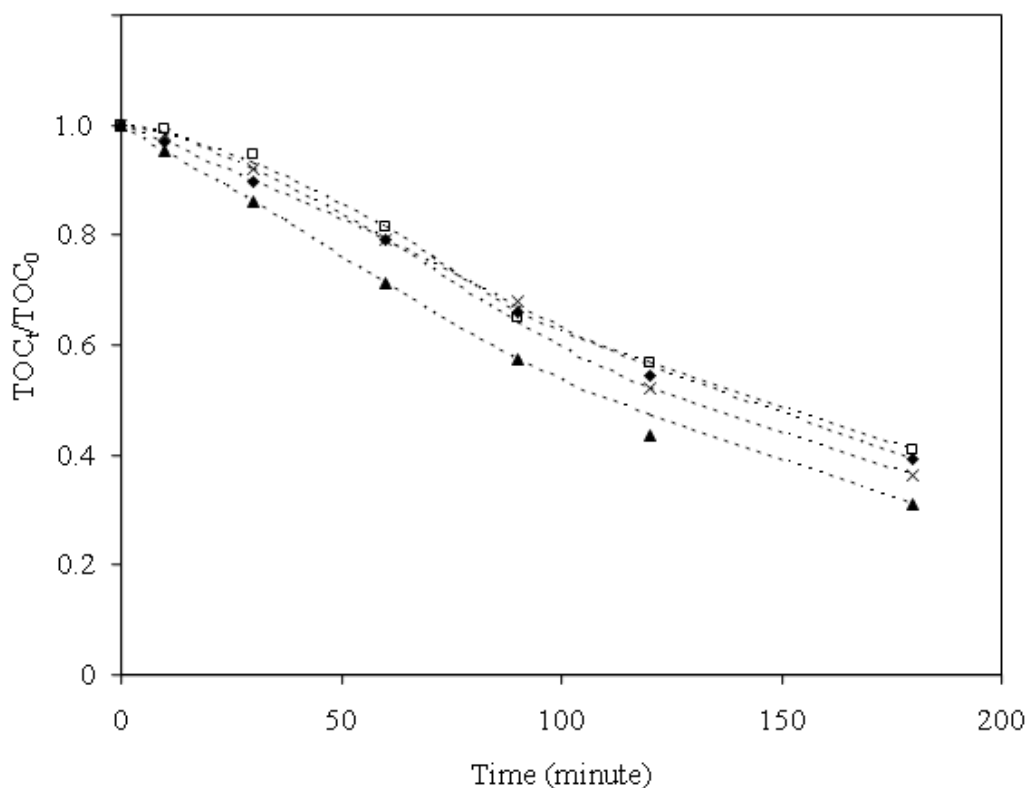


Figure 4. 13 The degradation profile of organic carbon at different temperature

♦ 20 °C; □ 30 °C; ▲ 40 °C; × 50 °C

When the temperature of reaction was at 10 °C, 80 minutes reaction time was required to nearly complete the degradation process, whereas the temperature of reaction was increased to 30 °C, a nearly complete degradation was achieved within 15 minutes of reaction time. In this present study, the reaction temperature beyond 40 °C was found to decrease the degradation rate. This might be due to the decomposition of H₂O₂ itself at higher temperatures [29, 155].

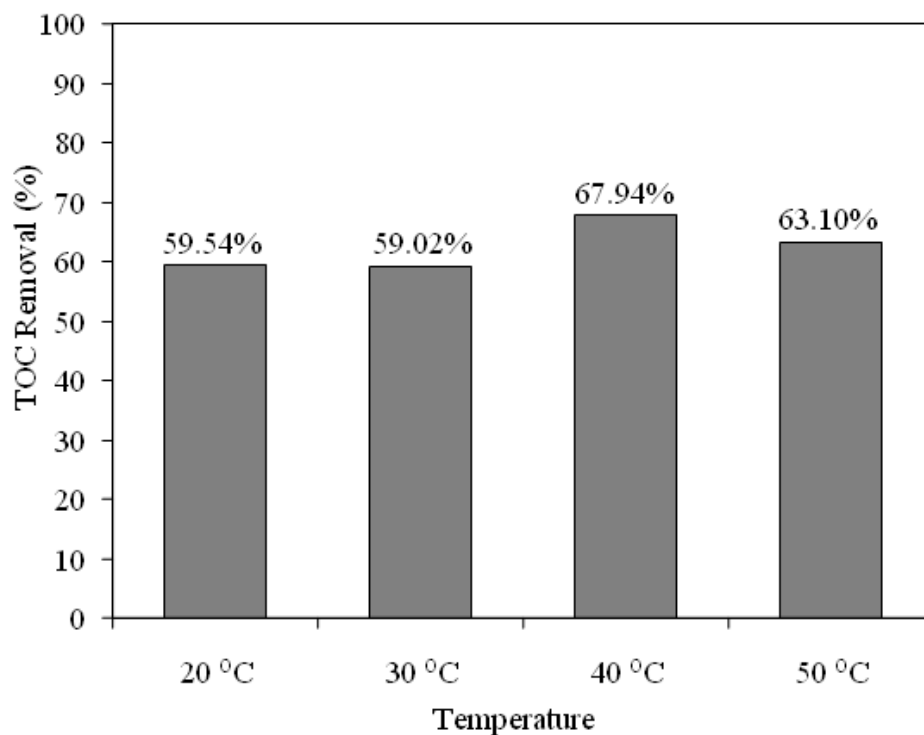


Figure 4. 14 Effect of temperature on TOC removal.

4.1.7 Optimization Process of MDEA Degradation by using UV/H₂O₂

The optimization of MDEA degradation process was initially conducted by screening of factors that influence the degradation process. Factors without optimum values during preliminary experiments were screened based on the limitation of the present equipment capability. The factors screened were UV intensity and initial MDEA concentration. UV intensity at 12.06 mW/cm² was the highest intensity of UV lamp available in the laboratory. The initial concentration of MDEA solution at 1000 ppm of organic carbon was the best concentration to monitor the degradation process. Therefore, these values were chosen for further experiments to screen the other factors. RSM is a well known process to evaluate the effect of each factor and their interaction. The factors screened using RSM were initial concentration of H₂O₂, initial pH, and temperature of reaction. Screening of independent factors affecting the TOC removal was carried out using Box-Behnken design. Three level factors consisting of 2² full factorials with 3 center point were created. The three levels that was chosen

based on the preliminary study was coded as low (-1), middle (0), and high (+1) are presented in Table 4.1.

Table 4. 1 The three levels chosen from the preliminary study.

Factors	Levels		
	Low (-1)	Middle (0)	High (+1)
A: H ₂ O ₂	0.12 M	0.18 M	0.24 M
B: Temperature	30 °C	40 °C	50 °C
C: pH	7	9	11

By applying the Box-Behnken design, the generated matrix design of the experiments is shown in Table 4.2. The combination of three level factors resulting in thirteen (13) experiments, with different possible combination to cover the entire range of variable.

Table 4. 2 Box-Behnken matrix design.

Experiment	Operational parameter		
	pH	H ₂ O ₂ (M)	Temperature (°C)
1	9.0	0.12	50.0
2	11.0	0.18	50.0
3	7.0	0.18	30.0
4	11.0	0.18	30.0
5	9.0	0.24	30.0
6	9.0	0.12	30.0
7	11.0	0.12	40.0
8	7.0	0.18	50.0
9	7.0	0.24	40.0
10	11.0	0.24	40.0
11	7.0	0.12	40.0
12	9.0	0.18	40.0
13	9.0	0.24	50.0

Based on the matrix design, experiments were conducted and the percentages of TOC removal obtained from the experiments were fitted to the second order polynomial equation to represent the present experimental results on TOC removal with other parameters (Equation 4.2).

$$\begin{aligned} \% \text{ TOC removal} = & -511.106 + 56.2002(\text{pH}) + 7.76336(\text{Temperature}) + \\ & 2212.35(\text{H}_2\text{O}_2) - 2.16741(\text{pH})^2 + 20.9167(\text{pH})(\text{H}_2\text{O}_2) - 0.620375(\text{pH})(\text{Temperature}) - \\ & 3954.27(\text{H}_2\text{O}_2)^2 - 21.2887(\text{H}_2\text{O}_2)(\text{Temperature}) + 0.00447125(\text{Temperature})^2 \end{aligned} \quad (4.2)$$

The predicted values according to Equation 4.2, are compared with those obtained from experiments (Table 4.3).

Table 4. 3 Box-Behnken matrix design with experimental and fitted value.

Experiment	Operational parameter			Response (% TOC removal)	
	pH	H ₂ O ₂	Temperature	Observed value	Fitted value
1	9.0	0.12	50.0	43.92	42.71
2	11.0	0.18	50.0	22.14	22.90
3	7.0	0.18	30.0	65.00	64.24
4	11.0	0.18	30.0	73.63	73.60
5	9.0	0.24	30.0	82.45	83.66
6	9.0	0.12	30.0	43.47	43.05
7	11.0	0.12	40.0	23.08	23.53
8	7.0	0.18	50.0	63.14	63.17
9	7.0	0.24	40.0	54.49	54.04
10	11.0	0.24	40.0	44.79	43.61
11	7.0	0.12	40.0	42.82	44.00
12	9.0	0.18	40.0	64.07	64.20
13	9.0	0.24	50.0	31.81	32.23

The experimental value ($R^2 = 0.9980$) of TOC removal satisfactory agree with those predicted using Equation 4.2, which are shown in Figure 4.15, proving the validity of the second order polynomial model (Equation 4.1) for representing the present degradation of MDEA using UV/H₂O₂ oxidation process.

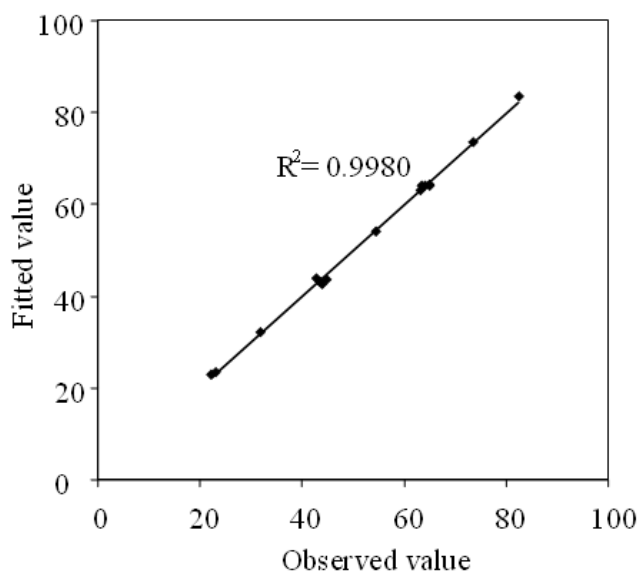


Figure 4. 15 Relation between experimental value and fitted value of TOC removal.

Pareto chart of the standardized effect at $P = 0.05$ (Figure 4.16) clearly shows the standardized effects of factors and interaction between each factor affecting TOC removal.

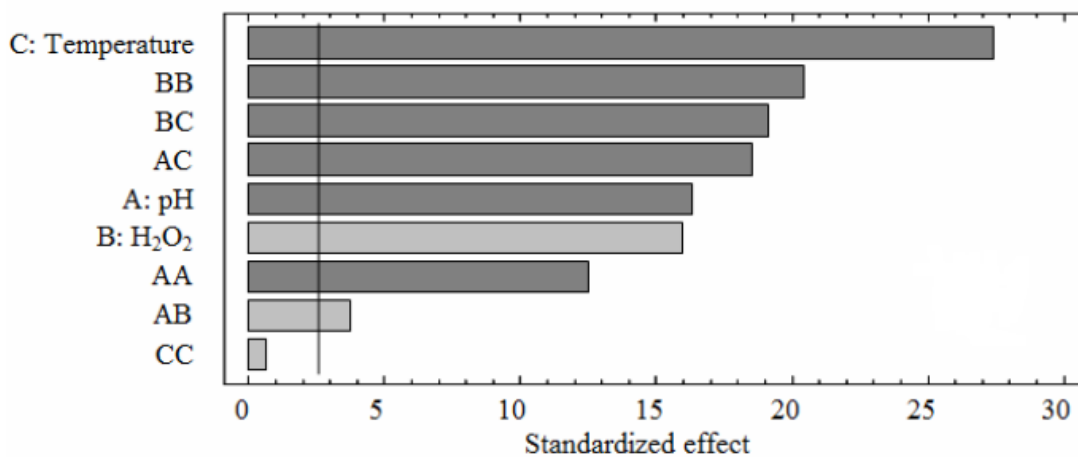


Figure 4. 16 Pareto chart of the standardized effect for percentage TOC removal for screening of significant factors for the degradation of MDEA.

□ + ; ■ -

The order of the most significant factor for increasing TOC removal is: initial concentration of H_2O_2 > interaction between pH and H_2O_2 > quadratic temperature. Meanwhile, the order of the most significant factor to reduce the TOC removal is: temperature > quadratic H_2O_2 > interaction between H_2O_2 and temperature > interaction between pH and temperature > pH > quadratic pH.

ANOVA analysis was performed to identify the significant factors affecting the TOC removal at P-value = 0.05 and the results of ANOVA analysis is presented in Table 4.4. A significant factor affecting the TOC removal was indicated by P-value of less than 0.05. Table 4.4 shows that the quadratic factor of temperature gave insignificant effect (P-value = 0.5489) and the other factors and their interaction gave a significant effect for TOC removal (P-value < 0.05).

Table 4. 4 ANOVA analysis for TOC removal of synthetic MDEA waste.

Source	Sum of Squares	Df	Mean Square	F-Ratio	P-Value
A:pH	477.56	1	477.56	267.01	0.0000
B: H_2O_2	453.713	1	453.713	253.68	0.0000
C:Temperature	1340.14	1	1340.14	749.29	0.0000
AA	277.523	1	277.523	155.17	0.0001
AB	25.2004	1	25.2004	14.09	0.0132
AC	615.784	1	615.784	344.29	0.0000
BB	748.231	1	748.231	418.35	0.0000
BC	652.624	1	652.624	364.89	0.0000
CC	0.738169	1	0.738169	0.41	0.5489
Total error	8.94274	5	1.78855		
Total (corr.)	4551.51	14			

In order to examine the effect of factors towards the responses, a graphical representation known as contour plots of regression model obtained using Equation 4.2 is shown in Figure 4.17. As illustrated in Figure 4.17, increasing concentrations of H_2O_2 to a certain level causes an increase in TOC removal, due to the increasing sources of available hydroxyl radicals.

Further increase of H_2O_2 will decrease TOC removal, which could be related to the scavenging effect of H_2O_2 itself, leading to a decrease in H_2O_2 concentration in the system. In addition, by increasing the pH to a certain level will increase the removal of TOC, which might be due to the reason that hydroxyl radical oxidation mechanism for compounds containing nitrogen atoms are favorable at higher pH levels [89]. However, further rise in pH lead to a reduction in TOC removal, due to the decomposition of H_2O_2 itself at higher pH.

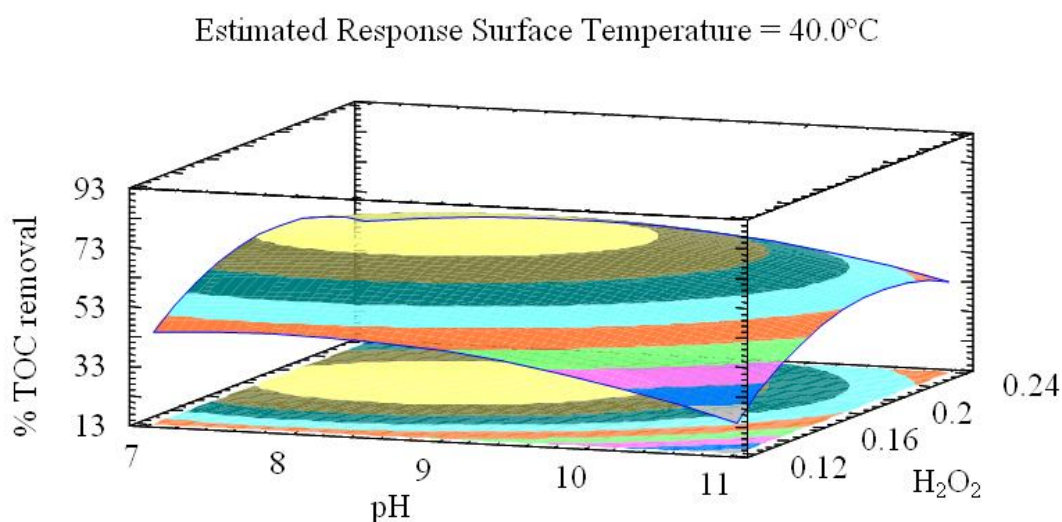
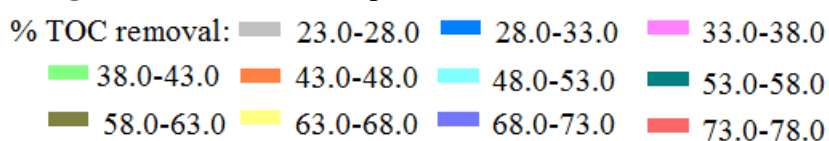


Figure 4. 17 3D Contour plots of TOC removal for MDEA.



Based on the contour plots of TOC removal (Figure 4.17), the optimum conditions for the degradation of MDEA using UV/ H_2O_2 process at initial concentration of MDEA = 2000 ppm (= 1000 ppm of TOC) and UV intensity = 12.06 mW/cm^2 are: temperature = 30 °C, pH = 9.76, and the concentration of H_2O_2 = 0.22 M (Table 4.5), in the other words, the molar ratio between MDEA (TOC (M)) to H_2O_2 (M) = 1:2.56.

Table 4. 5 Optimum condition for the degradation of MDEA by using UV/H₂O₂ at initial TOC = 1000 ppm; UV light intensity = 12.06 mW/cm².

Factor	Optimum condition
H ₂ O ₂	0.22 M
pH	9.76
Temperature	30 °C

Experiments were conducted (in duplicate), using the obtained optimum condition and the estimated TOC removal was 85.74%, which satisfactory agree with the predicted value of 86.05% (Figure 4.18) indicating the validity of the present proposed Equation 4.2. The deviation between the experimental value and the predicted value was estimated to be 0.31%.

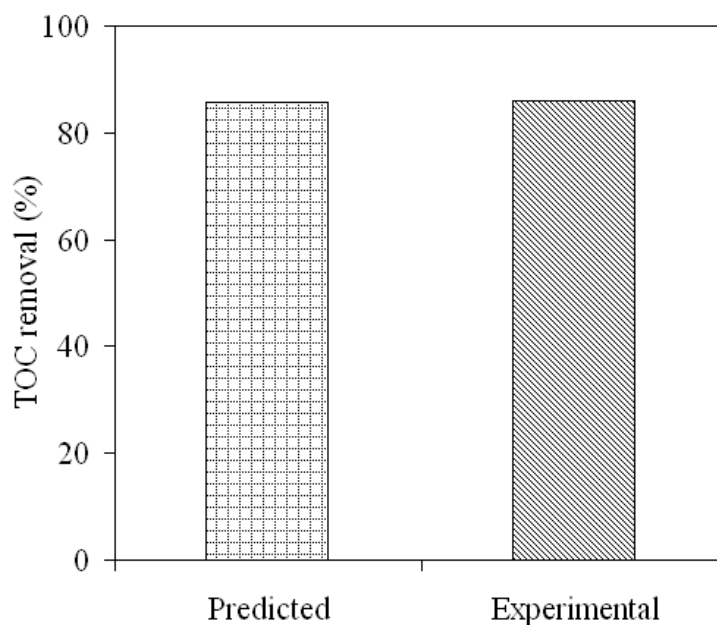


Figure 4. 18 Comparison of predicted and experimental TOC removal at optimum condition.

4.2 Degradation Intermediates Identification and Development of Degradation Mechanism

Degradation of aqueous MDEA solution using UV/H₂O₂ has been studied. MDEA (C₅H₁₃O₂N) is a compound containing the elements namely C, H, O, and N and the structure is shown in Figure 2.1. For the identification of degradation intermediates, experiments were conducted using the following conditions: [MDEA]₀ = 2000 ppm (= 1000 ppm TOC), [H₂O₂]₀ = 0.22 M, initial pH = 9.76, temperature = 30 °C, UV intensity = 12.06 mW/cm², and reaction time = 3 hours. The end products after the complete degradation of MDEA containing these elements, using hydroxyl radical (HO•) is expected to be CO₂, H₂O, NH₃/NH₄⁺, NO₂⁻, NO₃⁻, and N₂.

Based on the analysis of the degradation intermediates obtained during the degradation of MDEA, using UV/H₂O₂ process, the identified organic by-products are: oxalic acid (C₂H₂O₄), acetic acid (CH₃COOH), formic acid (HCOOH), and the inorganic by-product are: nitrate (NO₃⁻), nitrite (NO₂⁻), ammonium (NH₄⁺), and carbon dioxide (CO₂). Figure 4.19 shows the profile of inorganic by-products during UV/H₂O₂ process.

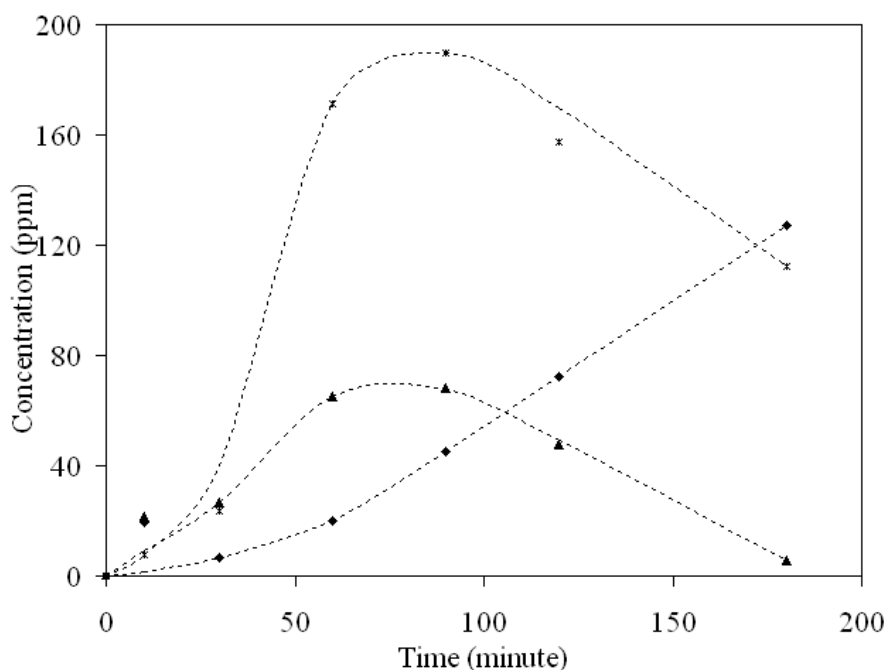


Figure 4. 19 Inorganic by-product profile during the UV/H₂O₂ process.

◆ Nitrate; ▲ Nitrite; × Ammonium

It can be seen that the concentration of ammonium and nitrite increased until 90 minutes and then decreased with reaction time. Oxidation of both ammonium and nitrite by hydroxyl radical resulted in the production of nitrate. The concentration of nitrate increased along with the decrease in ammonium (NH_4^+) and nitrite (NO_2^-) concentration.

Similar by-products such as ammonium and nitrate were also identified and reported by Klare *et al.* [89] and Low *et al.* [87]. Klare *et al.* identified $\text{NH}_3/\text{NH}_4^+$, nitrate (NO_3^-), and nitrite (NO_2^-) as intermediate products in the partially degraded secondary amine. Low *et al.* [87] also found ammonium (NH_4^+) and nitrate (NO_3^-) during the degradation of organic compound containing nitrogen atom. Both researchers used TiO_2 mediated photo-catalytic technique for degradation. Many other researchers who identified the inorganic by-products containing nitrogen atom during their study on AOP for the degradation of organic compound containing nitrogen atom are listed in Table 2.10.

Identification of organic by-products during the degradation of MDEA using UV/ H_2O_2 was conducted using high performance liquid chromatography (HPLC). The chromatogram obtained using YMC-Pack PolymerC18 column is shown in Figure 4.20. After 30 minutes of radiation, one of the intermediate products was identified as oxalic acid, which appeared at 3.9 minutes of retention time. Other by-products could not be identified using this column and hence Transgenomic column was used, which show the presence of two more organic acids. Those two by-products were identified as acetic acid (RT = 8.1 min) and formic acid (RT = 8.9 min), respectively (Figure 4.21). Organic by-products profile during UV/ H_2O_2 process is presented in Figure 4.22.

As reported by many researchers [60, 89, 143], degradation of organic compound containing amino group by using hydroxyl radical is highly dependent on pH. At low pH, free electron pair of nitrogen atom was protonated, and resulting in the deactivation of $\alpha - \text{CH}$ bond [33, 89]. Hence, the hydroxyl radical can only attack the further location of CH bond after $\alpha - \text{CH}$ bond. Meanwhile, at any $\text{pH} \geq 7$, free electron pair of nitrogen atom was un-protonated. In this condition, hydroxyl radical can attack the free electron pair of nitrogen atom and the $\alpha - \text{CH}$ bond [144 – 145]. However, steric effect of components attached to the nitrogen atom was also

identified. The steric effect drives the ability of hydroxyl radical to attack the electron pair of nitrogen atom [89].

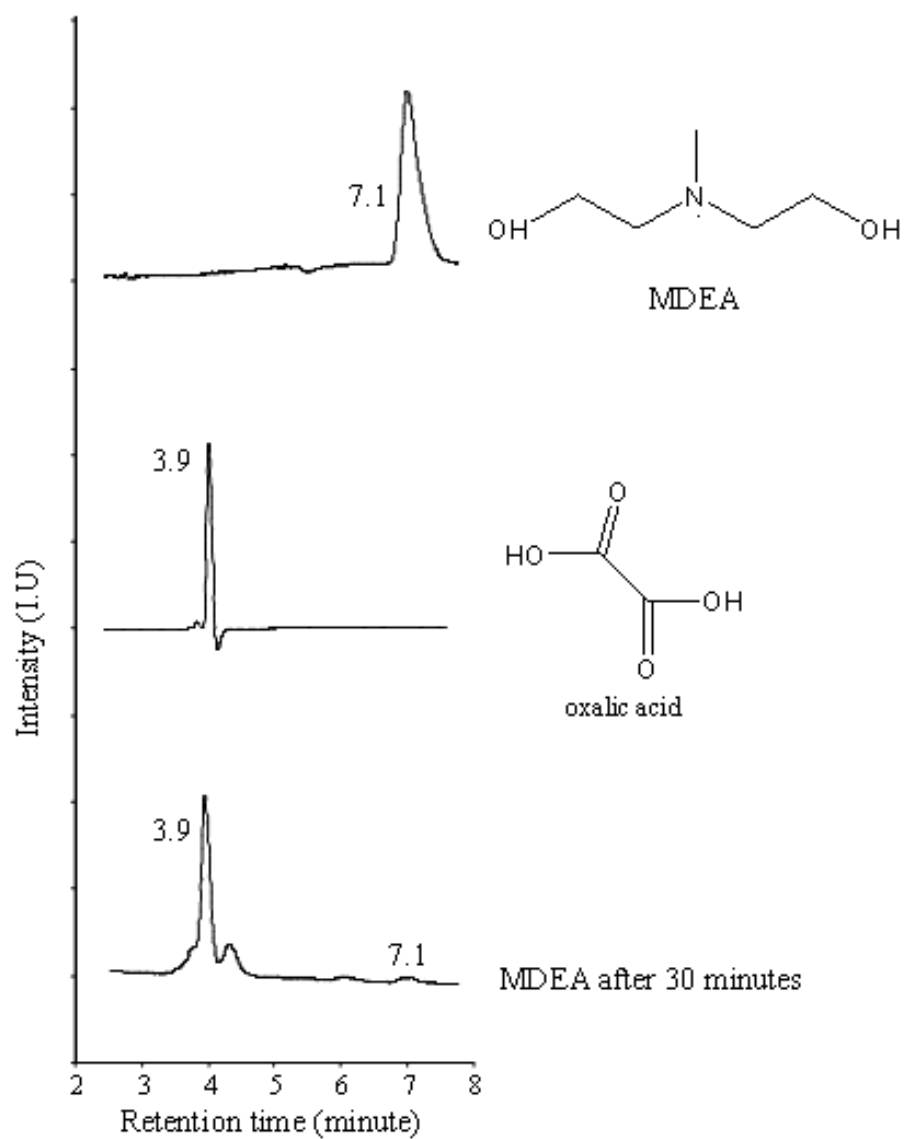


Figure 4. 20 Chromatogram of partially degraded MDEA after UV/H₂O₂ process using YMC-PolymerC18 column.

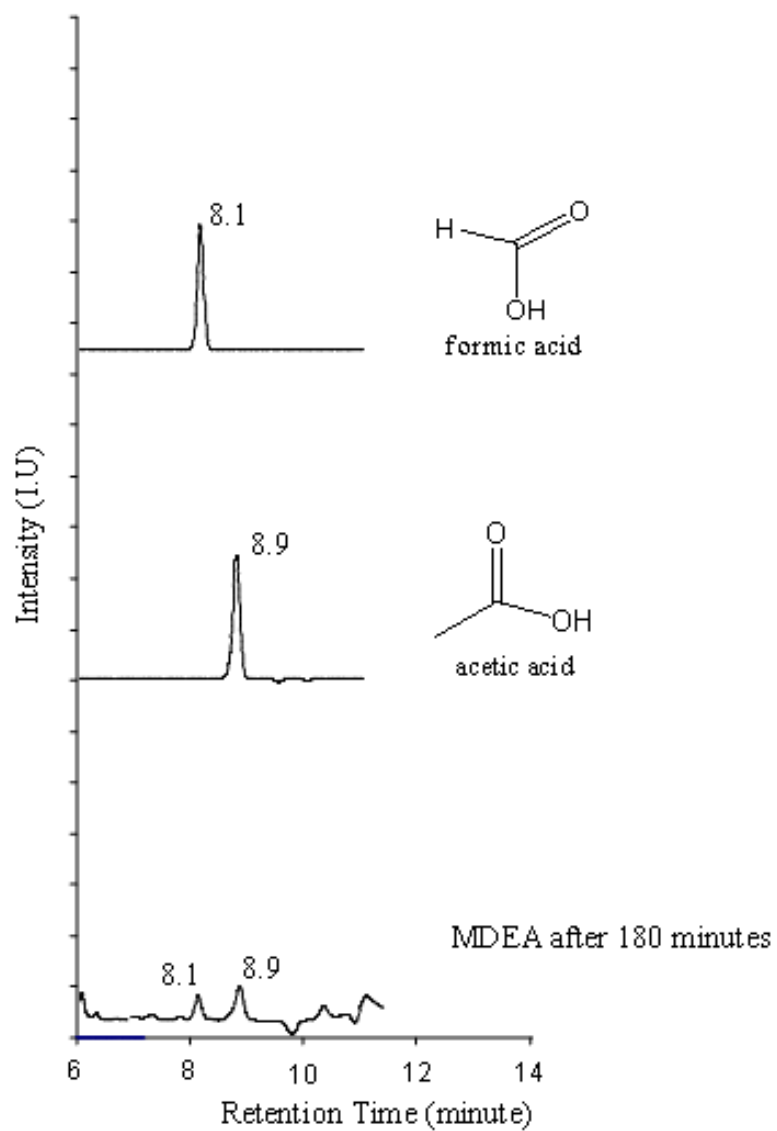


Figure 4. 21 Chromatogram of partially degraded MDEA after UV/H₂O₂ using Transgenomic column.

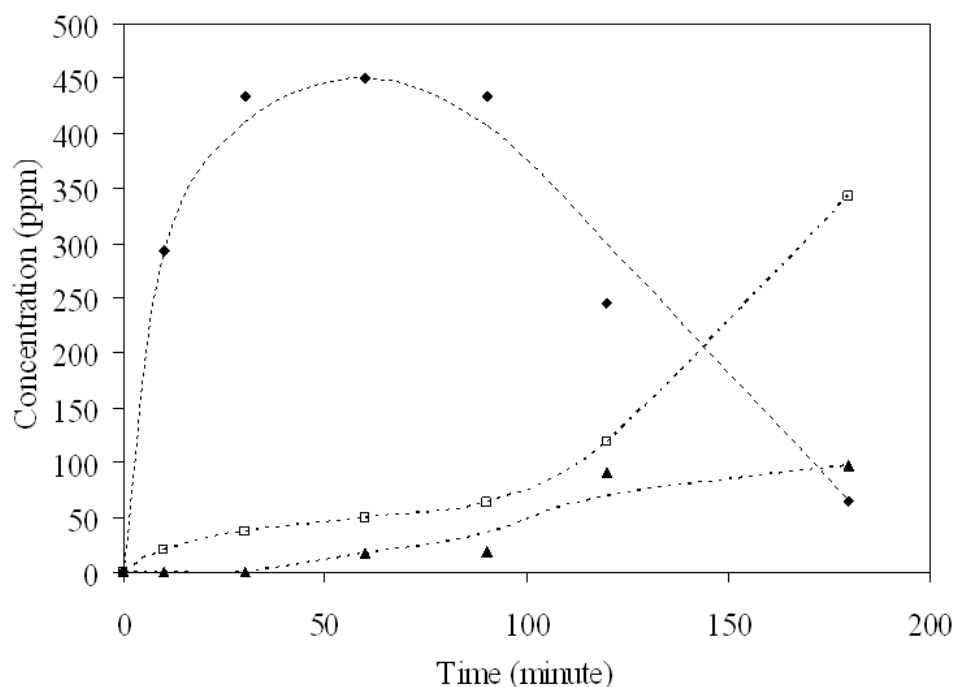


Figure 4. 22 Organic by-products profile during the UV/H₂O₂ process.

◆ Formic acid; □ Oxalic acid; ▲ Acetic acid

Based on the observation of inorganic (Figure 4.19) and organic by-products (Figure 4.22) profiles, initially formic acid was formed as a by-product. The proposed mechanism of MDEA mineralization by hydroxyl radical can be explained as follows. Initially hydroxyl radical was generated by H₂O₂ photolysis. MDEA consist of two groups of ethanol and one methyl. During the mineralization of MDEA by hydroxyl radical, initially hydroxyl radical attacked α – CH bond of methyl group by taking one H to form water (H₂O) [31] and a radical compound, through hydrogen abstraction (Figure 4.23, scheme 1). Further, the hydroxyl radical attacked the organic compound radical (electrophilic addition) [32] and then cleaved the C-N bonds. During the next step, formic acid was produced. Acetic and oxalic acids appeared later. The formation of these two organic acids occurred by cleavage of C-N bonds of the ethanol groups attached to the nitrogen atom of MDEA [89]. Further oxidation of by-products by hydroxyl radical (Figure 4.24, schemes 2, 3, 4, 5, and 6) would result in the formation of few end products such as ammonium (NH₄⁺), nitrate (NO₃⁻), nitrite (NO₂⁻), and carbon dioxide (CO₂). Figure 4.23 and 4.24 show the proposed mineralization mechanism of MDEA by hydroxyl radical.

Scheme 1

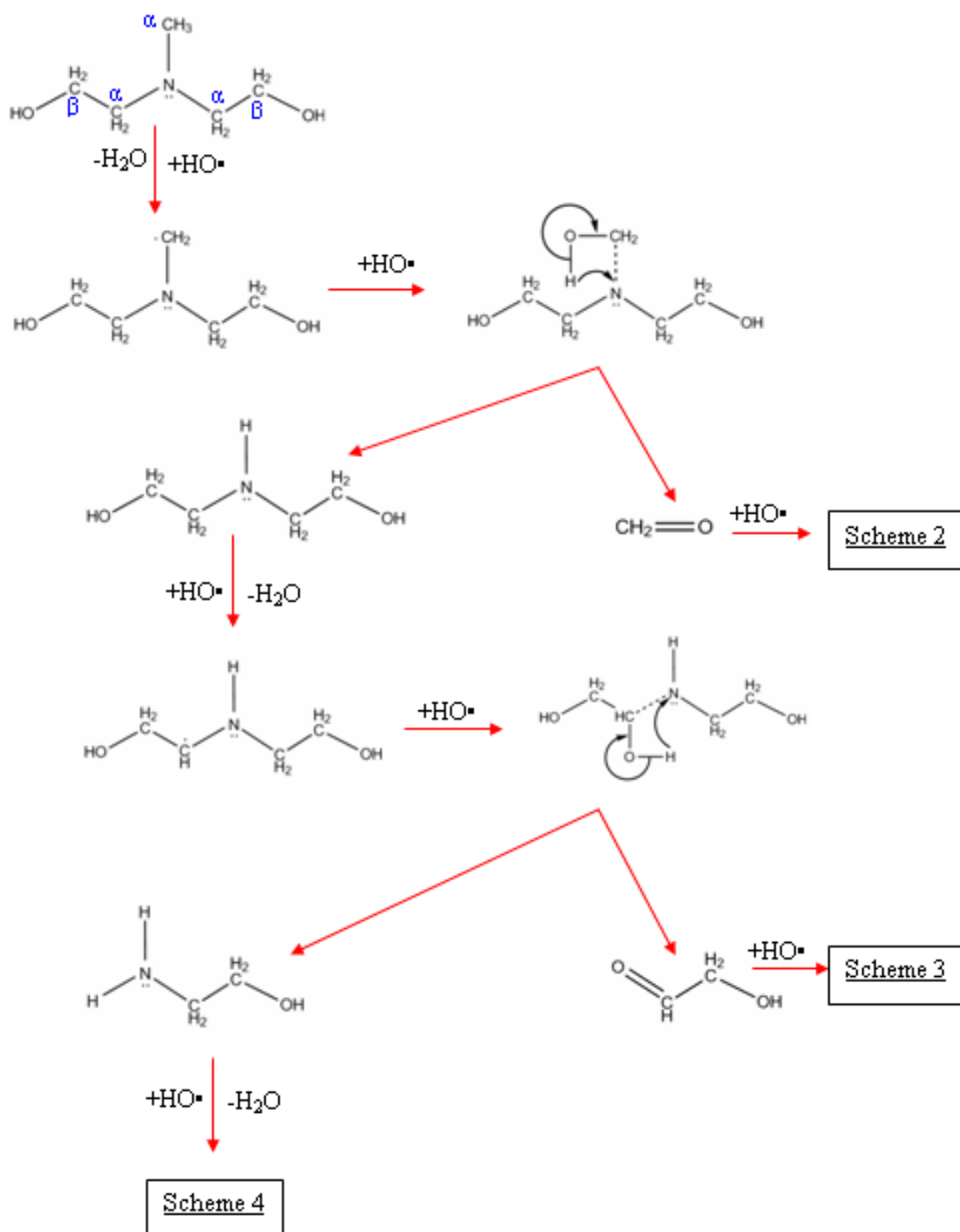
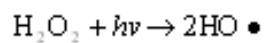
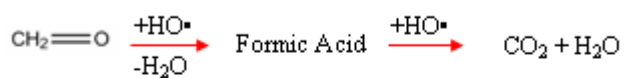
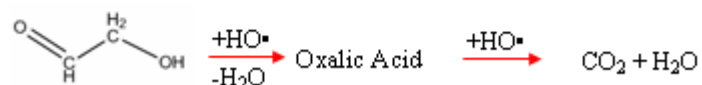


Figure 4. 23 The initial stages of MDEA mineralization by hydroxyl radical.

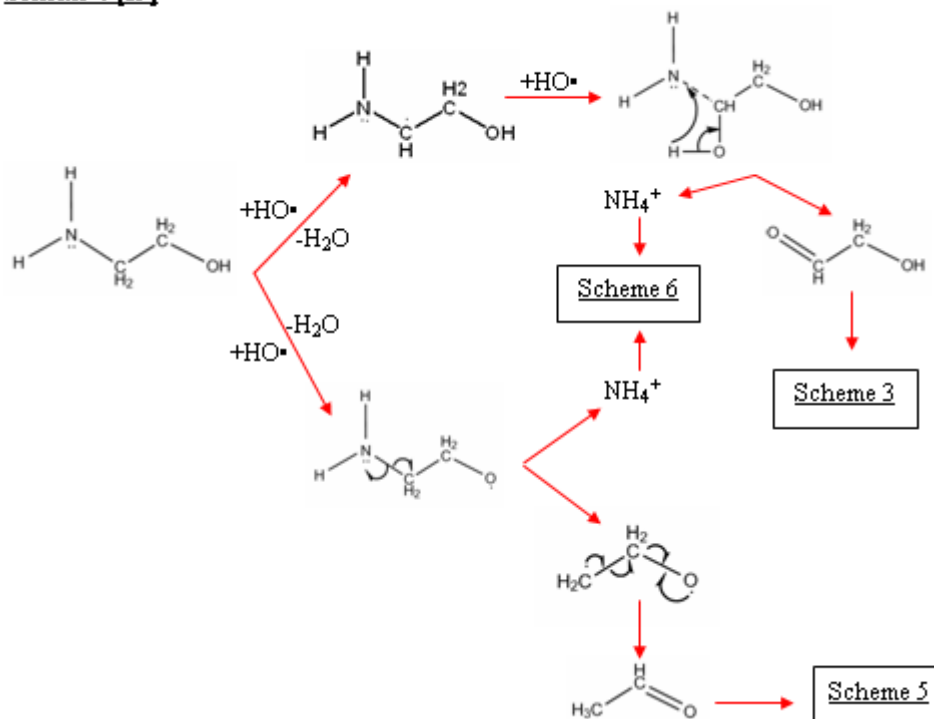
Scheme 2 [157]



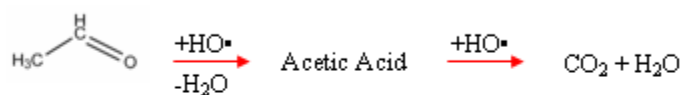
Scheme 3



Scheme 4 [89]



Scheme 5



Scheme 6 [87]

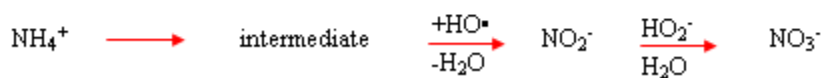


Figure 4. 24 Reaction pathways of intermediate degradation by hydroxyl radical.

4.3 Kinetics of MDEA Mineralization Process

4.3.1 Determination of Kinetic Constants of MDEA Mineralization

In order to follow the kinetics of MDEA mineralization, a set of experiments were conducted, using the following condition: intensity of UV lamp = 12.06 mW/cm², irradiation time = 3 hours, oxidation temperature = 20, 30, 40, and 50 °C, initial pH = 9.76 (optimum pH), and initial H₂O₂ concentration was varied from 0 - 0.22 M. In this study, the mineralization process was monitored by measuring the total organic carbon (TOC) of the samples during the process (Figure 4.25 and Figure 4.26).

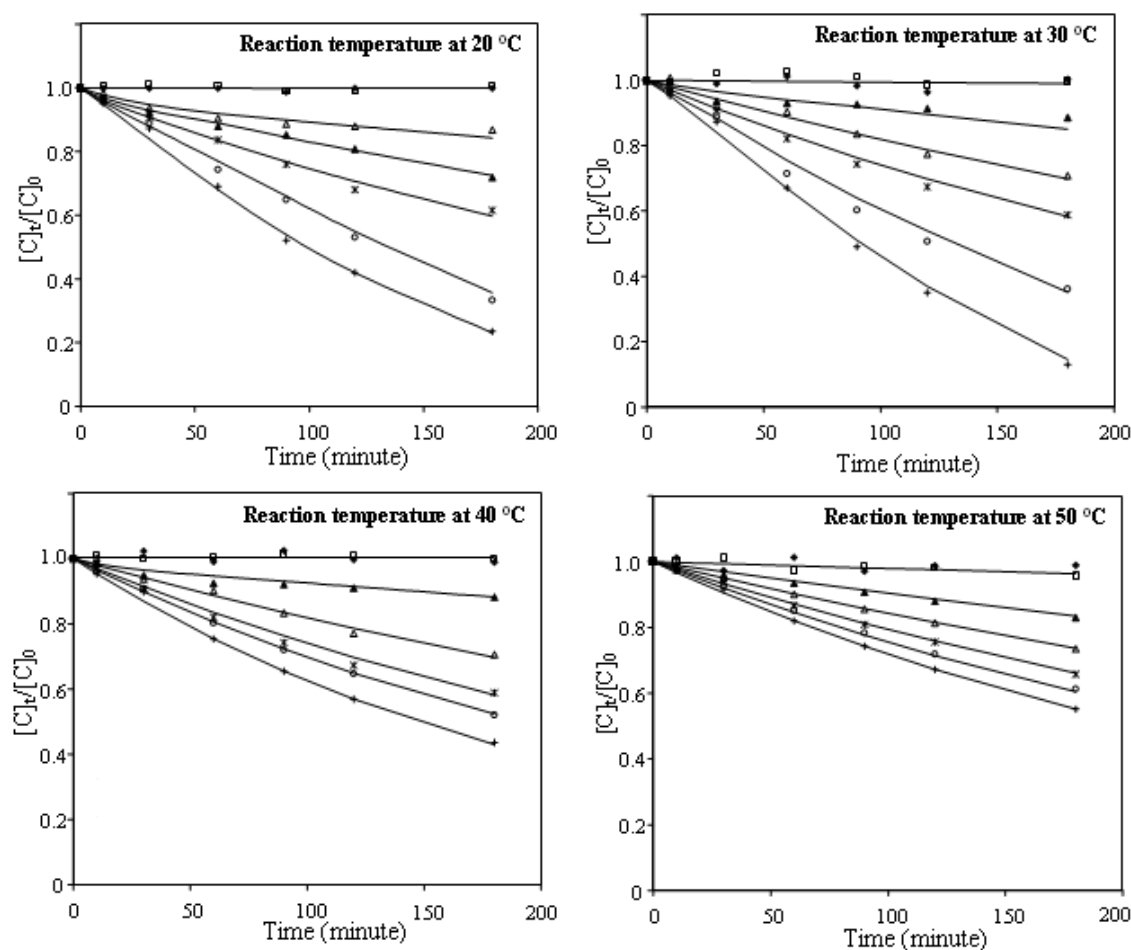


Figure 4. 25 MDEA mineralization profile at different initial concentration of H₂O₂.

• No UV □ 0 M ▲ 0.06 M ▲ 0.09 M * 0.12 M ° 0.18 M + 0.22 M

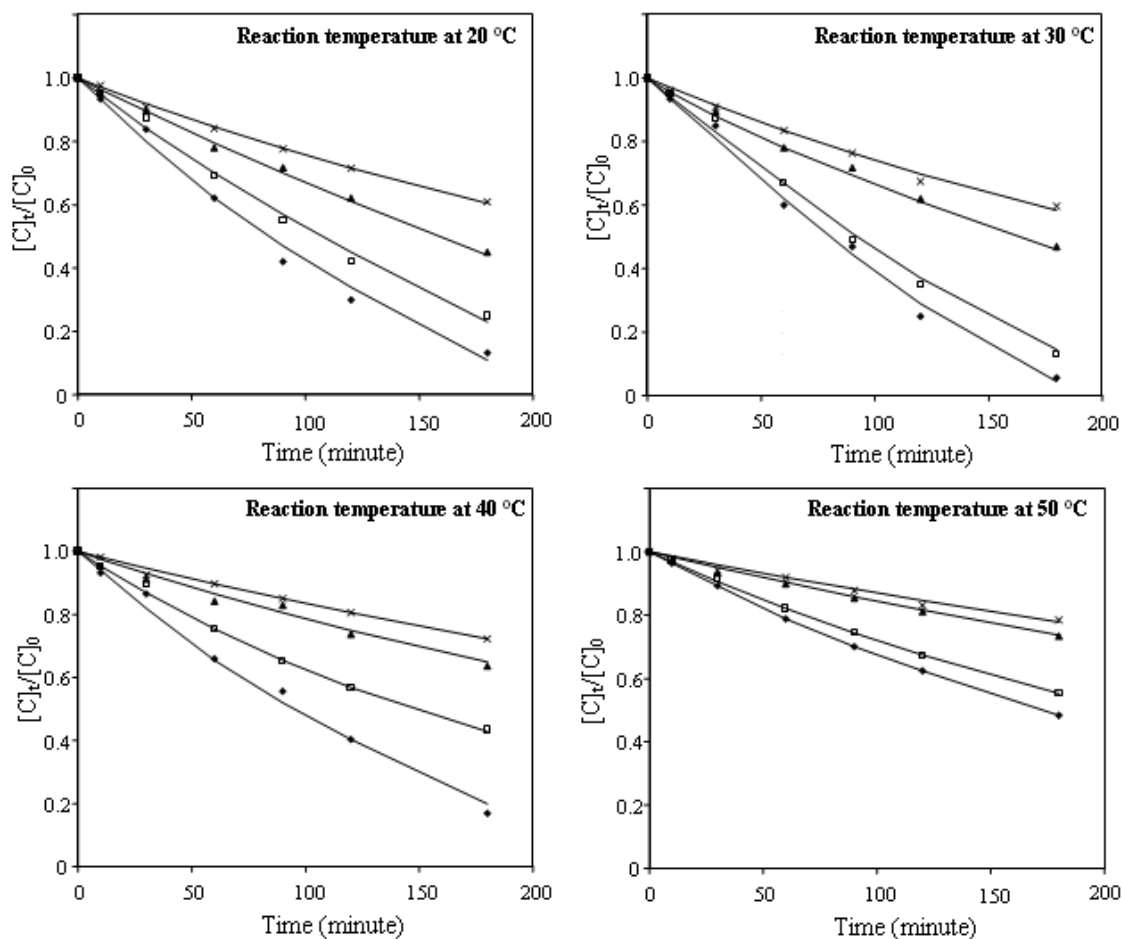


Figure 4. 26 MDEA mineralization profile at different initial concentration of contaminant.

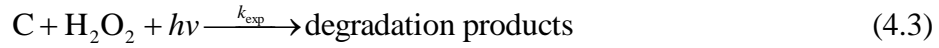
• 0.042 M □ 0.085 M ▲ 0.128 M × 0.180 M

Based on the proposed scheme of mechanism (Figure 4.23 and 4.24), during the mineralization process some intermediate products were formed, however not all the intermediate products could be detected using the analytical equipments available in the laboratory, hence the determination of rate constants were conducted based on the changes of TOC and H_2O_2 during the UV/ H_2O_2 process. The estimated experimental reduction rates of MDEA during the initial 30 minutes are presented in Table 4.6.

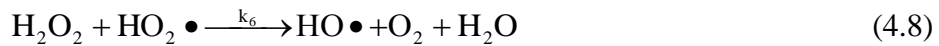
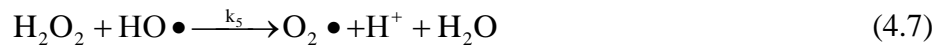
Table 4. 6 Estimated reduction rates at initial 30 minutes.

Temp. (°C)	Experimental	[C] ₀ (M)	[H ₂ O ₂] ₀ (M)	[-d[C] ₀ /dt] (M min ⁻¹)	Slope; R ²
20	[C] ₀ = constant	0.0847	0.0615	0.000180	Slope = 0.5350 R ² = 0.9991 (Figure 4.27)
		0.0847	0.0900	0.000221	
		0.0851	0.1210	0.000260	
		0.0847	0.1810	0.000317	
		0.0852	0.2220	0.000359	
	[H ₂ O ₂] ₀ = constant	0.0432	0.2230	0.000235	Slope = 0.5949 R ² = 0.9993 (Figure 4.28)
		0.0852	0.2220	0.000359	
		0.1280	0.2170	0.000449	
		0.1825	0.2170	0.000556	
30	[C] ₀ = constant	0.0847	0.0615	0.000179	Slope = 0.5354 R ² = 0.9991 (Figure 4.27)
		0.0847	0.0900	0.000221	
		0.0850	0.1210	0.000260	
		0.0847	0.1810	0.000317	
		0.0852	0.2230	0.000359	
	[H ₂ O ₂] ₀ = constant	0.0432	0.2220	0.000235	Slope = 0.5947 R ² = 0.9993 (Figure 4.28)
		0.0852	0.2230	0.000359	
		0.1280	0.2170	0.000448	
		0.1825	0.2170	0.000556	
40	[C] ₀ = constant	0.0851	0.0615	0.000144	Slope = 0.5544 R ² = 0.9995 (Figure 4.27)
		0.0850	0.0900	0.000178	
		0.0851	0.1210	0.000210	
		0.0853	0.1800	0.000263	
		0.0850	0.2210	0.000290	
	[H ₂ O ₂] ₀ = constant	0.0432	0.2220	0.000194	Slope = 0.5740 R ² = 0.9983 (Figure 4.28)
		0.0850	0.2210	0.000290	
		0.1278	0.2210	0.000370	
		0.1830	0.2210	0.000457	
50	[C] ₀ = constant	0.0848	0.0610	0.000113	Slope = 0.5672 R ² = 0.9998 (Figure 4.27)
		0.0848	0.0900	0.000140	
		0.0850	0.1210	0.000167	
		0.0850	0.1830	0.000210	
		0.0850	0.2210	0.000233	
	[H ₂ O ₂] ₀ = constant	0.0432	0.2220	0.000156	Slope = 0.5785 R ² = 0.9998 (Figure 4.28)
		0.0850	0.2210	0.000233	
		0.1280	0.2180	0.000293	
		0.1840	0.2180	0.000361	

The general mineralization process using UV/H₂O₂ process can be explained as follows (Equation 4.3 – 4.5):



where C is the substrate (MDEA). Hydroxyl radical is well known as a non selective oxidator. Consequently, the hydroxyl radical reacts with H₂O₂ during oxidation process to produce less reactive radicals such as hydroperoxyl radical (HO₂ •) and O₂ • [146]. This reaction is known as scavenging reaction. These scavenging reactions during MDEA mineralization can be expressed as follows (Equation 4.6 – 4.8):



De *et al.* [146] estimated the hydroxyl radical reaction rate constants for phenol and chlorinated phenols by using UV/H₂O₂ photo-oxidation. A similar approach is considered for the present study on the mineralization of MDEA. Hence the rate of mineralization $-\frac{d[C]}{dt}$ could be expressed as (Equation 4.9):

$$-\frac{d[C]}{dt} = k_3[C][HO \bullet] \quad (4.9)$$

where $[C]$ is the concentration of substrate, $[\text{HO}_2 \bullet]$ is the concentration of hydroxyl radical, and k_3 is the hydroxyl radical rate constants for MDEA mineralization. During the oxidation process, the scavenging reaction occurs and the hydroxyl radicals react with H_2O_2 to form other less reactive radicals such as $\text{HO}_2 \bullet$ and $\text{O}_2 \bullet$. UV photolysis of H_2O_2 (Equation 4.4) and the reaction of $\text{HO}_2 \bullet$ with H_2O_2 (Equation 4.8) led the formation of $\text{HO} \bullet$ radical, while the reaction of $\text{HO} \bullet$ with the substrate (Equation 4.5) and H_2O_2 (Equation 4.6 and 4.7) led to the disappearance of $\text{HO} \bullet$ in the system. Rate of formation of $\text{HO} \bullet$ by UV photolysis of H_2O_2 can be expressed as $\left[\frac{\Phi_{\text{H}_2\text{O}_2} W_{\text{abs},\text{H}_2\text{O}_2}}{V} \right]$

[32, 146], where $\Phi_{\text{H}_2\text{O}_2}$ is the quantum yields of the photolysis of H_2O_2 (mol/E), $W_{\text{abs},\text{H}_2\text{O}_2}$ is the radiation flow rate absorbed by H_2O_2 (E/s), and V is the volume of irradiated solution (L). The formation of $\text{HO}_2 \bullet$ is expressed by Equation 4.6 and the disappearance of $\text{HO}_2 \bullet$ is expressed by Equation 4.8. According to the above reactions (Equation 4.4 and 4.8), the rate of formation of $\text{HO} \bullet$ is equal to $\left[\frac{\Phi_{\text{H}_2\text{O}_2} W_{\text{abs},\text{H}_2\text{O}_2}}{V} \right]$ and $k_6[\text{HO}_2 \bullet][\text{H}_2\text{O}_2]$. Similarly the rate of disappearance of $\text{HO} \bullet$ can be represented as $-k_3[C][\text{HO} \bullet]$, $-k_4[\text{H}_2\text{O}_2][\text{HO} \bullet]$, and $-k_5[\text{HO} \bullet][\text{H}_2\text{O}_2]$, according to Equations 4.5, 4.6, and 4.7, respectively. Hence the net rate of formation can be represented as follows (Equation 10):

$$\frac{d[\text{HO} \bullet]}{dt} = \left[\frac{\Phi_{\text{H}_2\text{O}_2} W_{\text{abs},\text{H}_2\text{O}_2}}{V} \right] + k_6[\text{HO}_2 \bullet][\text{H}_2\text{O}_2] - k_3[C][\text{HO} \bullet] - k_4[\text{H}_2\text{O}_2][\text{HO} \bullet] - k_5[\text{HO} \bullet][\text{H}_2\text{O}_2] \quad (4.10)$$

Similarly the net rate of formation of $\text{HO}_2 \bullet$ (Equation 4.11) can be estimated from the rate of formation (Equation 4.6) and disappearance (Equation 4.8):

$$\frac{d[\text{HO}_2 \bullet]}{dt} = k_4[\text{H}_2\text{O}_2][\text{HO} \bullet] - k_6[\text{HO}_2 \bullet][\text{H}_2\text{O}_2] \quad (4.11)$$

where $[\text{HO}_2 \bullet]$ and $[\text{HO} \bullet]$ are the concentrations of $\text{HO}_2 \bullet$ and $\text{HO} \bullet$, respectively, and k_3 , k_4 , k_5 , and k_6 are the rate constants. The species involved in the reactions, namely $[\text{HO} \bullet]$ and $[\text{HO}_2 \bullet]$ are the intermediates and are very reactive and do not accumulate during the reaction. After the induction period, steady state approximation suggest that the rate of formation of the individual species ($[\text{HO} \bullet]$ and $[\text{HO}_2 \bullet]$) is equal to the rate of disappearance [6, 8, 126, 146 – 148] and hence $\frac{d[\text{HO} \bullet]}{dt} = 0$ and $\frac{d[\text{HO}_2 \bullet]}{dt} = 0$. Using this steady state conditions, an equation for $[\text{HO} \bullet]$ can be derived by rearranging Equation 4.11 and then substituting into Equation 4.10 to yield Equation 4.12:

$$[\text{HO} \bullet] = \frac{\left[\frac{\Phi_{\text{H}_2\text{O}_2} W_{\text{abs}, \text{H}_2\text{O}_2}}{V} \right]}{k_3[\text{C}] + k_5[\text{H}_2\text{O}_2]} \quad (4.12)$$

Further substitution of Equation (4.12) into Equation (4.9) yields Equation 4.13:

$$-\frac{d[\text{C}]}{dt} = k_3[\text{C}] \frac{\left[\frac{\Phi_{\text{H}_2\text{O}_2} W_{\text{abs}, \text{H}_2\text{O}_2}}{V} \right]}{k_3[\text{C}] + k_5[\text{H}_2\text{O}_2]} \quad (4.13)$$

During the start of the reaction (time $t \approx 0$), the reaction of H_2O_2 scavenging to hydroxyl radical ($\text{HO} \bullet$) can be neglected (Equation 4.6 and Equation 4.7) and hence the initial mineralization rate $-\frac{d[\text{C}]_0}{dt}$ is equal to the rate of formation of hydroxyl radical $\frac{d[\text{HO} \bullet]}{dt}$ by UV photolysis of H_2O_2 as represented by Equation 4.4. The rate of generation of hydroxyl radical at the initial time without any scavenging can be expressed as $\left[\frac{\Phi_{\text{H}_2\text{O}_2} W_{\text{abs}, \text{H}_2\text{O}_2}}{V} \right]$ [146], and hence $-\frac{d[\text{C}]_0}{dt}$ equal to $\left[\frac{\Phi_{\text{H}_2\text{O}_2} W_{\text{abs}, \text{H}_2\text{O}_2}}{V} \right]$.

Equation 4.13 can be modified as (Equation 4.14):

$$-\frac{d[C]}{dt} = k_3[C] \frac{-\frac{d[C]_0}{dt}}{k_3[C] + k_5[H_2O_2]} \quad (4.14)$$

Accordingly the initial rate can be expressed as Equation 4.15 [149]:

$$-\frac{d[C]_0}{dt} = k_{\text{exp.}} [C]_0^a [H_2O_2]_0^b \quad (4.15)$$

where k_{exp} is the observed mineralization rate constant, t is the oxidation time, and ‘ a ’ and ‘ b ’ are the order of reactions. By combining and rearranging Equation 4.14 and Equation 4.15, the mineralization rate can be expressed as Equation 4.16:

$$\left[\frac{[C]_0^a [H_2O_2]_0^b}{-\frac{d[C]}{dt}} \right] = \frac{1}{k_{\text{exp}}} + \frac{k_5}{k_{\text{exp}} k_3} \left[\frac{[H_2O_2]}{[C]} \right] \quad (4.16)$$

Furthermore, the order of reactions (‘ a ’ and ‘ b ’) may be calculated by initial rate method [149] using Equation (4.15). For the estimation of the order of reaction ‘ b ’, the experiments were conducted at five different concentrations of H_2O_2 (0.06 M, 0.09 M, 0.12 M, 0.18 M, and 0.22 M) at constant initial concentration of substrate $[C]_0$. Based on the above condition, the logarithmic form of Equation (4.15) has been used (Equation 4.17):

$$\ln \left[-\frac{d[C]_0}{dt} \right] = \ln k' + b \ln [H_2O_2]_0 \quad (4.17)$$

where $k' = k_{\text{exp}}[C]_0^a$. The present experimental results (Table 4.6) were used to estimate the order of reaction 'b' by plotting $\ln[-d[C]_0/dt]$ vs $\ln[H_2O_2]_0$ (Figure 4.27) and the estimated slope was approximately constant (0.535 – 0.567) for the four different reaction temperatures (20, 30, 40, and 50 °C).

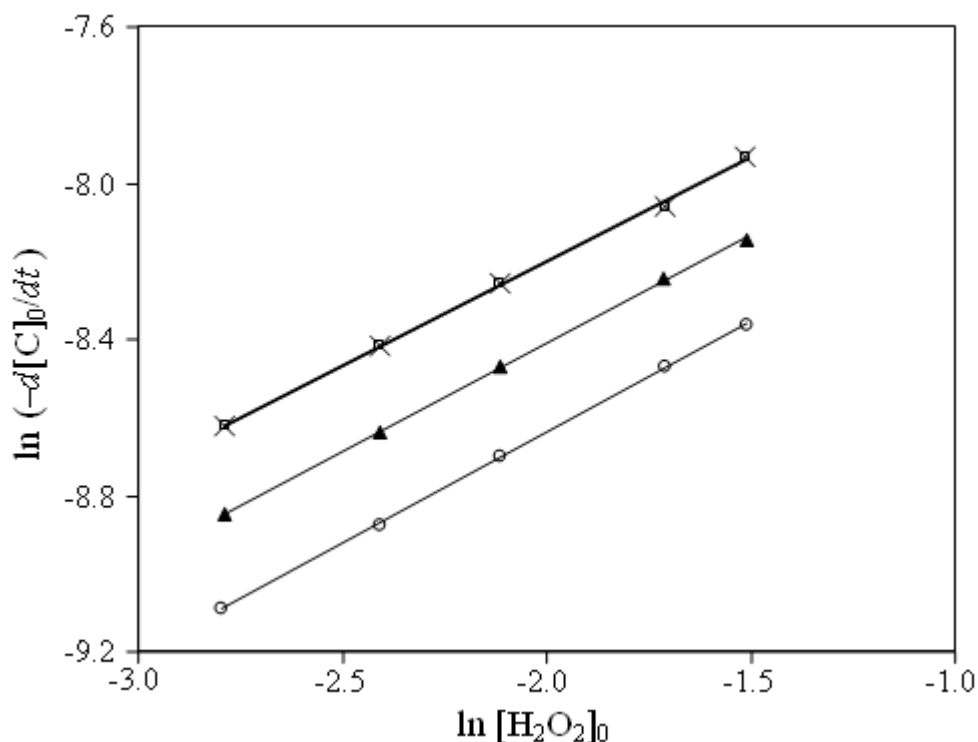


Figure 4. 27 Plot of $\ln[-d[C]_0/dt]$ vs $\ln[H_2O_2]_0$ at four different temperatures.

$$\times 20 \text{ } ^\circ\text{C}; y = 0.5350x - 7.1298; R^2 = 0.9991$$

$$\square 30 \text{ } ^\circ\text{C}; y = 0.5354x - 7.1289; R^2 = 0.9991$$

$$\blacktriangle 40 \text{ } ^\circ\text{C}; y = 0.5544x - 7.3005; R^2 = 0.9995$$

$$\circ 50 \text{ } ^\circ\text{C}; y = 0.5672x - 7.5034; R^2 = 0.9998$$

Similarly, for the estimation of 'a', the experiments were conducted at four different initial concentrations of substrates $[C]_0$ with constant initial concentration of $[H_2O_2]_0$ (0.22M). The logarithmic form of Equation (4.15) for the estimation of the order of reaction 'a' can be expressed as (Equation 4.18):

$$\ln\left[-\frac{d[C]_0}{dt}\right] = \ln k'' + a \ln[C]_0 \quad (4.18)$$

where $k'' = k_{\text{exp}}[\text{H}_2\text{O}_2]_0^b$. A plot of $\ln[-d[\text{C}]_0/dt]$ vs $\ln[\text{C}]_0$ shows a linear correlation (Figure 4.28), and the estimated slope was approximately 0.58 at all reaction temperatures tested.

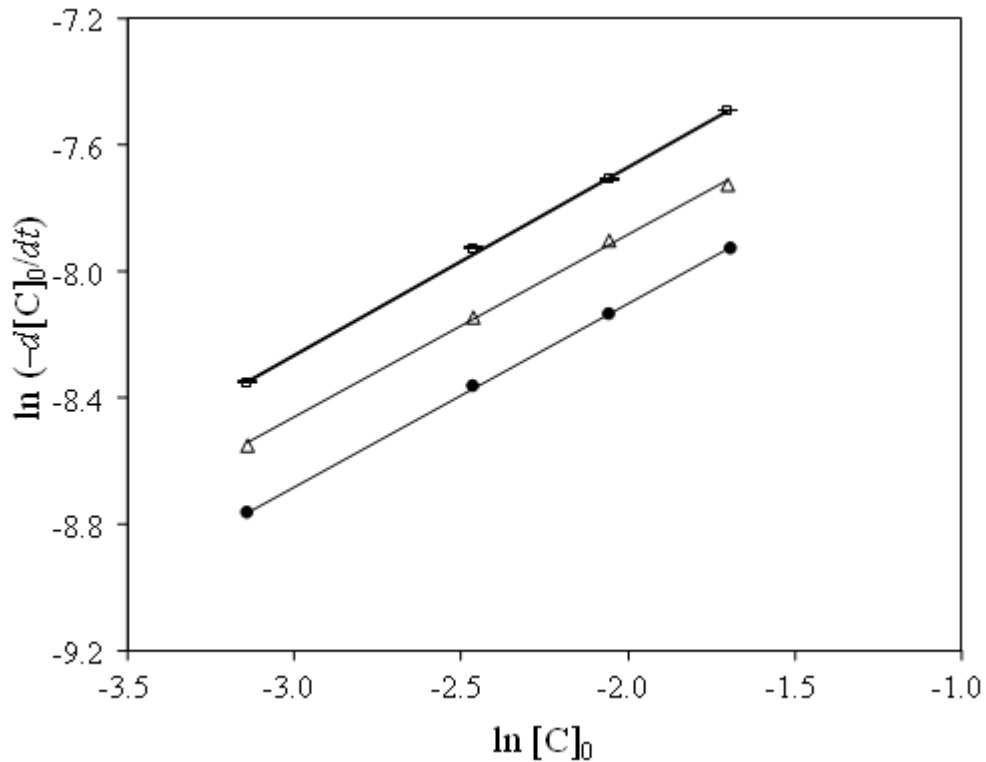


Figure 4. 28 Plot of $\ln[-d[\text{C}]_0/dt]$ vs $\ln[\text{C}]_0$ at four different temperature.

- 20 °C; $y = 0.5949x - 6.4806$; $R^2 = 0.9993$
- 30 °C; $y = 0.5947x - 6.4812$; $R^2 = 0.9993$
- △ 40 °C; $y = 0.5740x - 6.7380$; $R^2 = 0.9983$
- 50 °C; $y = 0.5785x - 6.9452$; $R^2 = 0.9998$

Using the estimated values for ‘a’ and ‘b’, then the Equation 4.15 can be written as:

$$-\frac{d[\text{C}]_0}{dt} = k_{\text{exp}} \cdot [\text{C}]_0^{0.58} [\text{H}_2\text{O}_2]_0^{0.55} \quad (4.15)$$

indicating that the overall mineralization process at the initial reaction time follows the pseudo first order reaction. Based on the above rate equation obtained using the present experimental results, it can be shown that the mineralization rate depends on both $[\text{C}]_0$ and $[\text{H}_2\text{O}_2]_0$ where $[\text{C}]_0$ is slightly dominant than $[\text{H}_2\text{O}_2]_0$. This might be

due to the presence of intermediate products such as organic acid, which could not be readily degraded by hydroxyl radical. Therefore, scavenging reaction occurs and the concentration of hydroxyl radical in the system decreases. Thus, the MDEA mineralization process was dominantly controlled by the initial concentration of the substrate $[C]_0$. De *et al.* [150] reported that the reaction rate of phenol degradation by UV/H₂O₂ at the second stage got affected by the formation of organic acid in the system. The formation of organic acid reduced the concentration of hydroxyl radical in the system. Therefore the reaction rate was controlled by the concentration of phenol available in the reaction medium. Acetic, maleic, and oxalic acid are the organic acids that were reported to be not readily degradable by hydroxyl radical [29 – 30]. The incomplete MDEA mineralization was probably due to the formation of those organic intermediate products which are not readily degradable by hydroxyl radicals.

The present experimental results (Table 4.6) were used for solving Equation 4.16 and the plot is shown in Figure 4.29. For the estimation of kinetic constants, the reported value for k_5 at pH 9.79 = $8 \times 10^7 \text{ M}^{-1}\text{sec}^{-1}$ was considered [151]. The rate of substrate degradation for the reaction during the first 30 minutes $[-d[C]_0/dt]$ was calculated from the experimental data (Table 4.6) for each experimental condition. Calculation of rate constant of MDEA mineralization by hydroxyl radical is presented in Appendix B. The results are summarized in Table 4.7.

Table 4. 7 Calculated values for k_{exp} and k_3 .

Temp. (°C)	T (°K)	1/T	1/ k_{exp}	Slope (Eq. 4.16)	k_{exp} ($\text{M}^{-1} \text{min}^{-1}$)	k_3 ($\text{M}^{-1} \text{min}^{-1}$)	$\ln k_3$
20	293	0.0034	287.95	2.4255	0.003473	5.69×10^{11}	27.06715
30	303	0.0033	286.94	2.3956	0.003485	5.75×10^{11}	27.07764
40	313	0.0032	353.74	2.6365	0.002827	6.44×10^{11}	27.19096
50	323	0.0031	439.37	2.5763	0.002276	8.19×10^{11}	27.43135

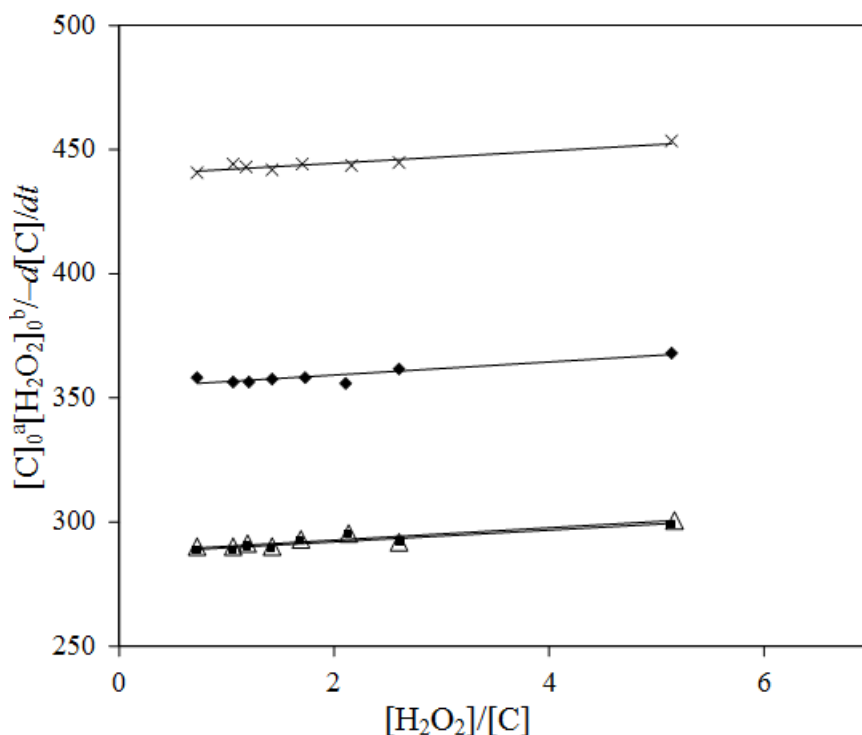


Figure 4. 29 Plot of Equation 4.16 at the initial period of mineralization
Temperature = 20, 30, 40, and 50 °C and pH = 9.76.

△ 20 °C; $y = 2.4255x + 287.95$; $R^2 = 0.8561$

■ 30 °C; $y = 2.3956x + 286.94$; $R^2 = 0.8586$

◆ 40 °C; $y = 2.6365x + 353.74$; $R^2 = 0.8385$

× 50 °C; $y = 2.5763x + 439.37$; $R^2 = 0.8990$

It can be seen in Table 4.7, the estimated hydroxyl radical rate constants (k_3) were similar at 20°C and 30°C of the oxidation process. As discussed earlier, based on the mineralization profile of MDEA, the oxidation process was not dependent on temperature up to 30°C. Above 30 °C, the hydroxyl radical rate constant (k_3) increased from $5.75 \times 10^{11} \text{ M}^{-1} \text{ min}^{-1}$ at 30°C to $8.19 \times 10^{11} \text{ M}^{-1} \text{ min}^{-1}$ at 50 °C ($9.58 \times 10^9 \text{ M}^{-1} \text{ s}^{-1}$ to $13.64 \times 10^9 \text{ M}^{-1} \text{ s}^{-1}$). Theoretically, this condition will result in an increase in total organic carbon removal when the oxidation is conducted at higher temperatures. In fact, the raise in temperature decreases the organic carbon removal (k_{exp} decreased from $3.49 \times 10^{-3} \text{ M}^{-1} \text{ min}^{-1}$ at 30 °C to $2.28 \times 10^{-3} \text{ M}^{-1} \text{ min}^{-1}$ at 50 °C). This might be due to the increase in oxidation temperature that resulted in the increase of scavenging reaction. The scavenging reaction reduced the concentration of hydroxyl radical in the system.

In addition, increase in oxidation temperature lead H_2O_2 to further undergo self-accelerating decomposition. For comparison, De *et al.* [146] reported an estimated hydroxyl radical rate constant of $1 \times 10^{10} \text{ g mol}^{-1} \text{ s}^{-1}$ for the degradation of 2- and 4-chlorophenol using UV/ H_2O_2 in aqueous solution at room temperature. During the mineralization of monoethanolamine (MEA) using Fenton's reagent at room temperature, the reported hydroxyl radical rate constant was $2.9 \times 10^6 \text{ M}^{-1} \text{ min}^{-1}$ ($4.8 \times 10^4 \text{ M}^{-1} \text{ s}^{-1}$) [6]. The present estimated hydroxyl radical rate constants for the mineralization of MDEA by using UV/ H_2O_2 are smaller compared to the reported rate constants for aromatic compounds such as phenol [146]. Nevertheless, the present estimated values are higher compared to those obtained using Fenton treatment for the oxidation of same group of compound i.e. monoethanolamine. Table 4.8 presents the comparison of the reported hydroxyl radical rate constants for different pollutants using various methods of oxidation process. The present estimated values are satisfactorily comparable with those reported in the literature.

4.3.2 Temperature Dependence of MDEA Mineralization

In this study, the experiments on the mineralization of MDEA by UV/ H_2O_2 were conducted at four different temperatures ranging from 20 °C to 50 °C, since the optimum oxidation temperature was found within this range. The activation energy of any reaction can be calculated using Arrhenius' law (Equation 4.19) [147, 153 – 154]:

$$k = A_0 e^{-Ea/RT} \quad (4.19)$$

where k = hydroxyl radical reaction rate constant; A_0 = preexponential factor; Ea = activation energy; R = ideal gas constant ($8.314 \text{ Joule K}^{-1} \text{ mol}^{-1}$); T = temperature °K. The logarithmic form of Arrhenius' law can be written as:

$$\ln k = \ln A_0 - \frac{Ea}{R} \left(\frac{1}{T} \right) \quad (4.20)$$

Table 4. 8 Literature values for hydroxyl radical rate constants for different compounds.

Process	Method	Rate constants	References
Degradation of: - Phenol - 2-chlorophenols - 4-chlorophenols	UV/H ₂ O ₂	(1.41±0.6) x 10 ¹⁰ g mol ⁻¹ s ⁻¹ (9.10±2.1) x 10 ¹⁰ g mol ⁻¹ s ⁻¹ (1.07±0.4) x 10 ¹⁰ g mol ⁻¹ s ⁻¹	De <i>et al.</i> , 1999 [146]
Degradation of methyl tert-butyl ether (MTBE)	UV/H ₂ O ₂	(3.9 ±0.73) x 10 ⁹ M ⁻¹ s ⁻¹	Chang <i>et al.</i> , 2000 [152]
Degradation of 4-chloro-3,5-dinitrobenzoic acid	UV/H ₂ O ₂	3.5 x 10 ⁹ M ⁻¹ s ⁻¹	Lopez <i>et al.</i> , 2000 [63]
Degradation of carbendazim	UV/H ₂ O ₂	(2.2±0.3) x 10 ⁹ M ⁻¹ s ⁻¹	Mazellier <i>et al.</i> , 2003 [69]
Degradation of sulphamethoxazole	UV/H ₂ O ₂	3.5 x 10 ⁹ M ⁻¹ s ⁻¹ to 6.8 x 10 ⁹ M ⁻¹ s ⁻¹	Lester <i>et al.</i> , 2010 [129]
Mineralization of monoethanolamine	UV/H ₂ O ₂	4.7 x 10 ¹⁰ M ⁻³ s ⁻¹ to 15 x 10 ¹⁰ M ⁻³ s ⁻¹	Ariff, 2010 [10]
Mineralization of monoethanolamine	Fenton's reagent	4.8 x 10 ⁴ M ⁻¹ s ⁻¹	Harimurti <i>et al.</i> , 2010 [6]
Mineralization of diisopropanolamine	Fenton's reagent	2.38 x 10 ⁵ M ⁻¹ s ⁻¹	Omar <i>et al.</i> , 2010 [8]
Mineralization of methyldiethanolamine - at 20 °C - at 30 °C - at 40 °C - at 50 °C	UV/H ₂ O ₂	9.50 x 10 ⁹ M ⁻¹ s ⁻¹ 9.58 x 10 ⁹ M ⁻¹ s ⁻¹ 10.73 x 10 ⁹ M ⁻¹ s ⁻¹ 13.64 x 10 ⁹ M ⁻¹ s ⁻¹	Present work

Using the present calculated rate constant values (Table 4.7), a plot of $\ln k_3$ vs $1/T$ is made (Figure 4.30) which shows a linear correlation with $R^2 = 0.8580$. From the slope, the activation energy was estimated as 10.20 kJ mol⁻¹. Table 4.9 compares the reported activation energy values for the hydroxyl radical oxidation process obtained using different pollutants. The present estimated activation energy (10.20 kJ mol⁻¹) obtained for the mineralization of MDEA is in similar range and comparable with the reported activation energies for degradation of formaldehyde [157] and less than that

reported for simple phenolic compounds such as *ortho*, *meta*, and *para* form of cresol [155], complex phenolic compounds such as 2,4,6-trichlorophenol [136], *p*-hydroxybenzoic acid [148], and 2,4-dichlorophenoxyacetic acid [156], which might also be attributed to the type of oxidation process involved.

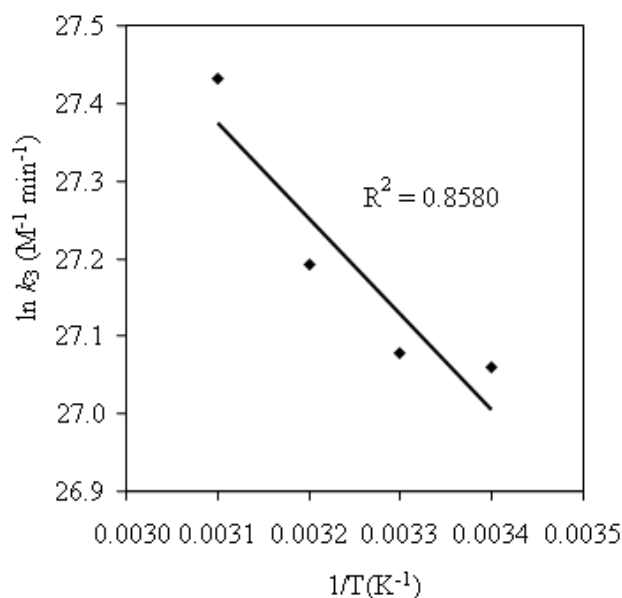


Figure 4.30 Plot of $\ln k_3$ vs $1/T$.

Table 4.9 Activation energies of hydroxyl radical oxidation for different pollutants.

Process	Method	Activation energy	References
Degradation of <i>p</i> -hydroxybenzoic acid	UV/Fenton's reagent	32.8 kJ mol ⁻¹	Beltran <i>et al.</i> , 2001 [148]
Degradation of 2,4-dichlorophenoxyacetic acid	Anodic Fenton	26.1 ± 0.9 kJ mol ⁻¹	Wang and Lemley, 2001 [156]
Destruction of:	Fenton's reagent		Kavitha and Palanivelu, 2005 [155]
- <i>o</i> -cresol		16.25 kJ mol ⁻¹	
- <i>m</i> -cresol		12.90 kJ mol ⁻¹	
- <i>p</i> -cresol		14.95 kJ mol ⁻¹	
Photocatalytic oxidation of 2,4,6-trichlorophenol	UV/O ₂ /TiO ₂	19.98 kJ mol ⁻¹	Ochuma <i>et al.</i> , 2007 [136]
Degradation of formaldehyde	UV-Fenton	9.85 kJ mol ⁻¹	Liu <i>et al.</i> , 2011 [157]
Mineralization of methyldiethanolamine	UV/H ₂ O ₂	10.20 kJ mol ⁻¹	Present work

4.4 Effect of Bicarbonate on MDEA Mineralization by UV/H₂O₂

During sweetening process of natural gas, bicarbonate (HCO₃⁻) is also expected to be present in the effluents leaving the unit. During the absorption and desorption of CO₂ using aqueous amine solution, the following reaction are expected to occur (Equation 4.21 – 4.24).

Ionization of water:



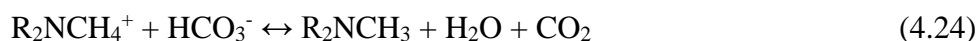
Hydrolysis and ionization of dissolve CO₂:



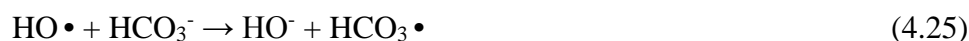
Protonation of MDEA:



Acid-basic reaction with the amine:



Generally, the presence of bicarbonate in the AOP's can act as a scavenger for hydroxyl radical. Bicarbonate (HCO₃⁻) reacts with hydroxyl radical (HO •) to form bicarbonate radical (HCO₃ •), which is also a well-known oxidant, but much less reactive compared to hydroxyl radical [29, 51, 71, 158 – 159]. Consequently, the degree of oxidation will be less. Bicarbonate radical is formed according to the following reaction (Equation 4.25) [32, 59, 158]:



Since the presence of bicarbonate in the AOP's is capable to reduce the degradation efficiency, the study of bicarbonate effect on degradation of MDEA using UV/H₂O₂ is essential.

The effect of bicarbonate in the degradation process of MDEA using UV/H₂O₂ was studied by conducting experiments with the addition of NaHCO₃ in the solution. The experiments were conducted using the following condition: intensity of UV lamp = 12.06 mW/cm², irradiation time = 3 hours, oxidation temperature = 30°C, initial concentration of MDEA = 2000 ppm (1000 ppm TOC), initial pH = 9.76 (optimum pH) and 7, initial concentration of H₂O₂ = 0.22 M, and concentration of NaHCO₃ = 0, 0.025, 0.05, 0.075, 0.1, 0.125, and 0.15 M. The addition of NaHCO₃ in the simulated MDEA solution increased the mineralization rate of MDEA when the initial pH of the process was approximately 7 (Figure 4.31). This result is not in agreement with the statement that bicarbonate is capable to decrease the degradation efficiency [29, 51, 71, 158 – 159].

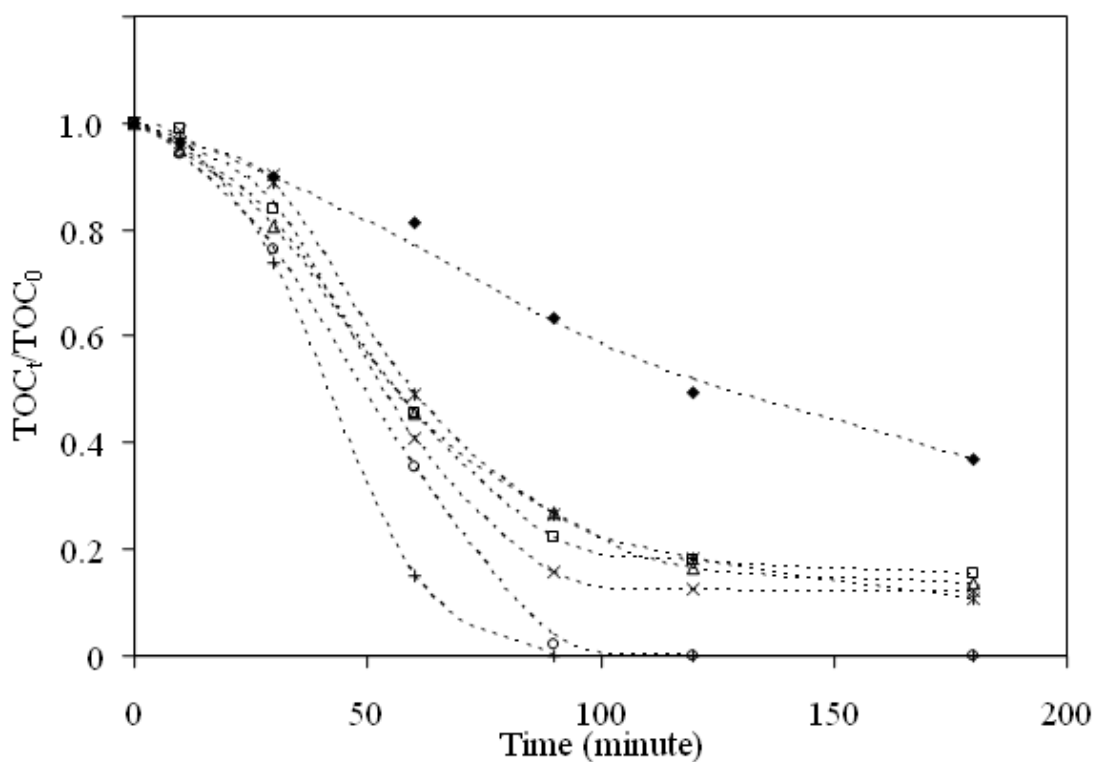


Figure 4. 31 The organic carbon profile during the degradation of MDEA using UV/H₂O₂, in the presence of NaHCO₃ at initial pH = 7.

- ◆ 0 M NaHCO₃ □ 0.025 M NaHCO₃
- △ 0.050 M NaHCO₃ × 0.075 M NaHCO₃
- * 0.100 M NaHCO₃ ○ 0.125 M NaHCO₃
- + 0.150 M NaHCO₃

At neutral pH, bicarbonate reacts with hydroxyl radical to form bicarbonate radical. This radical is less reactive compared to the hydroxyl radical, and hence the degree of TOC removal is expected to decrease. Nevertheless, the degree of TOC removal was increasing, which could be explained by other possibilities. The bicarbonate acts as a good buffer in the degradation process. HCO_3^- is an amphoteric ion that can act either as an acid which can donate its H^+ or as a base which can also accept an H^+ to form H_2CO_3 . Further, the H_2CO_3 can be directly converted to water and carbon dioxide ($\text{H}_2\text{CO}_3 \rightarrow \text{H}_2\text{O} (\text{l}) + \text{CO}_2 (\text{g})$).

When the degradation process was conducted without bicarbonate, the formation of organic acid during the degradation process decreases the pH of the system to a certain level (Figure 4.32) and the presence of bicarbonate in the system maintained the pH and did not allow the pH to drop into acidic condition (Figure 4.32 and Figure 4.33). Thus, the presence of HCO_3^- in the solution maintained the free electron pair of nitrogen atom of MDEA in un-protonated condition. Therefore, more active site for reaction was always provided and hence a higher degradation of MDEA could be achieved. Nonetheless when the initial pH of reaction was 9.76 (i.e. optimum pH value for degradation of MDEA using UV/ H_2O_2 [160]) with the presence of bicarbonate, then the enhancement of degradation process was not noticed (Figure 4.34).

The reduction in MDEA degradation at higher pH ($\text{pH} > 7$) in the presence of bicarbonate might be due to the conversion of bicarbonate to carbonate (CO_3^{2-}) at higher pH, and then reacted with hydroxyl radical to form carbonate radical (Equation 4.26):



The carbonate radical significantly reduces the concentration of hydroxyl radical in the system since the reaction rate between carbonate and hydroxyl radical is high ($3.9 \times 10^8 \text{ M}^{-1} \text{ s}^{-1}$). As a result, the TOC removal was less. At neutral pH, bicarbonate does not change to carbonate [51], and even though bicarbonate reacts with the hydroxyl radical at neutral pH (initial $\text{pH} = 7$), the presence of bicarbonate radical did

not give significant interference in the degradation process, since the reaction rate of bicarbonate and hydroxyl radical is less ($8.5 \times 10^6 \text{ M}^{-1} \text{ s}^{-1}$).

Reaction between hydroxyl radical and bicarbonate (HCO_3^-)/carbonate (CO_3^{2-}) produce a hydroxyl ion (HO^-) in the system (Equation 4.25 and 4.26). The hydroxyl ion will be neutralized by organic acid produced during the UV/ H_2O_2 process. The pH during the process slightly decreases when the concentration of bicarbonate is low and the pH profile during the process relatively unchange when the concentration of bicarbonate is higher (Figure 4.32 and 4.33). This may be due to the increase of the buffering capability. The hydroxyl ions (OH^-) neutralize the organic acid produced in the system during the UV/ H_2O_2 process and this capability increases along with the increase of bicarbonate concentration in the system.

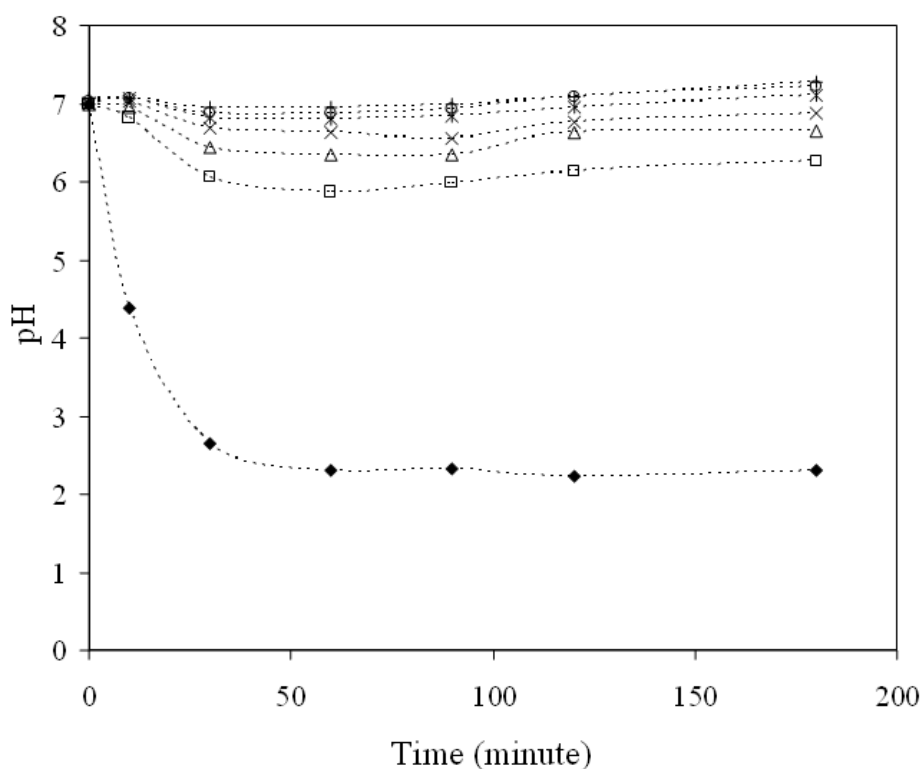
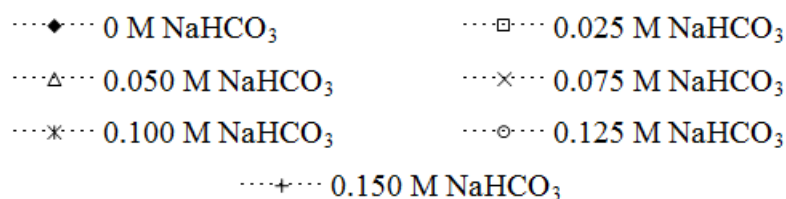


Figure 4. 32 The pH profile during the degradation of MDEA using UV/ H_2O_2 with the presence of NaHCO_3 at initial pH = 7.



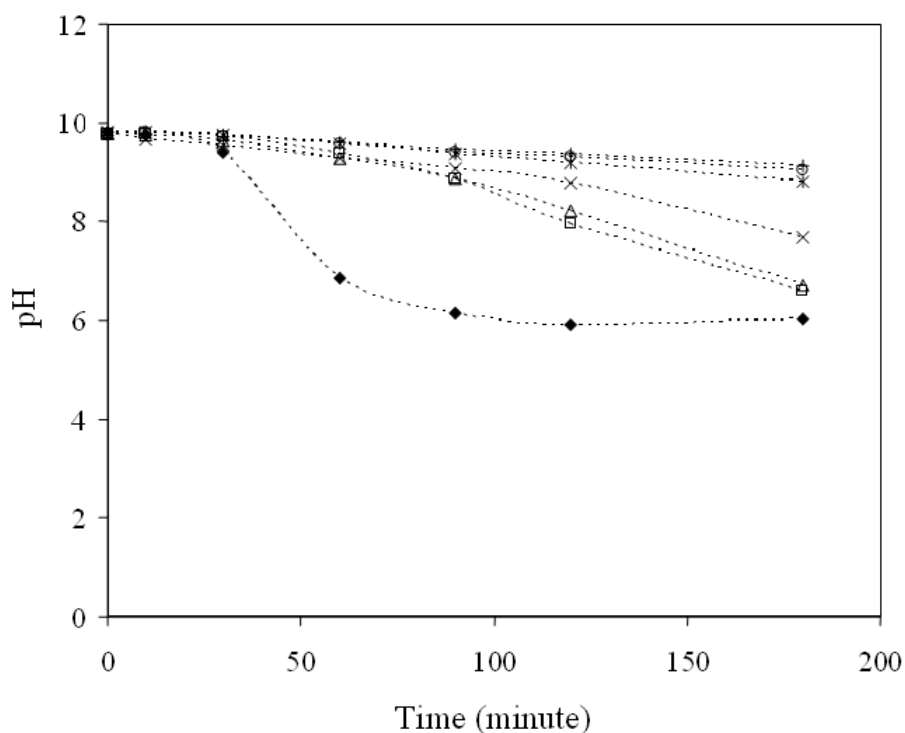


Figure 4.33 The pH profile during the degradation of MDEA using UV/H₂O₂ with the presence of NaHCO₃ at initial pH = 9.76.

.....◆..... 0 M NaHCO₃ ◻..... 0.025 M NaHCO₃
△..... 0.050 M NaHCO₃ ×..... 0.075 M NaHCO₃
*..... 0.100 M NaHCO₃ ○..... 0.125 M NaHCO₃
+..... 0.150 M NaHCO₃

Based on the previous discussion, it can be concluded that at neutral pH, bicarbonate increases the TOC removal by maintaining the pH at around 7 and hence the active site of MDEA for oxidation is always available. However at high initial pH of reaction, the bicarbonate acts as a scavenger to hydroxyl radical by converting into carbonate which further reacts with hydroxyl radical and hence reduce the TOC removal.

Complete mineralization was achieved when the bicarbonate at concentration = 0.125 M and 0.150 M present in the system with initial pH of reaction = 7 (Figure 4.35) and for an initial pH = 9.76 the TOC removal decreased approximately 25% (Figure 4.36).

This is a very good advantage for the future application of the treatment of effluent containing MDEA or any other alkanolamine, which is commonly rich with bicarbonate. Thus, the best set of degradation conditions can be predicted and an effective degradation process can be designed.

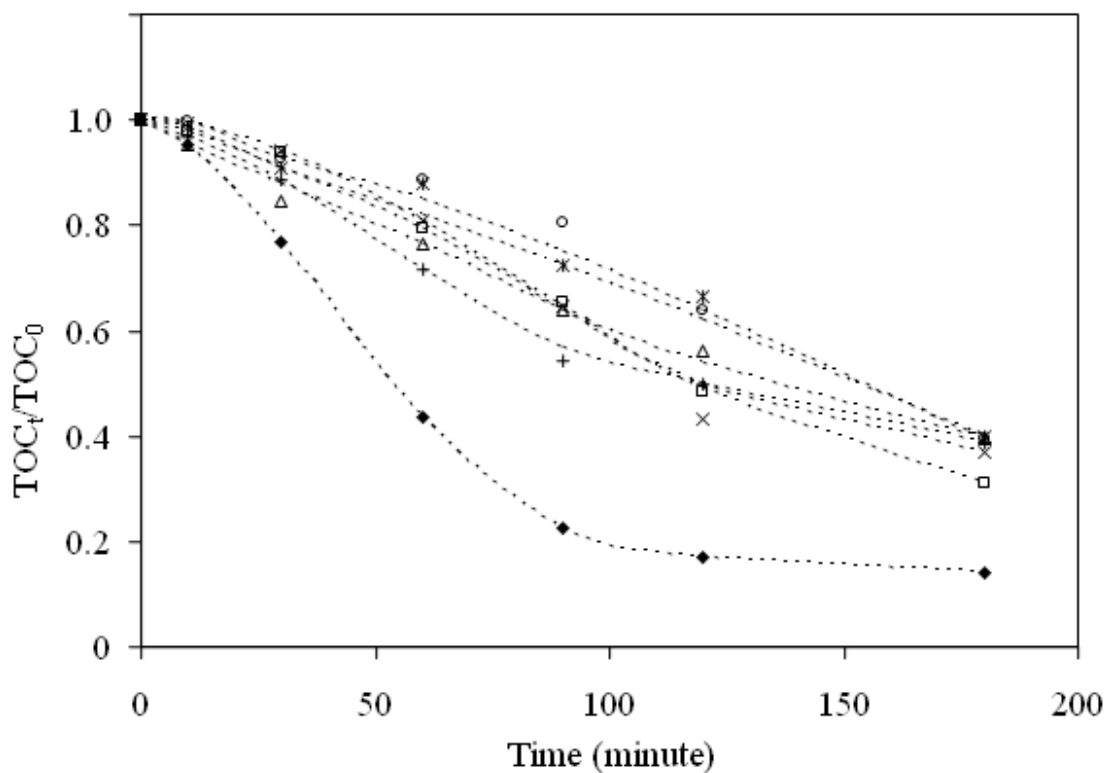


Figure 4.34 The organic carbon profile during the degradation of MDEA using UV/H₂O₂ with the presence of NaHCO₃ at initial pH = 9.76.

- ◆ 0 M NaHCO₃
- △ 0.050 M NaHCO₃
- ✱ 0.100 M NaHCO₃
- 0.025 M NaHCO₃
- × 0.075 M NaHCO₃
- 0.125 M NaHCO₃
- + 0.150 M NaHCO₃

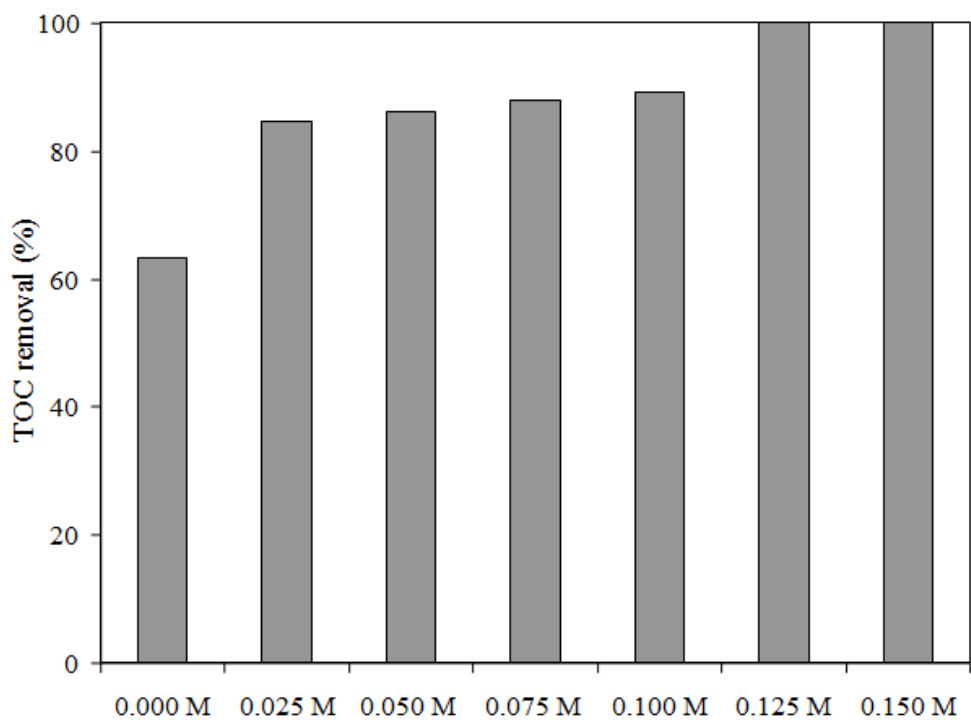


Figure 4. 35 Percentage TOC removal achieved at initial pH = 7, for different concentration of NaHCO₃.

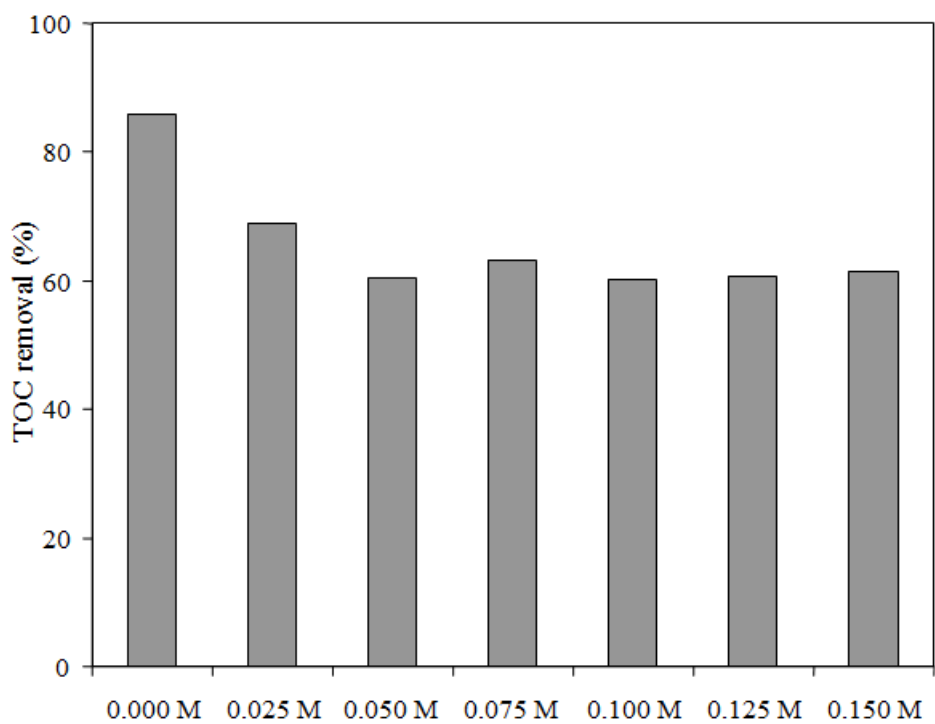


Figure 4. 36 Percentage TOC removal achieved at initial pH = 9.76, for different concentration of NaHCO₃.

4.5 Degradation of Refinery Effluent (PPMSB Effluent) using UV/H₂O₂

The actual effluent from gas processing plant of PETRONAS Penapisan Melaka Berhad (PPMSB) was also considered for the present study on the degradation of MDEA using UV/H₂O₂. The properties of the actual industrial effluent are presented in Table 3.2. The pre-treatments included the removal of hydrogen sulfide (H₂S), removal of oil, and removal of grease. H₂S has to be removed since it is very toxic to the environment. Meanwhile oil and grease has to be removed since these components might affect the penetration of UV light into the solution. The details of the removal of oil and grease and H₂S were discussed in section 3.1.1 of Chapter 3. The pre-treated effluent with high concentration of MDEA was diluted to an approximately 1000 ppm of initial concentration of organic carbon and then placed in the reactor. The 1000 ppm TOC of initial concentration of pollutant was chosen since this concentration was approximately equals with the 2000 ppm of MDEA (2000 ppm of MDEA \approx 1000 ppm TOC) which was the suitable concentration to monitor the TOC removal profile accurately during UV/H₂O₂ process using the present experiment set up. After adding the oxidant (H₂O₂), the solution was subjected to degradation process, by exposing to 8 watt UV lamp (intensity = 12.06 mW/cm²). The degradation was monitored by measuring the total organic carbon (TOC) at desired time intervals. The process was conducted for 3 hours and the % TOC removal was calculated accordingly by Equation (3.4).

During the optimization process of refinery effluent degradation using UV/H₂O₂, the RSM was used. Since the main component of the refinery effluent is MDEA, therefore the optimization process condition was based on the results obtained from the synthetic MDEA solution. Screening was carried out for three factors i.e. initial concentration of H₂O₂, initial pH, and temperature. TOC removal was used as the response. Box-Behnken design was used as the experimental design. Low and high level for screening was determined based on the preliminary study of synthetic MDEA solution (Table 4.1), and the Box-Behnken design of experiments were according to Table 4.2.

Based on the design of experiments in Table 4.2, the TOC removal (%) observed is fitted into second order polynomial equation to find the correlation between the factors and response (Equation 4.27).

$$\begin{aligned} \% \text{ TOC removal} = & -795.267 + 116.233(\text{pH}) + 2708.71(\text{H}_2\text{O}_2) + 5.2895(\text{Temperature}) \\ & - 3.72781(\text{pH})^2 - 147.104(\text{pH})(\text{H}_2\text{O}_2) - 0.6765(\text{pH})(\text{Temperature}) - 1828.13(\text{H}_2\text{O}_2)^2 - \\ & 11.9583(\text{H}_2\text{O}_2)(\text{Temperature}) + 0.0272625(\text{Temperature})^2 \end{aligned} \quad (4.27)$$

The predicted values according to equation 4.27, are compared with those obtained from experiments (Table 4.10).

Table 4. 10 Box-Behnken matrix design with observed and fitted value for refinery effluent.

Experiment	Operational parameter			Response (% TOC removal)	
	pH	H ₂ O ₂	Temperature	Observed value	Fitted value
1	9.0	0.12	50.0	45.73	45.18
2	11.0	0.18	50.0	21.84	22.23
3	7.0	0.18	30.0	55.65	55.26
4	11.0	0.18	30.0	67.35	64.70
5	9.0	0.24	30.0	89.83	90.38
6	9.0	0.12	30.0	43.75	46.24
7	11.0	0.12	40.0	36.74	36.91
8	7.0	0.18	50.0	64.26	66.91
9	7.0	0.24	40.0	84.50	84.33
10	11.0	0.24	40.0	29.30	31.40
11	7.0	0.12	40.0	21.33	19.23
12	9.0	0.18	40.0	64.73	64.46
13	9.0	0.24	50.0	63.11	60.62

Correlation between the observed values and fitted values of TOC removal are presented in Figure 4.37. The correlation gave $R^2 = 0.9935$. High value for R^2 indicated that the model generated is suitable for the prediction of TOC removal. The second order model of TOC removal percentage for refinery effluent was obtained with $R^2 = 0.9935$ and R^2 adjusted = 0.9818 and is presented in Equation 4.27.

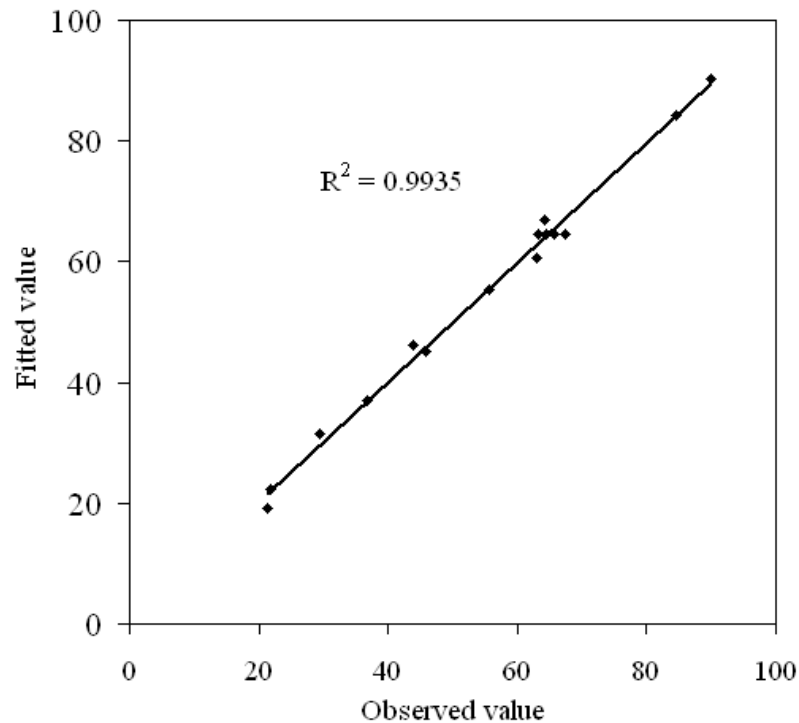


Figure 4. 37 Correlation between the experimental and fitted value (Equation 4.27) of TOC removal for refinery effluent.

Pareto chart of standardized effect at $P = 0.05$ (Figure 4.38) clearly shows the standardized effects of factors and interaction between each factor affecting TOC removal (increase or decrease).

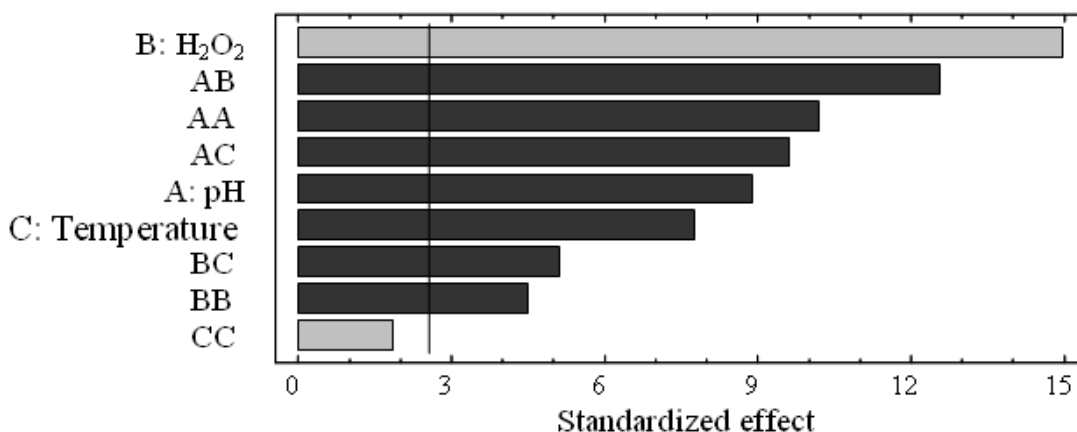


Figure 4.38 Pareto chart of the standardized effect for percentage TOC removal for screening of significant factors for degradation of actual effluent.

□ + ; ■ -

Hydrogen peroxide concentration (H_2O_2) gives the most significant effect toward TOC removal, followed by quadratic factor of temperature with insignificant effect, whilst other factors give significant effect on the decrease of TOC removal. The order of the most significant factor to decrease TOC removal is: interaction between pH and H_2O_2 > quadratic factor of pH > interaction between pH and temperature > pH > temperature > interaction between H_2O_2 and temperature > quadratic factor of H_2O_2 .

Identification of significant factors affecting the TOC removal was performed using ANOVA analysis at P-value = 0.05. The results of ANOVA analysis is presented in Table 4.11. Significant factors affecting the TOC removal was indicated by P-value of less than 0.05. From Table 4.11 it can be seen that all the factors and their interaction gave a significant effect for TOC removal, but the quadratic factor of temperature is not significant (P-value = to 0.1214).

Contour plot of regression model for refinery effluent is presented in Figure 4.39. The 3D curvature (Figure 4.39) shows that, increasing the concentration of H_2O_2 up to a certain level will increase the removal. A further increase of H_2O_2 concentration reduces the removal. A similar profile with the synthetic aqueous MDEA solution is also found in terms of initial of pH of reaction. The TOC removal increases with an increase in pH up to certain level and then start to decrease.

Table 4. 11 ANOVA analysis for TOC removal of refinery effluent.

Source	Sum of Squares	Df	Mean Square	F-Ratio	P-Value
A:pH	621.458	1	621.458	78.64	0.0003
B:H ₂ O ₂	1775.78	1	1775.78	224.71	0.0000
C:Temperature	474.936	1	474.936	60.10	0.0006
AA	820.968	1	820.968	103.89	0.0002
AB	1246.44	1	1246.44	157.73	0.0001
AC	732.244	1	732.244	92.66	0.0002
BB	159.924	1	159.924	20.24	0.0064
BC	205.922	1	205.922	26.06	0.0038
CC	27.4429	1	27.4429	3.47	0.1214
Total error	39.5128	5	7.90256		
Total (corr.)	6094.75	14			

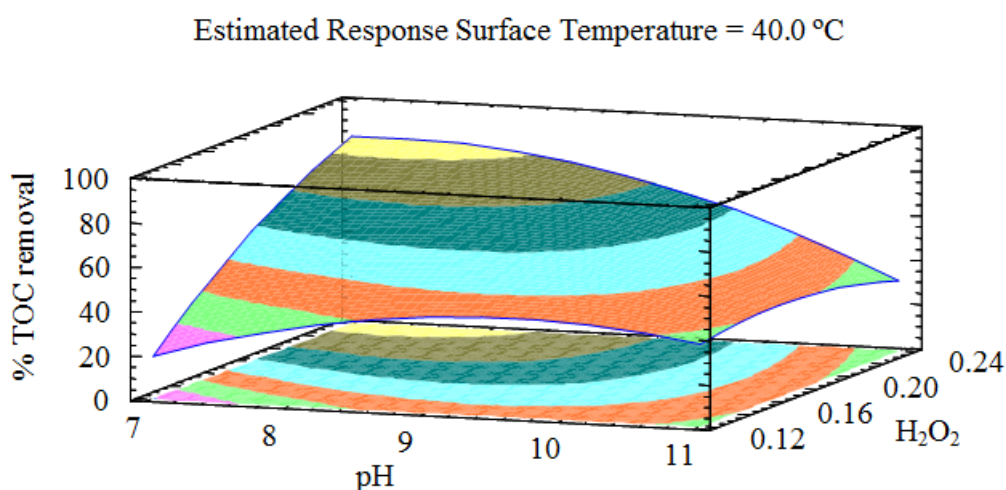
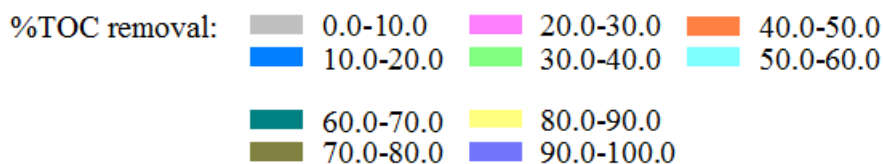


Figure 4. 39 Contour plots of TOC removal for refinery effluent.



The estimated optimum conditions for the degradation of refinery effluent using UV/H₂O₂ are: pH = 8.13, temperature = 30 °C, and initial concentration of H₂O₂ = 0.24 M (according to Table 4.12), in the other words, molar ratio between contaminant (TOC (M)) to oxidant (H₂O₂ (M)) = 1: 2.79.

Table 4. 12 Optimum condition for the degradation of PPMSB effluent by using UV/H₂O₂ at initial concentration of contaminant = 1000 ppm TOC; UV light intensity = 12.06 mW/cm².

Factor	Optimum
pH	8.13
H ₂ O ₂	0.24 M
Temperature	30.0 °C

Using the estimated optimum conditions (Table 4.12), the experiments were conducted in duplicate and the estimated %TOC removal was 92.05%, which satisfactorily agree with that predicted as 93.19% (Figure 4.40).

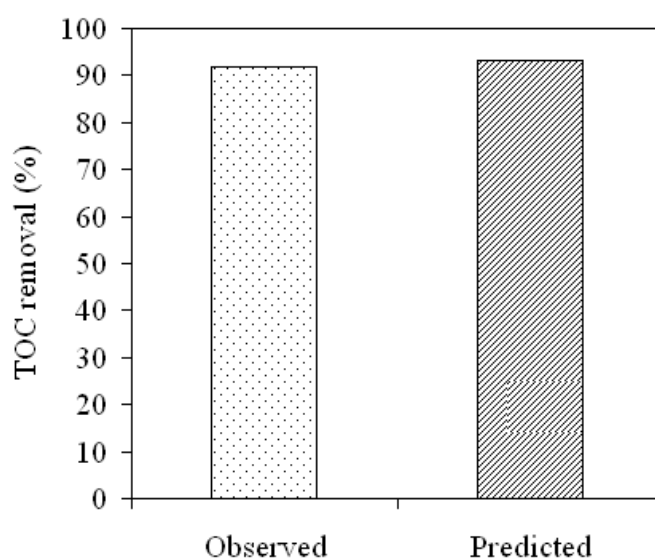


Figure 4. 40 Comparison of experimental and predicted TOC removal for refinery effluent.

The optimum condition of degradation process for refinery effluent using UV/H₂O₂ was slightly different from that of the simulated solution, even though the main component of the effluent was MDEA. The effluent requires higher amount of oxidant and lower pH condition. Since the actual effluents contains many other contaminants such as organic acids beside MDEA. These organic acids might have caused the reduction in pH value that are essential for the degradation.

4.6 Biodegradability Test on Partially Degraded MDEA Solution.

Generally, UV/H₂O₂ treatment is suitable for the degradation of organic compounds to form less toxic fragments compared to the parent compound. Based on the present results it was found that the degradation of synthetic aqueous MDEA solution and actual refinery effluent by UV/H₂O₂ oxidation resulted in approximately 85% and 93% of TOC removal, respectively. Complete TOC removal could not be achieved even with a high concentration of hydrogen peroxide.

The biodegradability estimation of the partially degraded effluent, after UV/H₂O₂ treatment was evaluated through the estimation of BOD₅/COD ratio [25, 37, 53, 90, 119, 161]. BOD₅ is a measure of the dissolved oxygen consumption during biological oxidation of organic contaminant, while the COD is a measure of the oxygen that is required to oxidize the oxidizable material present in the sample. According to the Europe Union (EU) regulation, if the BOD₅/COD ratio is greater than 0.5 (> 0.5), then the compounds are considered to be readily biodegradable [119]. The test was conducted for the partially degraded contaminant at approximately 40%, 60%, and maximum TOC removal achieved by using UV/H₂O₂. The UV/H₂O₂ process can increase the ratio of BOD₅/COD. Results of biodegradability evaluation are depicted in Figure 4.41 and Figure 4.42.

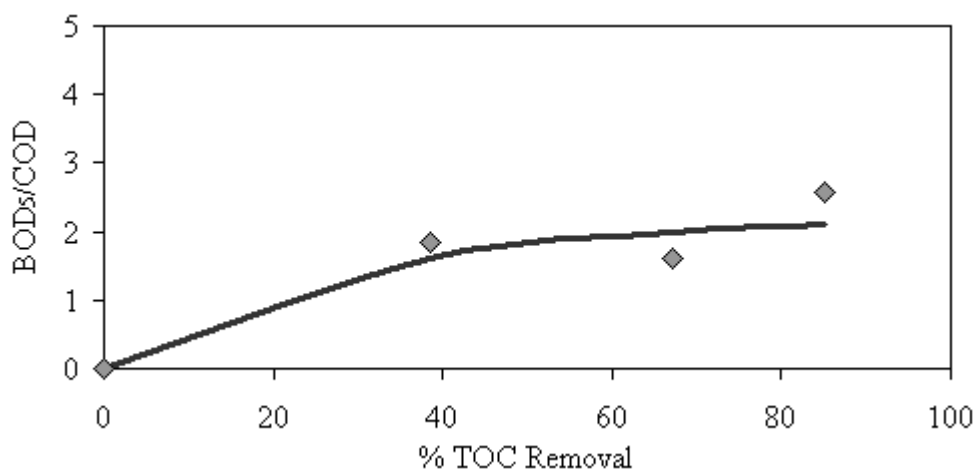


Figure 4. 41 The biodegradability evaluation of simulated MDEA solution.

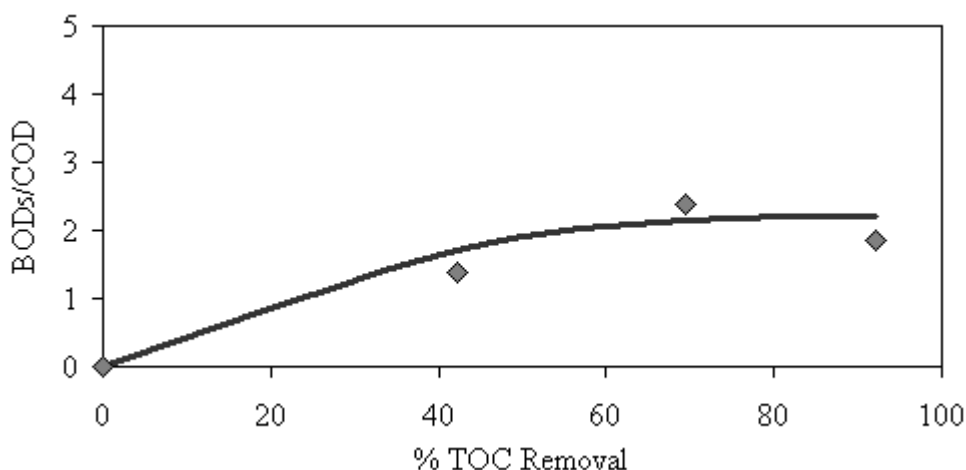


Figure 4. 42 The biodegradability evaluation of actual refinery effluent.

The higher ratio of BOD₅/COD approximately 2.0 indicates that partially degraded MDEA can be more easily degraded by biological oxidation. Based on these, it can be concluded that the UV/H₂O₂ oxidation can break down the MDEA structure and convert the non-biodegradable compounds into biodegradable compound.

4.7 Electrical Energy Consumption

UV/H₂O₂ treatment for the degradation of simulated MDEA solution and real effluent from refinery plant (PPMSB) have been conducted. The rate of degradation of actual effluent from refinery plant was slightly slower compared to the simulated aqueous MDEA solution (Figure 4.43). However, at the end of 180 minutes of reaction i.e. when all the oxidant (H₂O₂) was consumed, approximately 85% of TOC removal was achieved for both cases [160]. In order to compare the degradation rate, another method on degradation of simulated MDEA solution and real effluent from refinery plant (PPMSB) was also conducted using ZnO/SnO₂ coupled photocatalysts [4], and a similar trend was found (Figure 4.44). Approximately 23 % of TOC removal was achieved by using this method.

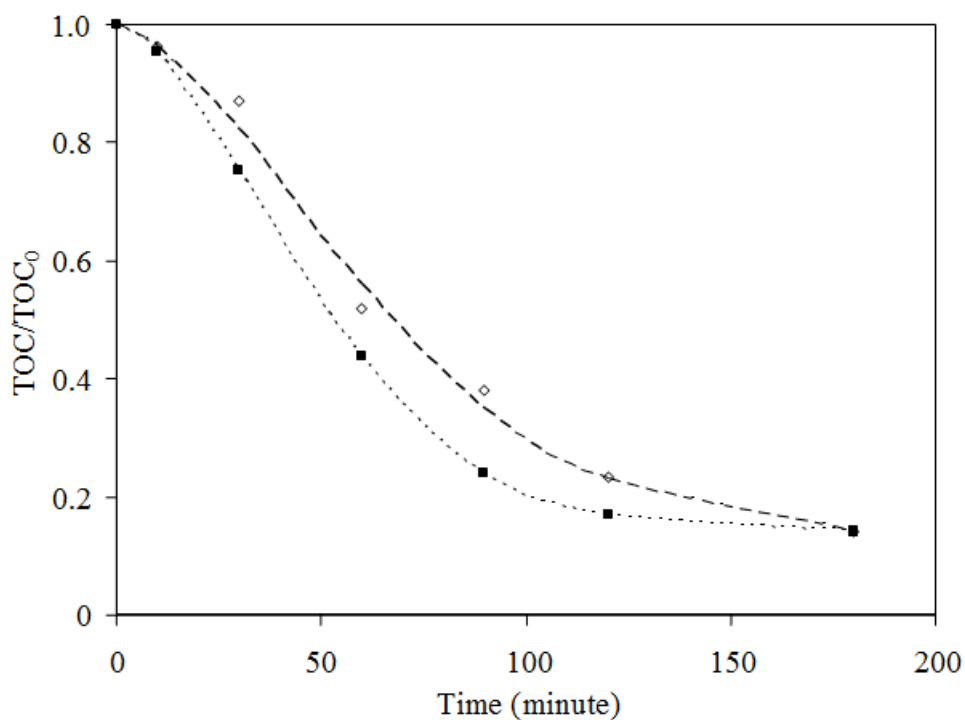


Figure 4.43 The TOC for photochemical degradation of MDEA by UV/H₂O₂
 ◊ A: refinery effluent (PPMSB); ■ B: simulated system.

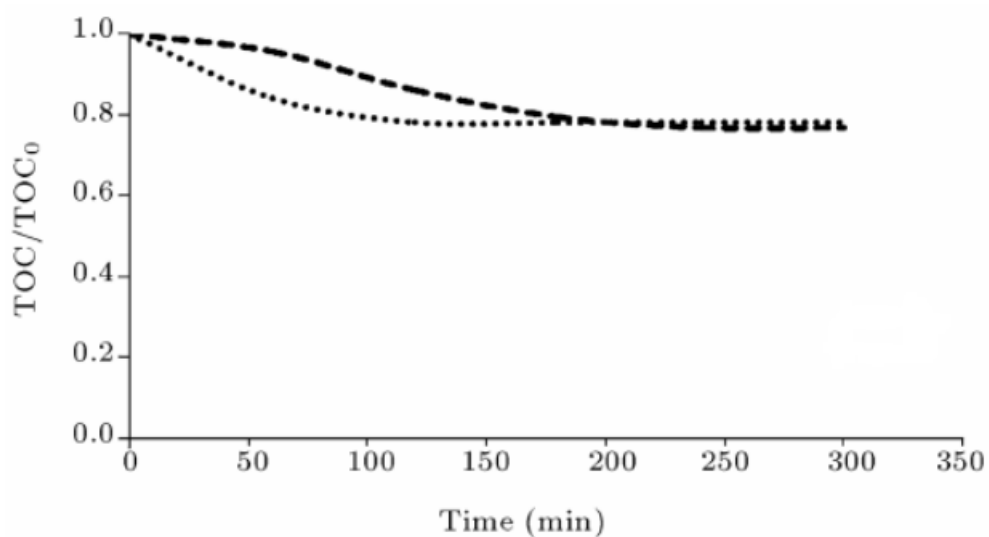


Figure 4.44 The TOC for the photocatalytic degradation of MDEA
 ---- A: refinery effluent (PPMSB); B: simulated MDEA solution [4].

Based on the observations of both UV/H₂O₂ photochemical and ZnO/SnO₂ coupled photocatalysts processes, the slower degradation rate of real effluent from refinery might be attributed to the reason that the effluent from refinery might contain many other components as impurities besides, MDEA that are capable to reduce the degradation rate.

Economics factor is often considered important during the selection of wastewater treatment technology rather than regulations, treatment outcome, and operations (maintenance, control, safety) [162]. Since the UV/H₂O₂ process for mineralization of MDEA is an electric-energy-intensive process and the electric energy can represent major consumption cost, hence the estimation of electrical energy demand is necessary. Legrini *et al.* in 1993 [34] proposed a general and simple method for the evaluation of electrical energy for advanced oxidation processes (AOP's). The electrical energy is expressed as the ratio of TOC (ppm) destroyed to electrical power consumed during the same time of irradiation. After the multiplication with the total volume of solution treated, then the calculation results in efficiency which is independent of equipment size. The energy efficiency is expressed in Equation 4.28.

$$\phi = \frac{\Delta\text{TOC} \times V}{P} \quad (4.28)$$

where ϕ is the energy efficiency, ΔTOC is the total organic carbon removed (ppm), V is the total volume of solution treated (L), and P is the electrical power consumed (kWh). The estimated energy consumption for the degradation of MDEA in synthetic solution and also in actual effluent using UV/H₂O₂ process are 0.069 kWh g⁻¹ and 0.064 kWh g⁻¹, respectively, whereas the reported values for ZnO/SnO₂ coupled photocatalysts is 1.298 kWh g⁻¹. The details of the results are presented in Table 4.13 and compared in Figure 4.45.

Table 4. 13 Comparison of electrical energy efficiency of MDEA mineralization using different process.

AOP method References	Experimental	Δ TOC (ppm)	ϕ (g kWh ⁻¹)	Energy consumed (kWh g ⁻¹)
ZnO/SnO ₂ Coupled Photocatalysts Ali <i>et al.</i> , 2010 [4]	Simulated MDEA solution [MDEA] ₀ = 1000 ppm [TOC] ₀ = 503.53 ppm Volume = 0.25 L UV lamp = 12 Watt (365 nm) Irradiation time = 3 hours Δ TOC = 22%	110.76	0.77	1.298
	Refinery effluent (PPMSB) [MDEA] ₀ = 1000 ppm [TOC] ₀ = 503.53 ppm Volume = 0.25 L UV lamp = 12 Watt (365 nm) Irradiation time = 3 hours Δ TOC = 23.15%	118.48	0.77	1.298
UV/H ₂ O ₂ Present work	Simulated MDEA solution [MDEA] ₀ = 2000 ppm [TOC] ₀ = 1006 ppm Volume = 0.4 L UV lamp = 8 Watt LP Hg lamp (254 nm) Irradiation time = 3 hours Δ TOC = 85.74%	857.4	14.29	0.069
	Refinery effluent (PPMSB) [MDEA] ₀ = 2000 ppm [TOC] ₀ = 1006 ppm Volume = 400 ml = 0.4 L UV lamp = 8 Watt LP Hg lamp (254 nm) Irradiation time = 3 hours Δ TOC = 92.05%	859.9	15.43	0.064

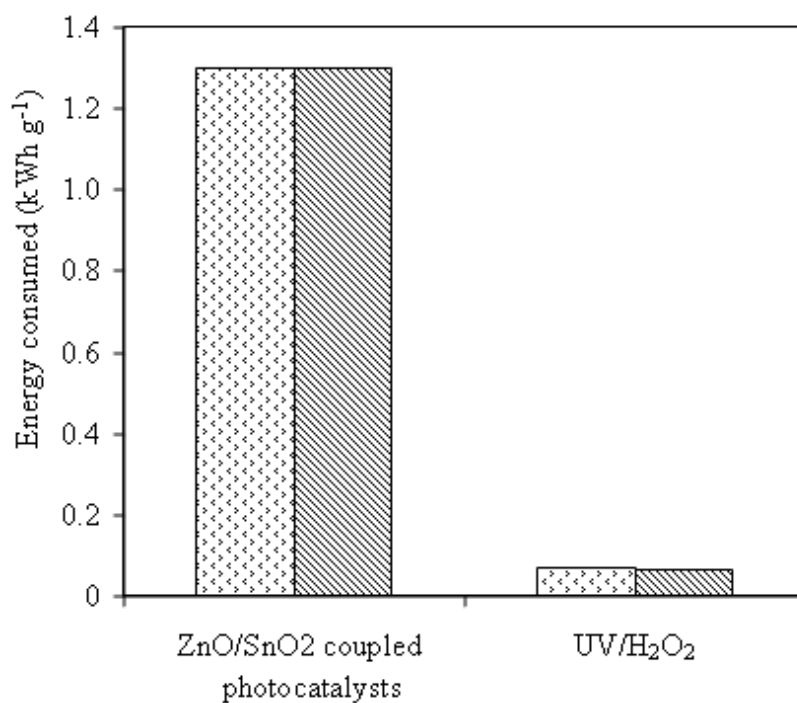


Figure 4. 45 Comparison of energy consumption per gram TOC of MDEA degradation in the present work using UV/H₂O₂ and using ZnO/SnO₂ coupled photocatalysts.

☒ Synthetic MDEA solution ☒ Refinery effluent

Based on Table 4.13 and Figure 4.45, it can be concluded that present UV/H₂O₂ process for the mineralization of MDEA is more electrical energy efficient, when compared with other similar process.

CHAPTER 5

CONCLUSIONS AND RECOMENDATIONS

5.1 Conclusions

The following conclusions can be drawn from the present research on the degradation of MDEA using UV/H₂O₂ advanced oxidation process:

1. The initial concentration of H₂O₂, initial pH, and temperature of reaction are the important factors affecting the TOC removal of MDEA mineralization using UV/H₂O₂. Increasing values of these factors up to a certain level increase the TOC removal, and further increase results in decrease in TOC removal. The maximum TOC removal, using UV/H₂O₂ oxidation, for simulated MDEA solution was achieved when the oxidation conditions were at initial pH = 9.76, temperature = 30 °C, and molar ratio between contaminant (TOC (M)) to oxidant (H₂O₂ (M)) = 1: 2.56. Meanwhile, the maximum TOC removal of UV/H₂O₂ oxidation for actual refinery effluent was achieved when the oxidation conditions were at initial pH = 8.13, temperature = 30 °C, and molar ratio between contaminant (TOC (M)) to oxidant (H₂O₂ (M)) = 1: 2.79.
2. Based on the by-products that were identified during the mineralization process using UV/H₂O₂ namely formic acid, oxalic acid, acetic acid, nitrate, nitrite, ammonium, and carbon dioxide, a mechanism of MDEA mineralization by hydroxyl radical was proposed. The mineralization mechanism was proposed through a hydrogen abstraction and then followed by electrophilic addition. Furthermore, based on the optimum conditions of the oxidation process that was estimated using RSM, the mineralization rate constants of MDEA have been estimated. It was found that the mineralization

rate constants were not dependent on temperature when the temperature of reaction ≤ 30 °C and the overall MDEA mineralization process at the initial reaction time follows the pseudo first order reaction.

3. The presence of bicarbonate during the UV/H₂O₂ process enhanced the mineralization of MDEA when the initial pH = 7, but decreased the mineralization of MDEA when the initial pH was at optimum condition for mineralization i.e. 9.76. At pH higher than 7, the bicarbonate changed to carbonate, which significantly reduces the concentration of hydroxyl radical in the system, therefore the mineralization was decreased. However, at pH approximately 7, the bicarbonate does not change and act as a good buffer, which could provide more active sites for hydroxyl radical to attack MDEA, hence the mineralization of MDEA was increased and reach 100% TOC removal when the concentration of bicarbonate ≥ 0.125 M.
4. The UV/H₂O₂ treatment for MDEA resulted in an increase in biodegradability, as indicated by the ratio between the BOD₅ to COD (i.e. > 0.5), when compared with untreated one. It is likely that the by-products are more biodegradable compared to the parent compound. In terms of energy efficiency, the UV/H₂O₂ was more effective to reduce the TOC of simulated MDEA solution and actual refinery effluent compared to the other removal technologies reported in the literature.

5.2 Recommendations

The following recommendations are proposed:

1. All the study has been done in the batch reactor. Since the volume of actual refinery effluent is very large, therefore a study in continuous mode is recommended for the real application to commercial operation.

2. Based on the results, both the partially degraded simulated aqueous MDEA solution and the actual refinery plant are readily biodegradable; therefore a detailed study on the biodegradation of partially degraded of MDEA solution using a bioreactor is important to estimate the operating condition for the biodegradation process using microorganism.

REFERENCES

- [1] M. Sandin, S. Allemark, and L. Edebo, "Selective Toxicity of Alkanolamines", *Antimicrob. Agents and Chemother.*, vol. 34(3), pp. 492 – 493, 1990.
- [2] A. Durán-Moreno, S.A. García-González, M.R. Gutiérrez-Lara, F. Rigas, and R.M. Ramírez-Zamora, "Assessment of Fenton's Reagent and Ozonation as Pre-treatment for Increasing the Biodegradability of Aqueous Diethanolamine Solutions from an Oil Refinery Gas Sweetening Process," *J. Hazard. Mater.*, vol. 186, pp.1652 – 1659, 2011.
- [3] M. Fürhacker, A. Pressl, and R. Allabashi, "Aerobic Biodegradability of Methyldiethanolamine (MDEA) used in Natural Gas Sweetening Plants in Batch Test and Continuous Flow Experiments", *Chemosphere*, vol. 52, pp. 1743 – 1748, 2003.
- [4] R. Ali, W.A.W. Abu Bakar, S.S. Mislán, and M.A. Sharifuddin, "Photodegradation of *N*-Methyldiethanolamine over ZnO/SnO₂ Coupled Photocatalysts", *Transaction C: Chemistry and Chemical Engineering*, vol. 17(2), pp. 124-130, 2010.
- [5] C. Walling, "Fenton Reagent Revisited", *Accounts Chem. Res.*, vol. 8(5), pp. 125 – 131, 1975.
- [6] S. Harimurti, B.K. Dutta, I.F.B.M. Ariff, S. Chakrabarti, and D. Vione, "Degradation of Monoethanolamine in Aqueous Solution by Fenton's Reagent with Biological Post-treatment", *Water Air Soil Pollut.*, vol. 211(1 – 4), pp. 273 – 286, 2010.

- [7] B.K. Dutta, S.Harimurti, I.F.B.M. Ariff, S. Chakrabarti, and D. Vione, "Degradation of Diethanolamine by Fenton's Reagent Combined with Biological Post-treatment", *Desalin. Water Treat.*, vol. 19(1 – 3), pp. 286 – 293, 2010.
- [8] A.A. Omar, R.M. Ramli, and P.N.F.M. Khamarudin, "Fenton Oxidation of Natural Gas Plant Wastewater", *Canadian Journal on Chemical Engineering & Technology*, vol. 1, pp. 1 – 6, 2010.
- [9] Q. Zhang and G. Yang, "The Removal of COD from Refinery Wastewater by Fenton Reagent," in *International Conference on Remote Sensing, Environment and Transportation Engineering (RSETE)*, pp. 7974-7977, Nanjing, China, 24-26 June 2011, ISBN: 978-1-4244-9172-8, Digital Object Identifier: 10.1109/RSETE.2011.5966300.
- [10] I.F.B.M. Ariff, "Studies on The Oxidation of Monoethanolamine using UV and H₂O₂ with Post-biological Treatment," M.S. thesis, Dept. Chem. Eng., Universiti Teknologi PETRONAS, Perak Darul Ridzuan, Malaysia, 2010.
- [11] British Petroleum (BP), BP Statistical Review of World Energy, (2011).
[Online]. Available :
http://www.bp.com/assets/bp_internet/globalbp/globalbp_uk_english/reports_and_publications/statistical_energy_review_2011/STAGING/local_assets/pdf/statistical_review_of_world_energy_full_report_2011.pdf.
- [12] Eia, U.S. Energy Information Administration Independent Statistic and Analysis, 2010. [Online]. Available : <http://www.eia.gov/countries/country-data.cfm?fips=MY>
- [13] A. I. Kohl, and R. Nielsen, *Gas Purification. 5th Ed*, Gulf Publishing Company, Houston, Texas, (1997).
- [14] J. A. Bullin, J. C. Polasek and J. W. Holmes, "Optimization of New and Existing Amine Gas Sweetening Plants Using Computer Simulation," in *Sixtieth GPA Annual Convention. Tulsa, OK: Gas Processors, Association, 1981: 142-8.*

- [15] Cameron Process System (2010 Cameron | Printed in USA, 1M | 07/10 TC9814-010), Amine Gas Sweetening Systems, pp. 1-2.
- [16] K. Mearkeltor, "Natural Gas Sweetening Process Design," *School of Doctoral Studies (European Union) Journal*, pp. 144-156, 2011.
- [17] The Dow Chemical Company (2010, March 24), Product Safety Assessment of N-methyldiethanolamine, pp. 1-6. [Online]. Available: http://msdssearch.dow.com/PublishedLiteratureDOWCOM/dh_0436/0901b80380436ae7.pdf?filepath=productsafety/pdfs/noreg/233-00470.pdf&fromPage=GetDoc.
- [18] L. Addington and C. Ness, An Evaluation of General "Rules of Thumb" in Amine Sweetening Unit Design and Operation, Bryan Research and Engineering, Inc., Bryan, Texas, USA. [Online]. Available: http://www.bre.com/portals/0/technicalarticles/Addington_Ness_RulesofThumb.pdf.
- [19] J. Polasek and J. Bullin, "Selecting Amines for Sweetening Units," in *GPA Regional Meeting*. Tulsa, OK: Gas Processor Association, 1994: up date from original paper in *Energy Progress* September 1984: 146-150.
- [20] M. S. Islam, R. Yusoff, B. S. Ali1, M. N. Islam and Chakrabarti, "Degradation studies of amines and alkanolamines during sour gas treatment process," *International Journal of the Physical Sciences*, vol. 6(25), pp. 5877-5890, 2011. ISSN 1992 - 1950 ©2011.
- [21] K. Arnold and M. Stewart, Surface Production Operation, Volume 2: Design of gas handling systems. *Gulf Publishing Company. Book Division. Houston.* , 1989, ISBN 087-201-175-5.
- [22] Metcalf and Eddy, *Wastewater engineering, 3rd edition*, McGraw-Hill, New York, USA, 1991.
- [23] J. E. Drinan, *Water and Wastewater Treatment: A guide for the Nonengineering Professional*, CRC Press LLC, Tecomic Publising, USA, 2001.

- [24] Laws of Malaysia; (act 127), Environmental Quality Act 1974 & Subsidiary Legislations International Law Book Services, 1999.
- [25] W.W. Eckenfelder and L. Musterman Jack, *Activated Sludge Treatment of Industrial Wastewater*, Technomic Publishing Company, Inc, Pennsylvania 17604, USA, 1995.
- [26] R. L. Stephenson and J.B. Blackburn Jr., *The Industrial Wastewater Systems Handbook*, Lewis Publishers, CRC Press LLC, USA, 1998.
- [27] D. L. Russell, *Practical Wastewater Treatment*, Global Environmental Operations, Inc. Lilburn, Georgia, 2006.
- [28] D. Mantzavinos, Advanced Oxidation Processes for Treatment of Industrial Effluent: Fundamental & Case Studies of Process Integration, in *Workshop on Advanced Oxidation Processes for Industrial Wastewater Treatment*, 4-5 October, 2007, Aula Magna, Aulario III, Universidad Rey Juan Carlos, Campus de Mostoles, Nadrid, Spain.
- [29] C.W. Jones, *Application of Hydrogen Peroxide and Derivatives*, RSC Clean Technology Monographs, Formerly of Solvay Interlox R & D, Widnes, UK, 1999.
- [30] Koprivanac and H. Kusic, *AOP as an Effective Tool for the minimization of Hazarduce Organic Pollutants in Colored Wastewater; Chemical and Photochemical Processes, Hazardous Material and Wastewater*, ISBN 1-60021-257-3, Nova Science Publiser, Inc, 2007, pp. 149-199.
- [31] W. J. Masschelein, *Ultraviolet Light in Water and Wastewater Sanitation*, Lewis Publishers, 2002.
- [32] T. Oppenländer, *Photochemical Purification of Water and Air*, WILLY-VCH, 2003.
- [33] M. M. Halmann, *Photodegradation of Water Pollutants*, CRC Press, Inc., US, 1996.
- [34] R. A. Buzzi, *Chemical Hazards at Water and Wastewater Treatment Plants*, Lewis Publisher, Chelsea, USA, (1992).

- [35] V. Homem, A. Alves, and L. Santos, "Amoxicillin degradation at ppb levels by Fenton's oxidation using design of experiments," *Sci. Total. Environ.*, vol. 408, pp. 6272-6280, 2010.
- [36] J. Berto, G. C. Rothenbach, M. A. B. Barreiros, A. X. R. Corrêa, S. Peluso-Silva, and C. M. Radetski, "Physico-chemical, Microbiological and Ecotoxicological Evaluation of A Septic Tank/Fenton reaction Combination for the Treatment of Hospital Wastewater," *Ecotox. Environ. Safe.*, vol. 72, pp. 1076-1081, 2009.
- [37] W. Jiang, G. Zhang, and W. Ying, "Integrated Fenton Oxidation Process for Advanced Treatment of Biologically Treated Coking Plant Effluent," in *3rd International Conference on Bioinformatics and Biomedical Engineering*, pp. 1-4, Digital Object Identifier: 10.1109/ICBBE.2009.5162974
- [38] J. Li, Z. Luan, L. Yu, and Z. Ji, "Pretreatment of Acrylic Fible Manufacturing Wastewater by the Fenton Process," *Desalination*, vol. 284, pp. 62-65, 2012.
- [39] M. I. Badawy, R. A. Wahaab, and A. S. El-Kalliny, "Fenton-biological Treatment Processes for the Removal of Some Pharmaceuticals from Industrial wastewater," *J. Hazard. Mater.*, vol. 167, pp. 576-574, 2009.
- [40] B. Lodha and S. Chaudhari, "Optimization of Fenton-biological Treatment Scheme for The Treatment of Aqueous Dye Solutions," *J. Hazard. Mater.*, vol. 148, pp. 459-466, 2007.
- [41] N. Boonrattanakij, M.-C. Lu, and J. Anotai, "Kinetics and Mechanism of 2,6-dimethyl-aniline Degradation by Hydroxyl Radical," *J. Hazard. Mater.*, vol. 172, pp. 952-957, 2009.
- [42] R. M. Ramli, "Degradation of Diisopropanolamine using Fenton's Reagent," M.S. Thesis, Dept. Chem. Eng., Tech. PETRONAS Univ., Seri Iskandar, Perak, MY, 2010.
- [43] S. Harimurti, "Degradation Kinetics of MEA and DEA by Fenton's Reagent with Biological Post-Treatment," M.S. Thesis, Dept. Chem. Eng., Tech. PETRONAS Univ., Seri Iskandar, Perak, MY, 2009.

- [44] P. F. Khamaruddin, M. A. Bustam, and A. A. Omar, "Using Fenton's Reagent for the Degradation of Diisopropanolamine: Effect of Temperature and pH," in *International Conference on Environment and Industrial Innovation (IPCBEI)*, vol. 12, pp. 12-17, Singapore, ©(2011) IACSIT Press.
- [45] L. Mingyu, W. Kunkun, T. Yillin, R. Gang, and S Lin, "Effect of Inorganic Ion on Fenton's Reagent Catalytic Degradation of Phenol in Water," in *International Conference on Computer Distributed Control and Intelligent Environmental Monitoring*, IEEE Computer Society, pp. 1144-1147, 2011, DOI 10.1109/CDIEM.2011.501
- [46] Lenntech, Water treatment & air purification holding B.V. Rotterdamseweg 402 M, 2629 HH Delft, (2008) The Netherlands.
- [47] D. L. Russell, *Practical Wastewater Treatment, Global Environmental Operations*, Inc. Lilburn, Georgia, 2006.
- [48] R. Andreozzi, V. Caprio, A. Insola, R. Marotta, and R. Sanchirico, "Advanced Oxidation Processes for the Treatment of Mineral Oil-Contaminated Wastewater," *Wat. Res.*, vol. 34 (2), pp. 620-628, 2000.
- [49] R. Hernandez, M. Zappi, J. Colucci, and Robert Jones, "Comparing the Performance of Various Advanced Oxidation Processes for Treatment of Aceton Contaminated Water," *J. Hazard. Mater.*, vol. 92, pp. 33-50, 2002.
- [50] L. Meuniur, S. Canonica, and U. von Guten, "Implication of Sequential Use of Ozone for Drinking Water Quality," *Wat. Res.*, vol.40, pp. 1864-1876, 2006.
- [51] J. Ma and N. J. D. Graham, "Degradation of Atrazine by Manganese-Catalysed Ozonation –Influence of Radical Scavengers," *Wat. Res.*, vol. 34 (15), pp. 3822-3828, 2000.
- [52] A. Safarzadeh-Amiri, "O₃/H₂O₂ Treatment of Methyl-*ter*-Butyl Ether (MTBE) in Contaminated Waters," *Wat. Res.*, vol. 35(15), pp. 3706-3714, 2001.
- [53] R. Rajeswari and S. Kanmani, "A study on Synergistic Effect of Photocatalytic Ozonation for Carbaryl Degradation," *Desalination*, vol. 242, pp. 277-285, 2009.

- [54] I. A. Katsoyiannis, S. Canonica, and U. von Guten, "Efficiency and Energy Requirements for the Transformation of Organic Micropollutants by Ozone, O₃/H₂O₂ and UV/H₂O₂," *Wat. Res.*, vol. 45, pp. 3811-3822, 2011.
- [55] S. H. Park, S.-J. Kim, S.-G. Seo, and S.-C. Jung, "Assessment of Microwave/UV/O₃ in the Photo-Catalytic Degradation of Bromothymol Blue in Aqueous Nano TiO₂ Particles Dispersions," *Nanoscale Res Lett*, vol. 5, pp. 1627-1632, 2010, DOI 10.1007/s11671-010-9686-y.
- [56] F. J. Beltrán, A. Aguinaco, and J. F. Garcí'a-Araya, "Mechanism and Kinetics of Sulfamethoxazole Photocatalytic Ozonation in Water," *Wat. Res.*, vol. 43, pp. 1359-1369, 2009.
- [57] R. Munter, "Advanced Oxidation Process – Current Status and Prospects," *Proc. Estonia. Sci. Chem.*, vol. 50(2), pp. 59-80, 2001.
- [58] O. Legrini, E. Oliveros, and A. M. Braun, "Photochemical Processes for Water Treatment," *Chem. Rev.*, vol. 93, pp. 671-698, 1993.
- [59] W.Z. Tang, *Physicochemical Treatment of Hazardous Waste*, Lewis Publishers, 2003.
- [60] S. Luňák and P. Sedlák, "Photoinitiated Reaction of Hydrogen Peroxide in the Liquid Phase," *J. Photochem. Photobiol. A: Chem.*, vol. 68, pp. 1-33, 1992.
- [61] I. Nicole, J. De Laat, M. Dore, J. P. Duguet, and C. Bonnel, "Use of U.V. Radiation in Water Treatment: Measurement of Photonic Flux by Hydrogen Peroxide Actinometry," *Wat. Res.*, vol. 24(2), pp. 157-168, 1990.
- [62] R. Andreozzi, V. Caprio, A. Insola, and R. Marotta, "Advanced Oxidation Process (AOP) for Water Purification and Recovery," *Catalysis Today*, vol. 53, pp. 51-59, 1999.
- [63] J. L. Lopez, F. S. G. Einschlag, M. C. Gonzáles, A. L. Capparelli, E. Oliveros, T. M. Haskem, and A. M. Braun, "Hydroxyl Radical Initiated Photodegradation of 4-chloro-3,5-dinitrobenzoic Acid in Aqueous Solution," *J. Photochem. Photobiol. A: Chem.*, vol. 137, pp. 177-184, 2000.

- [64] R.R. Giri, H. Ozaki, Y. Takayanagi, S. Taniguchi, and R. Takanami, “Efficacy of Ultraviolet Radiation and Hydrogen Peroxide Oxidation to Eliminate large number of Pharmaceutical Compounds in Mixed Solution,” *Int. J. Environ. Sci. Tech.*, vol. 8(1), pp. 19-30, Winter 2011.
- [65] Y. J. Jung, W. G. Kim, Y. Yoon, J. Kang, Y. M. Hong, and H. W. Kim, “Removal of Amoxicillin by UV and UV/H₂O₂ Processes,” *Sci. Total Environ.*, vol. 420, pp. 160-167, 2012.
- [66] K. Li, M. I. Stefan, and J. C. Crittenden, “Trichloroethane Degradation by UV/H₂O₂ Advanced Oxidation Process: Product Study and Kinetic Modeling,” *Environ. Sci. Technol.*, vol. 41, pp. 1696-1703, 2007.
- [67] M. I. Stefan and J. R. Bolton, “Mechanism of the Degradation of 1,4-Dioxane in Dilute Aqueous Solution Using the UV/Hydrogen Peroxide Process,” *Environ. Sci. Technol.*, vol. 32, pp. 1588-1595, 1998.
- [68] N. K. V. Leitner and M. Dore, “Hydroxyl Radical Induced Decomposition of Aliphatic Acid in Oxygenated and Deoxygenated Aqueous Solution,” *J. Photochem. Photobiol. A: Chem.*, vol. 99, pp. 137-143, 1996.
- [69] P. Mazellier, É. Leroy, J. De Laat, and B. Legube, “Degradation of Carbendazim by UV/H₂O₂ Investigated by Kinetic Modeling,” *Environ. Chem. Lett.*, vol. 1, pp. 68-72, 1 February 2003.
- [70] M. Muruganandham and M. Swaminathan, “Photochemical Oxidation of Reactive Azo Dye with UV-H₂O₂ Process,” *Dyes Pigments.*, vol. 62, pp. 269-275, 2004.
- [71] A. Riga, K. Soutsas, K. Ntampeglitis, V. Karayannis, and G. Papapolymerou, “Effect of System Parameters and of Inorganic Salts on the Decolorization and Degradation of Procion H-ex1 Dyes. Comparison of H₂O₂/UV, Fenton, UV/Fenton, TiO₂/UV and TiO₂/UV/H₂O₂ Processes,” *Desalination*, vol. 211, pp. 72-86, 2007.
- [72] W. Chu, “Modeling the Quantum Yields of Herbicide 2,4-D decay in UV/H₂O₂ process,” *Chemosphere*, vol. 44, pp. 935-941, 2001.

- [73] I. F. M. Ariff, P. N. F. M. Khamaruddin, S. Harimurti, and B. K. Dutta, "Optimization of UV/H₂O₂ Treatment of Monoethanolamine Using Taguchi Method of Experimental Design," in *International Conference on Environmental Research and Technology (ICERT 2008)*, Cleaner tech, control, treatment & remediation technique, Kuala Lumpur, Malaysia, 2008, pp. 930-934.
- [74] B. K. Körbathi and M.A. Rauf, "Application of Response Surface Analysis to the Photolytic Degradation of Basic Red 2 Dye," *Chem. Eng. J.*, vol. 138, pp. 166-171, 2008.
- [75] D. Salari, N. Daneshvar, F. Aghazadeh, and A.R. Khatae, "Application of Artificial Neural Network for Modeling of the Treatment of Wastewater Contaminated with Methyl *tert*-butyl ether (MTBE) by UV/H₂O₂ Process," *J. Hazard. Mater.*, vol. B125, pp. 205-210, 2005.
- [76] H. Mamane, H. Shemer, and K. G. Linden, "Inactivation of *E. coli*, *B. subtilis* spores and MS2, T4 and T7 phage using UV/H₂O₂ Advanced Oxidation," *J. Hazard. Mater.*, vol. 146, pp. 476-486, 2007.
- [77] E. M. Elkanzi and G. B. Kheng, "H₂O₂/UV Degradation kinetic of Isoprene in Aqueous Solution," *J. Hazard. Mater.*, vol. B73, pp. 55-62, 2000.
- [78] S. Esplugas, J. Giménez, S. Contreras, E. Pascual, and M. Rodríguez, "Comparison of Different Advanced Oxidation Processes for Phenol Degradation," *Water Res.*, vol. 36, pp. 1034-1042, 2002.
- [79] P. K. Malik and S. K. Sanyal, "Kinetics of Decolorization of Azo Dyes in Water by UV/H₂O₂ process," *Sep. Purif. Technol.*, vol. 36, pp. 167-175, 2004.
- [80] N. Daneshvar, M. A. Behnajady, and Y. Z. Asghar, "Photooxidative Degradation of 4-nitrophenol (4-NP) in UV/H₂O₂ Process: Influence of Operational Parameters and Reaction Mechanism," *J. Hazard. Mater.*, vol. B139, pp. 275-279, 2007.
- [81] P. Kajitvichyanukul, M. Lu, C. Liao, W. Wirojanagud, and T. Koottatep, "Degradation and Detoxification of Formaline Wastewater by Advanced Oxidation Processes," *J. Hazard. Mater.*, vol. B135, pp. 337-343, 2006.

- [82] K. Li, D. R. Hokanson, J. C. Crittenden, R. R. Trussell, and D. Minakata, "Evaluating UV/H₂O₂ Processes for Methyl tert-butyl Ether and Tertiary Butyl Alcohol removal: Effect of Pretreatment Options and Light Sources," *Water Res.*, vol. 42, pp. 5045-5053, 2008.
- [83] W. Song, V. Ravindran, and M. Pirbazari, "Process optimization using A Kinetic Model for the Ultraviolet Radiation-Hydrogen Peroxide Decomposition of Natural and Synthetic Organic Compounds in Groundwater," *Chem. Eng. J.*, vol. 63, pp. 3249-3270, 2008.
- [84] H. Chen, C. Chen, and G. Wang, "Performance evaluation of the UV/H₂O₂ Process on Selected Nitrogenous Organic Compounds: Reduction of Organic Contains vs. Corresponding C-,N-DBPs Formation," *Chemosphere*, vol. 85, pp. 591-597, 2011.
- [85] R. R. Sheha and H. H. Someda, *Hazardous Waste: Classification and Treatment Technologies*, Nova Science Publisher, Inc, New York, 2009.
- [86] C. Chang, J. Chen, M. Lu, and H. Yang, "Photocatalytic Oxidation of Gaseous DMF using Thin Film TiO₂ Photocatalyst," *Chemosphere*, vol. 58, pp. 1071-1078, 2005.
- [87] G.K.-C. Low, S. R. McEvoy, and R. W. Matthews, "Formation of Nitrate and Ammonium Ion in Titanium Dioxide Mediated Photocatalytic Degradation of Organic Compounds Containing Nitrogen Atoms," *Environ. Sci. Technol.*, vol. 25, pp. 460-467, 1991.
- [88] R. M. Alberici, M. C. Canela, M. N. Eberlin, and W. F. Jardim, "Catalyst Deactivation in Gas Phase Destruction of Nitrogen-Containing Organic Compounds using TiO₂/UV-VIS," *Appl. Catal. B-Environ.*, vol. 793, pp. 1-9, 2000.
- [89] M. Klare, J. Scheen, K. Vogelsang, H. Jacobs, and J. A. C. Broekaert, "Degradation of Short-chain Alkanolamines by TiO₂- and Pt/TiO₂-assisted Photocatalysis," *Chemosphere*, vol. 41, pp. 353-362, 2000.

- [90] H. Chun and W. Yizhong, "Decolorization and Biodegradability of Photocatalytic Treated Azo Dyes and Woll Textile Wastewater," *Chemosphere*, vol. 39(12), pp. 2107-2115, 1999.
- [91] M. A. Barakat, J. M. Tseng, and C. P. Huang, "Hydrogen Peroxide-assisted Photocatalytic Oxidation of Phenolic Compounds," *Appl. Catal. B-Environ.*, vol. 59, pp. 99-104, 2005.
- [92] A. Dixit, A. K. Mungray, and Chakraborty, "Photochemical Oxidation of Phenol and Chlorophenol by UV/H₂O₂/TiO₂ Process: A Kinetic Study," *International Journal of Chemical Engineering and Application*, vol. 1(3), October 2010, ISSN: 2010-0221.
- [93] D. Vione, V. Maurino, M. Vincenti, and E. Pelizzetti, "Formation of Nitrophenols upon UV Irradiation of Phenol and nitrate in Aqueous Solution and in TiO₂ Aqueous Suspension," *Chemosphere*, vol. 44, pp. 237-248, 2001.
- [94] M. Addamo, V. Augugliaro, E. García-López, V. Loddo, G. Marci, and L. Palmisano, "Oxidation of Oxalate Ion in Aqueous Suspension of TiO₂ by Photocatalysis and Ozonation," *Catal. Today.*, vol. 107-108, pp. 612-618, 2005.
- [95] M. A. Behnajady, H. Eskandarloo, N. Modirshahla, and M. Shokri, "Influence of the Chemical Structure of Organic Pollutants on Photocatalytic Activity of TiO₂ Nanoparticles: Kinetic Analysis and Evaluation of Electrical Energy per Order (E_{EO})," *Digest Journal of Nanomaterials and Biostructures*, vol. 6(4), pp. 1887-1895, October-December 2011.
- [96] F. Méndez-Arriaga, M. I. Maldonado, J. Gimenez, S. Esplugas, and S. Malato, "Abatement of Ibuprofen by Solar Photocatalysis Process: Enhancement and Scale up," *Catal. Today.*, vol. 144, pp. 112-116, 2009.
- [97] G. P. Anipsitakis and D. D. Dionysious, "Transition Metal/UV-based Advanced Oxidation Technologies for Water Decontamination," *Appl. Catal. B-Environ.*, vol. 54, pp. 155-163, 2004.
- [98] W.G. Cochran and G.M. Cox, *Experimental Design*, 2nd ed., John Wiley & Sons, New York, USA, 1992.

- [99] R. K. Roy, *Design of experiments using the Taguchi approach: 16 steps to product and process improvements*. New York: John Wiley and Sons, 2001.
- [100] A. I. Khuri, *Response Surface Methodology and Related Topics*, World Scientific Publishing Co. Pte. Ltd., 2005.
- [101] K. Hinkelmann and O. Kempthorne, *Design and Analysis of Experiments: Volume 1 Introduction of Experimental Design*, 2nd edition, Wiley-Interscience, A John Wiley & Sons, Inc., 2008.
- [102] M. Ahmadi, F. Vahabzadeh, B. Bonakdarpour, E. Mofarrah, and M. Mehranian, "Application of the Central Composite Design and Response Surface Methodology to the Advanced Treatment of Olive Oil Processing Wastewater using Fenton's Peroxidation," *J. Hazard. Mater.*, vol. B123, pp. 187-195, 2005.
- [103] C. T. Benatti, C. R. G. Tavares, and T. A. Guedes, "Optimization of Fenton's Oxidation of Chemical Laboratory Wastewaters using The Response Surface Methodology," *J. Environ. Manage.*, vol. 80, pp. 66-74, 2006.
- [104] D. Basheer. Hasan, A. R. Abdul Aziz, and W. M. A. Wan Daud, "Application of Response Surface Methodology in Process Parameters Optimization for Phenol Mineralization using Fenton's Peroxidation," *Afr. J. Biotechnol.*, vol. 10(50), pp. 10218-10231, 5 September 2011. ISSN 1684-5315©2011 Academic Journal. [Online] Available: <http://www.academicjournals.org/AJB>
- [105] H. Li, S. Zhou, Y. Sun, and J. Lv, "Nitrogen and Carbon Removal from Fenton-treated Leachate by Denitrification and Biofiltration," *Bioresour. Technol.*, vol. 101, pp. 7736-7743, 2010.
- [106] A. Naseri and H. Ayadi-Anzabi, "Monitoring of Decolorization of a Two Dyes Mixture using Spectrophotometric Data and Multivariate Curve Resolution: Modeling the Removal Process using An Experimental Design Method," *Anal. Methods*, vol. 4, pp. 153-161, 2012.

- [107] A. U. Rahmah, S. Harimurti, A. A. Omar, and T. Murugesan, "Optimization of Oxitetracycline Degradation Inside UV/H₂O₂ Reactor Using Box-Behnken Experimental Design," *J. Applied. Sci.*, 2012, ISSN 1812-5654/ DOI: 10.3923/jas.2012, © 2012 Asian Network for Scientific Information.
- [108] C. L. Lim, N. Morad, T. T. Teng, and N. Ismail, "Treatment of terasil Red R Dye wastewater using H₂O₂/pyridine/Cu(II) system", *J. Hazard. Mater.*, vol. 168, pp. 383-389, 2009.
- [109] A. R. Khataee, M. Zarei, and L Moradkhannejhad, "Appllication of Response Surface Methodology for Optimization of Azo Dye Removal by Oxalate Catalyzed Photoelectro-Fenton Process Using Carbone nanotube-PTEE Cathode," *Desalination*, vol. 258, pp. 112-119, 2010.
- [110] P. Maletzky and R. Bauer, "The Photo-Fenton method – Degradation of Nitrogen Containing Organic Compounds," *Chemospher*, vol. 37(5), pp. 899-909, 1998.
- [111] M. Mare, G. Waldner, R. Bauer, H. Jacobs, J. A. C. Broekaert, "Degradation of Nitrogen Containing Organic Compounds by Combined Photocatalysis and Ozonation," *Chemosphere*, vol. 38(9), pp. 2013-2027, 1999.
- [112] J. Jing, M. Liu, V. L. Colvin, W. Li, and W. W. Yu, "Photocatalytic Degradation of Nitrogen-containing Organic Compounds over TiO₂," *J. Mol. Catal. A: Chem.*, vol. 351, pp. 17-28, December 2011.
- [113] *Oxford Dictionary & Thesaurus of Current English*, Oxford University Press, 2004.
- [114] S. K. Ong, R. Y. Surampalli, A. Bhandari, P. Champagne, R. D. Tyagi, and I. Lo, *Natural Processes and Systems for Hazardous Waste Treatment*, ASCE and American Society of Civil Engineers, 2008.
- [115] R. R. Sheha and H. H. Someda, *Hazardous Waste: Classification and Treatment Technologies*, Nova Science Publishers, Inc., New York, 2008.
- [116] US EP A, *The Toxic-Release Inventory: A National Perspective*. Us Environmental Protection Agency, Office of Pesticides and Toxic Substances. EP A 5604-89-005, 1989.

- [117] W. W. Jr. Eckenfelder, D. L Ford, and A. J. Jr. Englande, *Industrial Water Quality*, 4th edition, Mc Graw Hill, 2009.
- [118] OECD, *Introduction to The OECD Guidlines for Testing of Chemicals Section 3; Part 1: Principles and Strategies Related to The Testing of Degradation of Organic Chemicals*, pp. 1-12, July 2003.
- [119] EUR-Lex, *Commission Decision 26.4.2005 Establishing Ecological Criteria and The Realated Assessment and Verification Eco-Label to Lubricans*, Official J. Eur. Union, L118, pp. 26-34, 2005.
- [120] P. Kajitvichyanukul and N. Suntrovipart, "Evaluation of Biodegradability and Oxidation Degree of Hospital Wastewater using Photo-Fenton Process as the Pretreatment method," *J. Hazard. Mater.*, vol. 138(2), pp. 384-391, 2006.
- [121] J. -S. Guo, A. A. Abbas, Y. -P. Chen, Z. -P. Liu, F. Fang, and P. Chen, "Treatment of Leachete Using a Combined Stripping, Fenton, SBR, and Coagulation Process," *J. Hazard. Mater.*, vol. 178, pp. 699-705, 2010.
- [122] T. -H. Kim, Jae. -K. Lee, and M. -J. Lee, "Biodegradability Enhancement of Textile Wastewater by Electrone Beam Irradiation," *Radiat. Phys. Chem.*, vol 76, pp. 1037-1041, 2007.
- [123] Y. Yang, P. Wang, S. Shi, and Y. Liu, "Microwave Enhanced Fenton-like Process for The Treatment of High Concentration Pharmaceutical Wastewater," *J. Hazard. Mater.*, vol. 168, pp. 238-245, 2009.
- [124] J. Mendham, R.C. Denney, J.D. Barnes, and M.J.K. Thomas, *Vogel's Textbook off Quantitative Chemical Analysis*, 6th edition, Practice Hall, UK, 2000.
- [125] Hach Company. "Hach Methods approved/accepted by the USEPA." *Hach-Downloads - Hach Methods EPA Acceptance Letters*. 1999. <http://www.hach.com/cms/documents/pdf/EPA/HachMethodsapprovedacceptedbytheUSEPA.pdf> (accessed June 9, 2012).
- [126] Clescerl, L S, A. E Greenberg, and A D Eaton, *Standard Methods for the Examination of Water and Wastewater*. 20th Edition. Baltimore: American Public Health Association, 1999.

- [127] R. H. Leonard. "Quantitative Range of Nessler's Reaction with Ammonia," *Clinical Chemistry*, vol. 9(4), pp. 417-422, 1963.
- [128] J. L. Brunty, R. A. Bucklin, J. Davis, C. D. Baird, and R. A. Nordstedt. "The Influence of Feed Protein Intake on Tilapia Ammonia Production," *Aquacult. Eng.*, vol. 16, pp. 161-166, 1997.
- [129] Y. Lester, D. Avisar, and H. Mamane, "Photodegradation of Antibiotic Sulphamethoxazole in Water with UV/H₂O₂ Advanced Oxidation Process," *Environ. Technol.*, vol. 31(2), 175-183, 2010.
- [130] N. Seraghni, S. Belattar, Y. Mameri, N. Debbache, and T. Sehili, "Fe(III)-Citrate-Complex-Induced Photooxidation of 3-Methylphenol in Aqueous Solution," *Int. J. Photoenergy*, doi:10.1155/2012/630425, 2012.
- [131] B. G. Petri, R. J. Watts, A. L. Teel, S. G. Huling, and R. A. Brown, "Fundamental of ISCO using hydrogen peroxide," in: *In situ chemical oxidation for groundwater remediation*, R. L. Siegrist, M. Crimi, T. J. Simpkin, Ed., Springer Inc., pp. 35-36, 2011.
- [132] B. Xua, N.-Y. Gaoa, H. Chengb, S. -J. Xi, M. Rui, and D. -D. Zhao, "Oxidative degradation of dimethyl phthalate (DMP) by UV/H₂O₂ process." *J. Hazard. Mater.*, vol. 162, pp. 954-959, 2009.
- [133] M.A. Behnajady, N. Modishahla, M. Shokri, and B. Vahid, "Investigation of The Effect of Ultrasonic Wave on The Enhancement of Efficiency of Direct Photolysis and Photooxidation Processes on The Removal of A Model Contaminant from Textile Industry," *Global NEST Journal.*, vol. 10(1), pp. 8-15, 2008.
- [134] B.F. Abramović, N.D. Banić, and D.V. Šojić, "Degradation of Thiocloprid in Aqueous Solution by UV and UV/H₂O₂ Treatments," *Chemosphere.*, vol. 81, pp. 114-119, 2010.
- [135] S. Haji, B. Benstaali, and N. Al-Bastaki, "Degradation of Methyl Orange by UV/H₂O₂ Advanced Oxidation Process," *Chem. Eng. J.*, vol. 168, pp. 134-139, 2011.

- [136] I.J. Ochuma, R.P. Fishwick, J. Wood, and J.M. Winterbottom, "Photocatalytic Oxidation of 2,4,6-Trichlorophenol in Water using A Cocurrent Downflow Contactor Reactor (CDCR)," *J. Hazard. Mater.*, vol. 144, pp. 627-633, 2007.
- [137] R. -P. Qiao, N. Li, X. -H. Qi, Q. -S. Wang, and Y. -Y. Zhuang, "Degradation of Microcystin-RR by UV Radiation in The Presence of Hydrogen Peroxide," *Toxicon*, vol. 45, pp. 745-752, 2005.
- [138] H. Asilian, R. Gholamnia, B. Rezaee, A. J. Jafari, A. Khavanin, and E. Darabi, "Photochemical of Polychlorinated Biphenyl by The Photolysis and Solvent," *J. App. Sci. Environ. Manage.*, vol. 14(4), pp. 107-112, December 2010.
- [139] B. Xu, N. -Y. Gao, X. -F. Sun, S. -J. Xia, M. Rui, M. -O. Simonnot, C. Causserand, and J. -F. Zhao, "Photochemical Degradation of Diethyl Phthalate with UV/H₂O₂," *J. Hazard. Mater.*, vol. B 139, pp. 132-139, 2007.
- [140] J. Ren, Q. -W. Ma, H. -H. Huang, X. -R. Wang, S. -B. Wang, and Z. -Q. Fan. (2010, Feb). Oxidative degradation of microcystin-LR by combination of UV/H₂O₂. *Fresenius Environmental Bulletin*. Vol. 19(12a). Pp. 3037-3044.
- [141] M. -W. Chang, C. -C. Chung, J.-M. Chern, and T. -S. Chen. "Dye Decomposition Kinetics by UV/H₂O₂: Initial Rate Analysis by Effective Kinetic Modelling Methodology," *Chem. Eng. Sci.*, vol. 65, pp. 135-140, 2010.
- [142] W. Li, S. Lu, Z. Qiu, and K. Lin. "Clofibric Acid Degradation in UV254/H₂O₂ Process: Effect of Temperature," *J. Hazard. Mater.*, vol. 176, pp. 151-157, 2010.
- [143] P. Neta, P. Muruthamuthu, P.M. Carton, and R.W. Fessenden, "Formation and Reactivity of the Amino Radical¹", *Journal of Physical Chemistry*, vol. 82(17), pp: 1875-1878, 1978.
- [144] A. C. Knipe and W. E. Watts, "Organic Reaction Mechanisms 1998," An Interscience Publication, John Wiley & Sons Ltd, 2003.
- [145] V. K. Ahluwalia and R. K. Parashar, "Organic Reaction Mechanisms", 2nd edition, Alpha Science International Ltd, 2005.

- [146] A.K. De, B. Chaudhuri, S. Bhattacharjee, and B.K. Dutta, "Estimation of HO• Radical Reaction Rate Constants for Phenol and Chlorinated Phenols using UV/H₂O₂ Photo-Oxidation," *J. Hazard. Mater.*, vol. B 64, pp. 91 – 104, 1999.
- [147] I.R. Levine, *Physical Chemistry*, 6th edition, Mc Grow Hill, New York, 2009.
- [148] J. Beltran, J. Torregrosa, J.R. Domiguez, and J.A. Peres, "Advanced Oxidation Processes for The Degradation of *p*-Hydroxybenzoic Acid 2: Photo-assisted Fenton Oxidation," *J. Chem. Technol. Biotechnol.*, vol. 76, pp. 1243 – 1248, 2001.
- [149] K.Y. Li, C.C. Liu, Q. Ni, Z. F. Liu, and F.Y.C. Huang, Colapret, "Kinetic Study of UV Peroxidation of Bis(2-chloroethyl) Ether in Aqueous Solution," *Ind. Eng. Chem. Res.*, vol. 34, pp. 1960 – 1968, 1995.
- [150] A. K. De, S. Bhattacharjee, and B. K. Dutta, "Kinetics of Phenol Photooxidation by Hydrogen Peroxide and Ultraviolet Radiation," *Ind. Eng. Chem. Res.*, vol. 36, pp. 3607 – 3612, 1997.
- [151] H. Christensen, K. Sehested, and H. Corfitzen, "Reaction of Hydroxyl Radical with Hydrogen Peroxide at Ambient and Elevated Temperatures," *J. Phys.Chem.*, vol. 86(9), pp. 1588 – 1590, 1982.
- [152] P.B.L. Chang and T. M. Young, "Kinetics of Methyl *ter*-Butyl Ether Degradation and By-product Formation during UV/Hydrogen Peroxide Water Treatment," *Water Res.*, vol. 38(8), pp. 2233 – 2240, 2000.
- [153] O. Levenspiel, *Chemical Reaction Engineering*, 3th edition, John Wiley & Sons, USA, 1999.
- [154] H.S. Fogler, *Elements of Chemical Reaction Engineering*, 4th edition, Practice Hall, 2006.
- [155] V. Kavitha and K. Palanivelu, "Destruction of Cresols by Fenton Oxidation Process," *Water Res.*, vol. 39, pp. 3062 – 3072, 2005.
- [156] Q. Wang and A.T. Lemley, "Kinetic Model and Optimization of 2,4-D Degradation by Anodic Fenton Treatment," *Environ. Sci. Technol.*, vol. 35, pp. 4509 – 4514, 2001.

- [157] X. Liu, J. Liang, and X. Wang, "Kinetics and Reaction Pathways of Formaldehyde Degradation using the UV-Fenton Method," *Water Environ. Res.*, vol. 83(5), pp. 418 – 426, 2011.
- [158] Andreazzi R., Caprio V., Insola A., and Marotta R., "Advanced Oxidation Processes (AOP) for Water Purification and Recovery", *Catalysis Today*, Vol. 53, pp. 51-59, 1999.
- [159] Y. -P. Chiang, Y. -Y. Liang, C. -N. Chang, and A. C. Chao, "Differentiating Ozone Direct and Indirect Reactions on Decomposition of Humic Substances," *Chemosphere*, vol. 65, pp. 2395 – 2400, 2006.
- [160] S. Harimurti, A. U. Rahmah, A. A. Omar, and T. Murugesan, Application of Response Surface Method in the Degradation of Wastewater containing MDEA using UV/H₂O₂ Advance Oxidation Process, *J. Applied. Sci.*, vol. 12(11), pp. 1093-1099, 2012.
- [161] H. Kim, J. Lee, and M. Lee, "Biodegradability enhancement of textile wastewater by electron beam irradiation," *Radiat. Phys. Chem.*, vol. 76, pp. 1037-1041, 2007.
- [162] N. Daneshvar, A. Aleboyeh, and A.R. Khataee, "The evaluation of electrical energy per order (EEo) for Photooxidative Decolorization of Four Textile Dye Solution by The Kinetic Model," *Chemosphere*, vol. 59, pp. 761 – 767, 2005.

PUBLICATIONS

Journals

No.	Title	Remark
1	Application of Response Surface Method in The Degradation of Wastewater Containing MDEA using UV/H ₂ O ₂ Advanced Oxidation Process	Journal of Applied Sciences, 12(11) – 1093 – 1099, 2012.
2	Kinetics of Methyl-diethanolamine Mineralization by Using UV/H ₂ O ₂ Process	CLEAN – Soil, Air, Water. On line DOI: 10.1002/clen.201200121

Conferences

No.	Title	Remark
1	Effect of Hydrogen Peroxide (H ₂ O ₂) on Mineralization of Methyl-diethanolamine (MDEA) using UV/H ₂ O ₂	ICPEAM 2010 (KLCC, 15 – 17 June 2010)
2	The Degradation Mechanism of Wastewater Containing MDEA using UV/H ₂ O ₂ Advanced Oxidation Process	NPC 2011 (UTP – Perak, 19 – 20 Sept 2011), DOI: 10.1109/NatPC.2011.6136283
3	Application of Response Surface Method in The Degradation of Wastewater Containing MDEA using UV/H ₂ O ₂ Advanced Oxidation Process	ICCEIB 2011 (Kuantan, Pahang, 28 – 30 Nov 2011)
4	Application of Response Surface Methodology for Screening of Factors Influencing in The Refinery Waste Mineralization by UV/H ₂ O ₂	ICPEAM 2012 (KLCC, 12 – 14 June 2012)
5	Effect of bicarbonate on the mineralization of methyl-diethanolamine by using UV/H ₂ O ₂	Will be presented in IOGSE 2013 (Kota Kinabalu, Sabah, 9 – 11 October 2013)

APPENDIX A
CALIBRATION CURVE

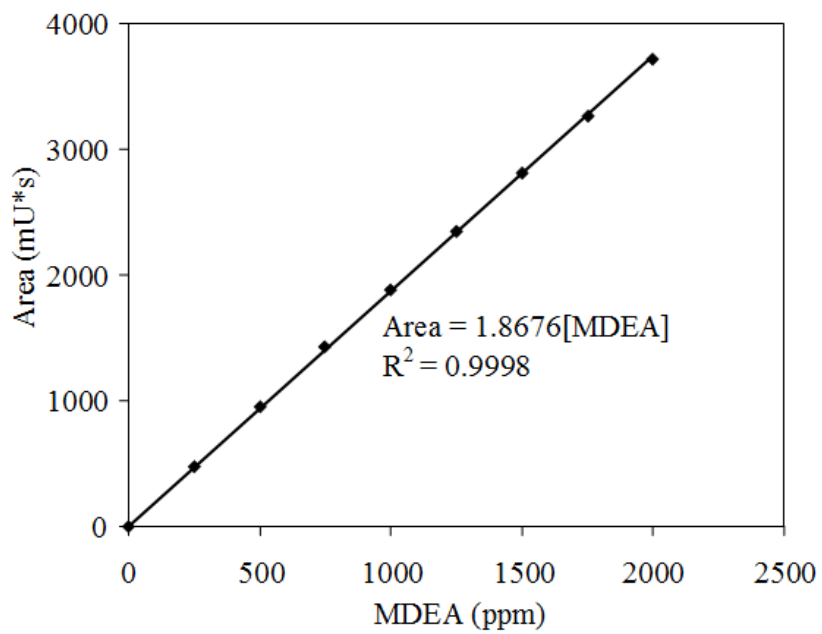


Figure A1. Calibration curve for MDEA (The plot of concentration of MDEA vs. area from HPLC analysis)

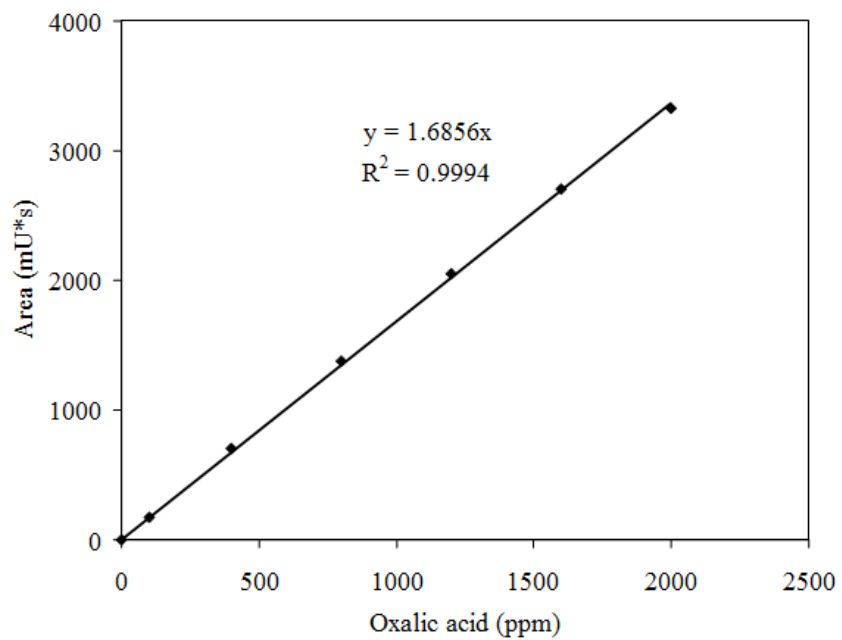


Figure A2. Calibration curve for oxalic acid (The plot of concentration of oxalic acid vs. area from HPLC analysis)

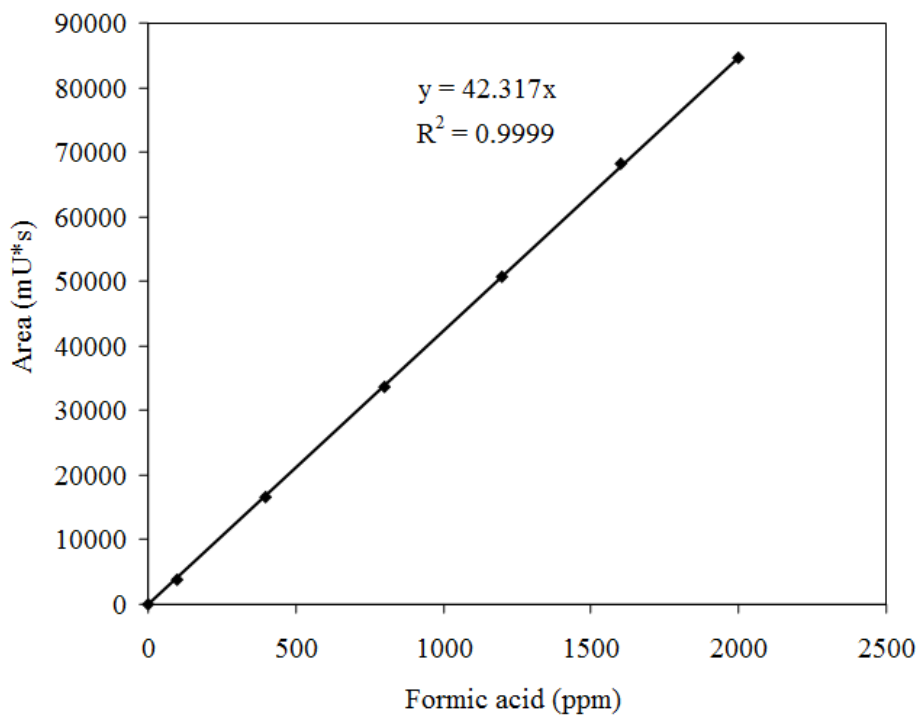


Figure A3. Calibration curve for formic acid (The plot of concentration of formic acid vs. area from HPLC analysis)

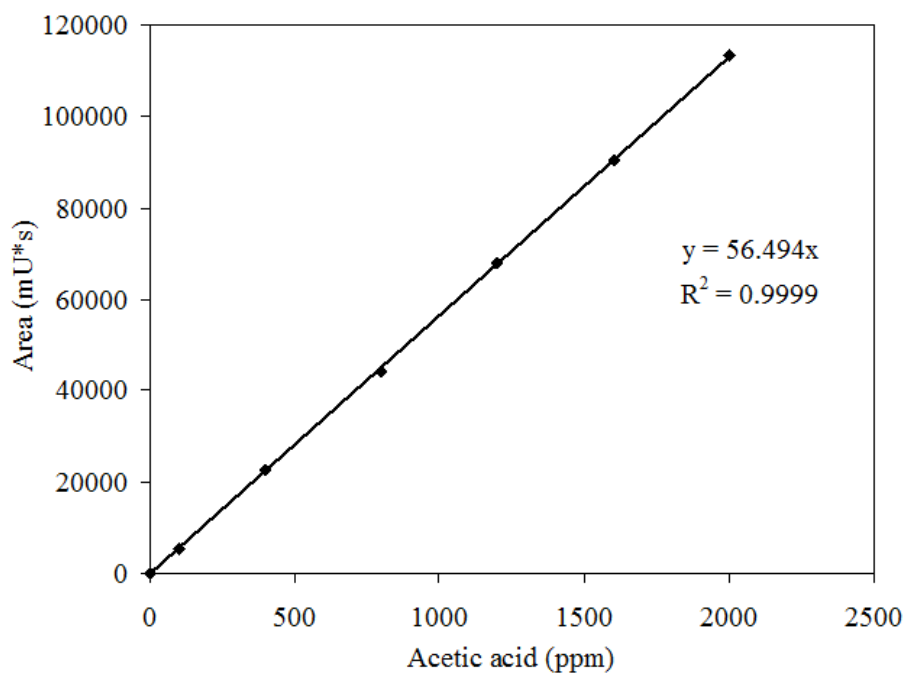


Figure A4. Calibration curve for acetic acid (The plot of concentration of acetic acid vs. area from HPLC analysis)

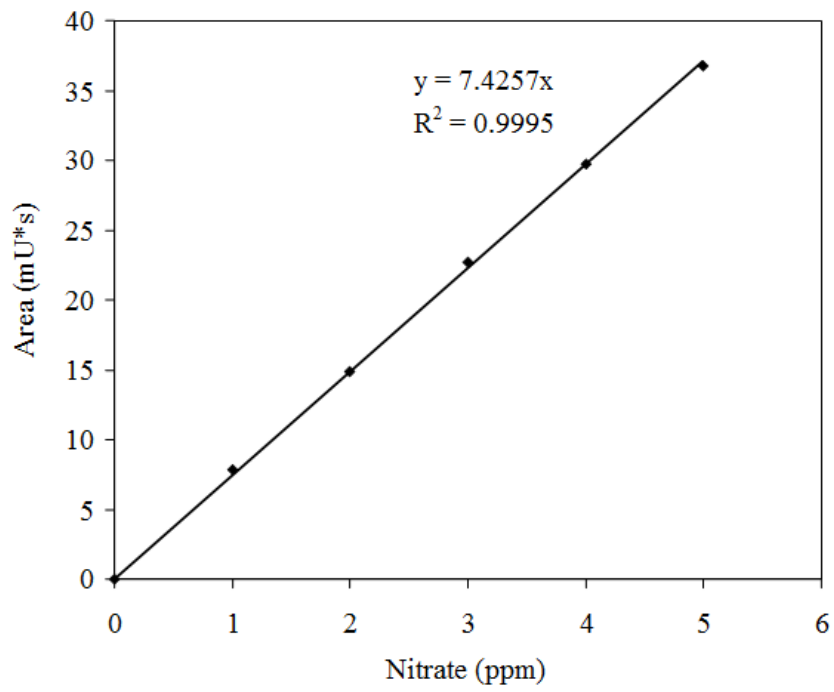


Figure A5. Calibration curve for nitrate (The plot of concentration of nitrate vs. area from IC analysis)

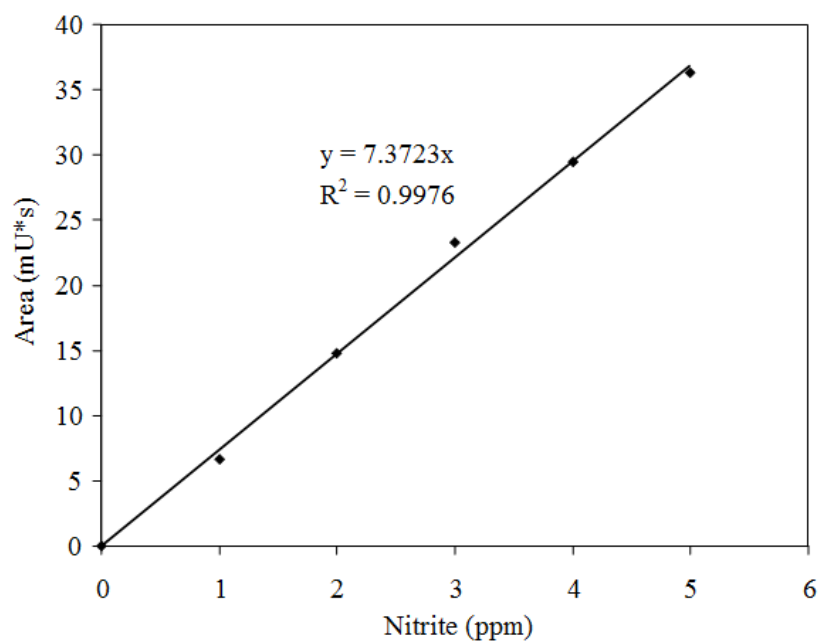


Figure A6. Calibration curve for nitrite (The plot of concentration of nitrite vs. area from IC analysis)

APPENDIX B

Rate constant of MDEA mineralization by hydroxyl radical at different temperature
based on Figure 4.29

Estimation of k_3 (rate constant of MDEA mineralization by hydroxyl radical) based on Figure 2.9.

Based on Equation 4.16;

$$\text{slope} = \frac{k_5}{k_{\text{exp}} k_3} \quad \text{hence;} \quad k_3 = \frac{k_5}{k_{\text{exp}} \text{slope}}$$

$$\begin{aligned} \text{Where } k_5 \text{ at experimental condition} &= 8 \times 10^7 \text{ M}^{-1} \text{ sec}^{-1} \\ &= 4.8 \times 10^9 \text{ M}^{-1} \text{ min}^{-1} \end{aligned}$$

Based on Figure 4.29, the *slope* and k_{exp} at different temperature are summarized in table bellow

Temp.(°C)	1/ k_{exp}	Slope (Eq. 4.16)	$k_{\text{exp}}(\text{M}^{-1} \text{ min}^{-1})$
20	287.95	2.4255	0.003473
30	286.94	2.3956	0.003485
40	353.74	2.6365	0.002827
50	439.37	2.5763	0.002276

At 20 °C

$$k_3 = \frac{k_5}{k_{\text{exp}} \text{slope}} = \frac{4.8 \times 10^9}{2.4255 \times 0.003473} = 5.69 \times 10^{11} \text{ M}^{-1} \text{ min}^{-1} = 9.50 \times 10^9 \text{ M}^{-1} \text{ sec}^{-1}$$

At 30 °C

$$k_3 = \frac{k_5}{k_{\text{exp}} \text{slope}} = \frac{4.8 \times 10^9}{2.3956 \times 0.003485} = 5.75 \times 10^{11} \text{ M}^{-1} \text{ min}^{-1} = 9.58 \times 10^9 \text{ M}^{-1} \text{ sec}^{-1}$$

At 40 °C

$$k_3 = \frac{k_5}{k_{\text{exp}} \text{slope}} = \frac{4.8 \times 10^9}{2.6365 \times 0.002827} = 6.44 \times 10^{11} \text{ M}^{-1} \text{ min}^{-1} = 10.73 \times 10^9 \text{ M}^{-1} \text{ sec}^{-1}$$

At 50 °C

$$k_3 = \frac{k_5}{k_{\text{exp}} \text{slope}} = \frac{4.8 \times 10^9}{2.5763 \times 0.002276} = 8.19 \times 10^{11} \text{ M}^{-1} \text{ min}^{-1} = 13.64 \times 10^9 \text{ M}^{-1} \text{ sec}^{-1}$$